


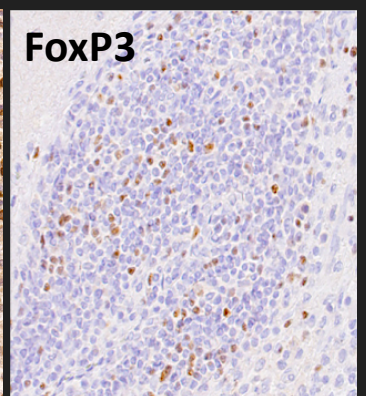
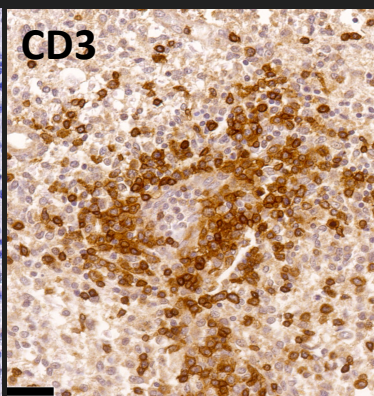
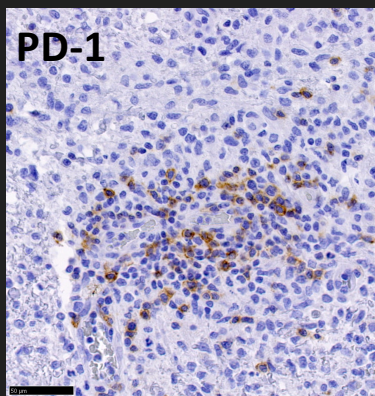
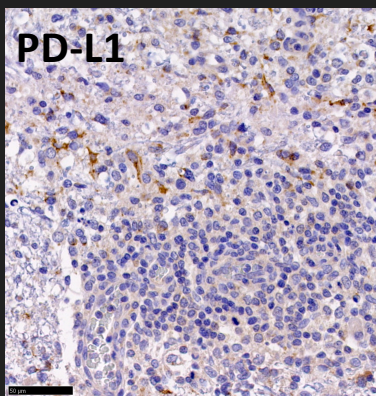
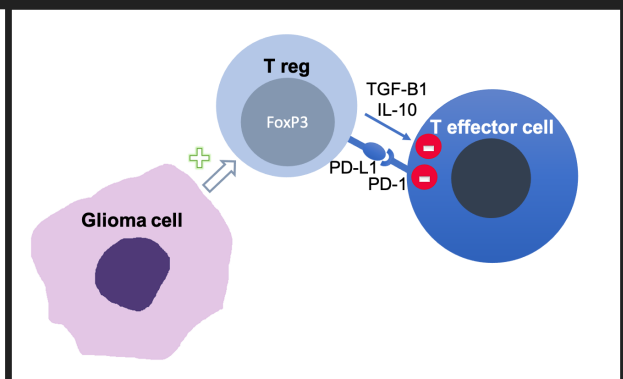
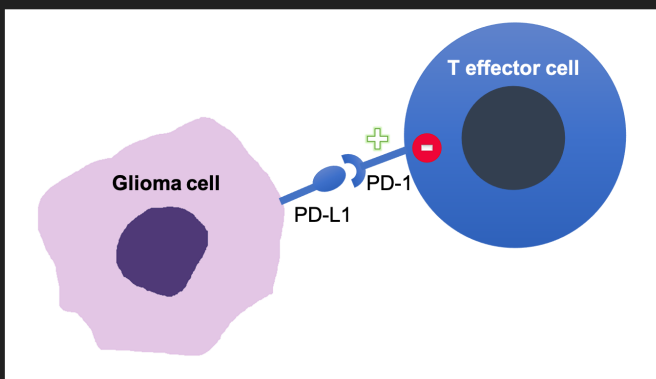
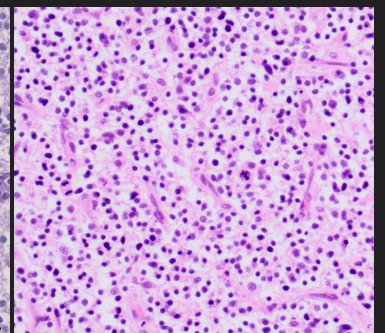
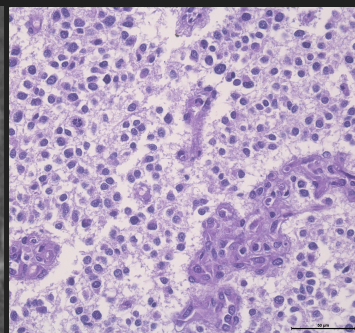
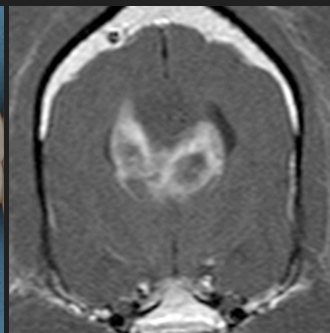
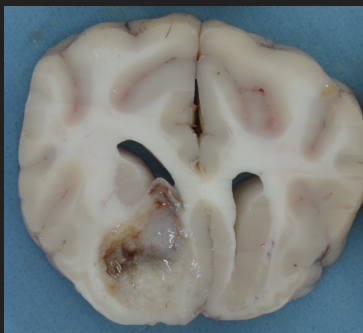
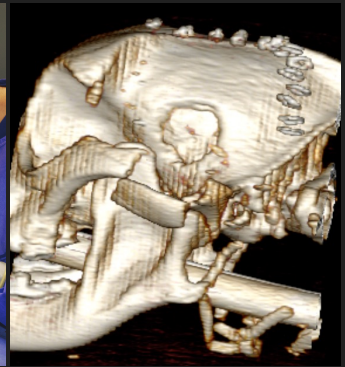
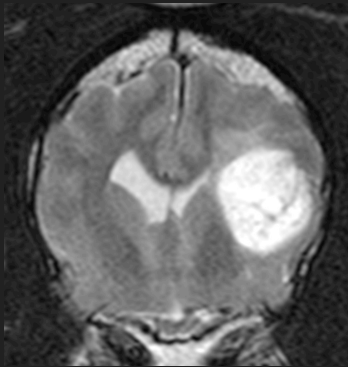


ADVERTIMENT. L'accés als continguts d'aquesta tesi queda condicionat a l'acceptació de les condicions d'ús establertes per la següent llicència Creative Commons:  http://cat.creativecommons.org/?page_id=184

ADVERTENCIA. El acceso a los contenidos de esta tesis queda condicionado a la aceptación de las condiciones de uso establecidas por la siguiente licencia Creative Commons:  <http://es.creativecommons.org/blog/licencias/>

WARNING. The access to the contents of this doctoral thesis it is limited to the acceptance of the use conditions set by the following Creative Commons license:  <https://creativecommons.org/licenses/?lang=en>

Characterizing Canine Glioma as a Naturally Occurring Model for Immune Evasion in Human Glioma



PhD Thesis
Roberto José-López
Barcelona, 2021



**Universitat Autònoma
de Barcelona**

Characterizing Canine Glioma as a Naturally Occurring Model for Immune Evasion in Human Glioma



FACULTAT DE VETERINÀRIA DE BARCELONA

Departament de Medicina i Cirurgia Animals

Thesis presented by
Roberto José López

To attain the degree of
Doctor en Medicina i Cirurgia Animals

Bellaterra, September 2021

Doctoral thesis directed by
Martí Pumarola i Batlle
Paul M. Brennan

UAB

Universitat Autònoma de Barcelona

MARTÍ PUMAROLA I BATLLE, Professor in Veterinary Pathology at the Departament de Medicina i Cirurgia Animals of the Universitat Autònoma de Barcelona

AND

PAUL M. BRENNAN, Senior Clinical Lecturer and Honorary Consultant Neurosurgeon at the Centre for Clinical Brain Sciences of the University of Edinburgh

DECLARE

that the doctoral thesis titled “Characterizing canine glioma as a naturally occurring model for immune evasion in human glioma” submitted by Roberto José López to attain the title of Doctor en Medicina i Cirurgia Animals, has been conducted under our supervision and we now consider it completed. Thus, we authorize its submission for evaluation by the corresponding examining panel.

We hereby confirm the above information is true on 17th of September 2021.

**MARTÍ
PUMAROLA
I BATLLE -
DNI
40425926E**

Firmado
digitalmente por
MARTÍ
PUMAROLA
BATLLE - DNI
40425926E
Fecha: 2021.09.17
09:41:13 +02'00'



Dr. Martí Pumarola i Batlle

Dr. Paul M. Brennan

AGRADECIMIENTOS

Después de 5 años de duro trabajo, no habría sido posible completar esta tesis sin el apoyo, la colaboración, la motivación y la orientación de grandes colegas, amigos y compañeros que de algún modo han aportado su granito de arena. ¡Espero no olvidarme de ninguno de vosotros!

En primer lugar, quiero agradecer a mi director y tutor de tesis **Martí**, por ofrecerme la oportunidad de llevar a cabo esta investigación en un tema que me apasiona, y por su apoyo y orientación constantes. Desde mi residencia en el Hospital Clínic UAB, quise desarrollar la investigación clínica en gliomas caninos que incluimos en esta tesis y, además, gracias a su ayuda y orientación, hemos podido caracterizar parte de la interacción de los gliomas en perros con el sistema inmune, que esperamos contribuya al desarrollo de estudios translacionales que ayuden a mejorar el manejo de los gliomas humanos. Es un orgullo para mí haber trabajado estos años contigo, Martí, y siempre recordaré tu *“mientras viva, yo te apoyo en lo que sea”*. Ha habido momentos difíciles por la complejidad de combinar esta tesis con mi puesto como profesor asociado y clínico en la Universidad de Glasgow, ¡pero finalmente lo logramos!

También quiero agradecer todo su apoyo y colaboración a mi segundo director **Paul M Brennan**. Nos encontramos gracias a un golpe de suerte y eso nos permitió desarrollar esta investigación comparativa con el glioma humano. Muchas gracias por aportar siempre otro punto de vista. Ha resultado muy enriquecedor para nuestros estudios. A través de Paul conocimos a **Ted Hupp**, él y su equipo, a los que también les doy mil gracias, desarrollaron el anticuerpo canino anti-PD-1 que nos permitió llevar a cabo parte de nuestra investigación doctoral y su contribución ha sido de gran utilidad.

No puedo olvidarme de **Dolors Pi Castro**, cuya contribución a los trabajos aquí incluidos ha sido descomunal. Muchas gracias por todo tu esfuerzo y tesón. ¡Parte de esta tesis también es tuya! Y cómo no, muchas gracias, **Ester Blasco**. Sin tu buen hacer con la inmunohistoquímica y tu organización y disponibilidad, nada de esto habría sido posible.

Un agradecimiento muy especial va también para mi compañero de fatigas durante los últimos 6 años y amigo incondicional, **Rodrigo Gutiérrez Quintana**. Gracias por ser tan buen amigo y por toda tu ayuda, sin ello, no hubiese podido combinar el trabajo con mi tesis, ¡además que fuiste el nexo con Paul! Hemos hecho un gran equipo durante estos años y

hemos llegado lejos juntos. Aunque ya no estemos en el mismo lugar, espero que la dupla Ro-Ro tenga para mucho rato y sigamos siendo los Winchester de la neurología, ¡jaja!

Nancy, Eduardo, Sebastián y tú siempre seréis mi familia.

A todos los colaboradores en los estudios aquí incluidos, ¡muchas gracias! Esta tesis no sería posible sin vuestra contribución. ¡Gracias también por vuestra paciencia mientras os perseguía pidiéndoos cosas! En particular quiero agradecer a **Sonia** y **Cristian**, además de colaborar en esta tesis, a Sonia por formarme como neurólogo y a Cristian por las vivencias compartidas durante la residencia, fue duro, ¡pero nos echamos unas buenas risas!

No puedo olvidarme tampoco de todos aquellos que me han inspirado y motivado desde el inicio de mi carrera hasta ahora. **Artur Font** durante mis estancias en Ars, él me inspiró a buscar la especialización, **Albert Lloret**, mi mestre Miyagui particular, **Jo Morris**, sin su apoyo y ayuda jamás hubiese conseguido la beca de la Universidad de Glasgow que ha financiado parte de esta investigación, y muchos más! Me habéis ayudado a llegar a donde estoy y por eso os doy las gracias.

También dar las gracias aquí y a la vida por los amigos que me ha brindado. **Paco, Ana, Luís, Laura, Miquel, Carlos, Nacho, Aina, Clara, Charlie, Raquel, Tim, Josep, Liza...** y un largo etc., soy un afortunado por disfrutar de vuestra compañía, cariño y apoyo.

A mi familia, mis padres **Laureano** y **Olimpia**, mi hermana, **Miriam**, y mis abuelos, **Rosa, Laureano** y **Claudina**. Papas, muchas gracias por todo el amor que me habéis profesado y todo vuestro duro trabajo para que pudiésemos ser lo que quisiéramos. Sin vosotros no sería nada. Miriam, eres la mejor hermana del mundo, recuerda siempre que vales mucho! Yaya Rosa, ¡eres la mejor abuela del mundo! Gracias por criarnos y por todo tu cariño, consejos y risas. A pesar de que a veces riñamos, me alegro mucho de parecerme a ti y de haber podido disfrutar este verano contigo en tu pueblito, Robledo de Donís, donde he completado esta tesis. Finalmente, gracias a **Nora**, mi compañera y mejor amiga. Sin tu amor, consejos y apoyo tampoco hubiera sido posible. He crecido mucho a tu lado.

Ahora, ¡a disfrutar la vida que son 2 días!

A mis padres, Olimpia y Laureano

A mi hermana, Miriam

A mi abuela, Rosa

A mi mejor amiga, Nora

INDEX

1. LIST OF ABBREVIATIONS.....	12
2. SUMMARY.....	16
3. RESUMEN.....	22
4. INTRODUCTION.....	28
4.1 Gliomas.....	30
4.1.1 Morphologic diagnosis and classification.....	30
4.1.2 Epidemiology: tumor subtype distribution, anatomic location within the CNS and patient demographics.....	32
4.1.3 Clinical diagnosis.....	33
4.1.4 Treatment and outcome.....	35
4.2 The mechanisms of tumor immune evasion in gliomas.....	36
4.2.1 Interaction of tumor cells with the immune system.....	36
4.2.2 Mechanisms of glioma immune escape.....	38
4.2.3 Regulatory T-cells.....	40
4.2.4 PD-1-PD-L1 immune checkpoint.....	41
5. OBJECTIVES.....	48
6. MATERIALS, METHODS AND RESULTS.....	50
6.1 Article 1. Clinical features, diagnosis, and survival analysis of dogs with glioma.....	54
6.2 Article 2. Expression of FOXP3 in canine gliomas: Immunohistochemical study of tumor-infiltrating regulatory lymphocytes.....	78
6.3 Article 3. Immunohistochemical study of programmed death ligand 1 expression and tumor-infiltrating lymphocytes in canine gliomas.....	90

7. DISCUSSION.....	126
8. CONCLUSIONS.....	138
9. BIBLIOGRAPHY.....	140

1. LIST OF ABBREVIATIONS

APC, antigen presenting cell

CBTC, Comparative Brain Tumor Consortium

CE, contrast enhancement

CI, confidence interval

CNS, central nervous system

CSF, cerebrospinal fluid

CSF-1, colony stimulating factor 1

CT, computed tomography

CTL, cytotoxic T-lymphocyte

CTLA4, cytotoxic T-lymphocyte-associated protein 4

DC, dendritic cell

FGL2, fibrinogen-like protein 2

FLAIR, fluid-attenuation inversion recovery

FOXP3, forkhead box P3

GFAP, glial fibrillary acidic protein

GRE, gradient recall echo

HA, high-grade astrocytoma

HO, high-grade oligodendroglioma

HU, high-grade undefined glioma

IDH, isocitrate dehydrogenase

IFN- γ , interferon-gamma

IL, interleukin

ITFs, intratumoral accumulations of fluid

LA, low-grade astrocytoma

LO, low-grade oligodendroglioma

MHC, major histocompatibility complex

MRI, magnetic resonance imaging

MST, median survival time

NCI, National Cancer Institute

NOS, not otherwise specified

OR, odds ratio

PD-1, programmed cell death protein 1

PD-L1, programmed death ligand 1

PGE, prostaglandin E

STAT3; signal transducer and activator of transcription 3

TC, tumor cell

TGF β , tumor growth factor beta

TIL, tumor-infiltrating lymphocyte

Treg, regulatory T-cell

WHO, World Health Organization

SUMMARY

2. SUMMARY

Growing evidence suggests human gliomas exploit immune inhibitory pathways to suppress antitumor immunity and promote tumor progression. Thus, there is an emerging need to characterize the contribution of the immune system to glioma biology so novel treatments can be developed to improve the poor outcomes associated with the current standard of care in human medicine.

To achieve this, animal models that recapitulate human gliomas with fidelity are necessary. Genetically engineered mice are frequently used to model human gliomas; however, murine models of disease have failed to reliably predict which of the therapies that are efficacious in pre-clinical studies will be effective in the clinic. As a result, the dog has been postulated as a promising model for human gliomas because of the size and structure of its brain, the high incidence of spontaneous gliomas, and the coexistence with an active immune system. Nevertheless, to validate canine glioma as a model for human glioma, there are many gaps in knowledge related to tumor natural biology as well as its molecular characteristics and immunologic profile that need to be addressed.

Binding of programmed cell death protein 1 (PD-1) to its ligand (PD-L1) promotes activated T-cell exhaustion. Tumor cells (TCs) evade host's immune attack by expressing PD-L1 and stimulating PD-1 expression on tumor-infiltrating lymphocytes (TILs). Accumulation of intratumoral FoxP3⁺ regulatory T-cells (Tregs) also results in effector T-cell inhibition and decreased antitumor response. Both, PD-1-PD-L1 immune checkpoint expression and Tregs accumulation are considered central to human glioma immune evasion.

In this thesis, we analyzed the epidemiologic features, clinical findings, diagnosis, and survival of a cohort of 91 dogs with glioma and assessed the relationship between these and tumor histologic type and grade. Also, we evaluated the immunohistochemical expression of

Tregs and the PD-1-PD-L1 immune checkpoint in a subset of 43 and 21 canine gliomas, respectively.

Despite the difference in tumor histologic subtype distribution between species, astrocytic gliomas are most common in humans whereas oligodendrogliomas are most prevalent in dogs, we found several key demographics and clinicopathologic similarities including tumor location in the fronto-olfactory, temporal, and parietal regions of the cerebral cortex, middle-to old-age at diagnosis, a male sex predilection, and seizures as the common presenting sign prompting diagnosis.

Although no associations were found between clinicopathologic findings or survival and canine glioma type or grade, definitive treatments (surgery, radiotherapy and/or chemotherapy) provided significantly improved median survival time (MST) compared to palliative treatment. On magnetic resonance imaging (MRI) of intracranial gliomas, oligodendrogliomas were associated with smooth margins and T1-weighted hypointensity compared to astrocytomas and undefined gliomas and were more commonly in contact with the ventricles than astrocytomas. Tumor spread to adjacent brain structures was associated with high-grade glioma. New onset seizures were associated with a more favorable prognosis. By contrast, MRI observed irregular or indistinct tumor margins, T2-weighted heterogeneity and drop metastases were associated with shorter survival.

The immunohistochemical study of expression of FOXP3+ Tregs in our sample of canine gliomas revealed FOXP3+ Treg infiltration in all tumor types and grades. Additionally, accumulation of FOXP3+ TILs within the tumor was more pronounced in astrocytic than oligodendroglial tumors.

We also demonstrated PD-1 and PD-L1 are immunohistochemically detectable in canine gliomas of different types and grades. PD-L1 expression of variable extent was observed in

all glioma specimens and astrocytomas were associated with higher levels of expression than oligodendrogliomas.

Finally, immunohistochemical evaluation of the TIL infiltrate in canine gliomas included the CD3⁺ and CD20⁺ TIL subsets, corresponding to T- and B-lymphocytes, respectively. TILs could be seen scattered throughout the tumor tissue, though they tended to cluster perivascularly in the tumor margins and infiltration zone, and CD3⁺ TILs were present in higher numbers than CD20⁺ TILs. Furthermore, FOXP3⁺ and PD1⁺ TIL subsets showed regional overlap with CD3⁺ TILs on adjacent tissue sections.

The results of the studies conducted in this thesis further the current knowledge on canine gliomas diagnosis, treatment outcome and prognosis, critical for assessment of therapies. Additionally, characterization of intratumoral FOXP3⁺ Treg accumulation and PD-L1 expression in canine gliomas, demonstrates that spontaneous canine glioma models immune evasion in its human counterpart. This supports the use of canine gliomas in translational human studies.

RESUMEN

3. RESUMEN

Cada vez hay más evidencia sugiriendo que los gliomas humanos explotan vías inhibitorias del sistema inmune para suprimir la inmunidad antitumoral y promover la progresión del tumor. Por tanto, urge caracterizar la contribución del sistema inmune a la biología de los gliomas para poder desarrollar nuevas terapias que mejoren los pobres resultados del tratamiento estándar actual en medicina humana.

Para lograr esto, hacen falta modelos animales que recapitulen los gliomas humanos con fidelidad. Es habitual usar ratones manipulados genéticamente como modelo del glioma humano, sin embargo, los modelos murinos de este tipo de cáncer han fracasado a la hora de predecir de manera fiable qué tratamientos aparentemente eficaces en estudios preclínicos son efectivos en la clínica. A consecuencia de esto, el perro se ha postulado como un modelo prometedor para los gliomas humanos debido al tamaño y estructura de su encéfalo, la alta incidencia de gliomas espontáneos, y la coexistencia con un sistema inmune activo. Sin embargo, para validar el glioma canino como modelo para el glioma humano, primero hay que resolver muchas incógnitas relacionadas con la biología natural de los gliomas caninos, así como con sus características moleculares e inmunofenotipo.

La unión entre la proteína de muerte celular programada 1 (PD-1) con su ligando (PD-L1) promueve el agotamiento y apoptosis de las células T activadas. Las células tumorales (TCs) evaden el ataque inmune de su huésped expresando PD-L1 e induciendo la expresión de PD-1 en los linfocitos que infiltran el tumor (TILs). La acumulación intratumoral de células T reguladoras (Tregs) también resulta en inhibición de las células T efectoras y disminución de la respuesta antitumoral. Estos mecanismos de expresión del punto de control inmune de la PD-1-PD-L1 y acumulación de Tregs, se consideran clave para la evasión del sistema inmune en los gliomas humanos.

En esta tesis, analizamos las características epidemiológicas, hallazgos clínicos, diagnóstico, y supervivencia de una muestra de 91 perros con glioma y evaluamos la relación entre estos parámetros y el tipo y grado histológico de los tumores. Además, evaluamos la expresión inmunohistoquímica de Tregs y el punto de control del sistema inmune PD-PD-L1 en 43 y 21 gliomas caninos, respectivamente.

A pesar de las diferencias entre especies en la distribución de los subtipos histológicos de tumor (los gliomas astrocíticos son más frecuentes en personas, mientras que los oligodendrogliomas son los más prevalentes en perros), encontramos varias similitudes demográficas y clinicopatológicas clave entre perros y humanos como la frecuente localización del tumor en las regiones fronto-olfatoria, temporal y parietal del córtex cerebral, una edad media-avanzada al diagnóstico, predilección por los machos, y crisis convulsivas como típico signo detonante del diagnóstico.

Aunque no pudimos demostrar asociaciones entre ningún hallazgo clinicopatológico o la supervivencia y el tipo o grado de glioma canino, las terapias más definitivas (cirugía, radioterapia y/o quimioterapia) proporcionaron un tiempo de supervivencia media significativamente superior al tratamiento paliativo. En resonancia magnética de los gliomas intracraneales, observamos que los oligodendrogliomas estaban asociados a márgenes bien definidos e hipointensidad en secuencias en T1 en comparación con los astrocitomas y los gliomas indefinidos, y más comúnmente en contacto con los ventrículos que los astrocitomas. La extensión del tumor a estructuras encefálicas adyacentes estaba asociada a glioma de alto grado. Las crisis convulsivas de nueva presentación se asociaron con un pronóstico más favorable. Por el contrario, la observación en resonancia de márgenes tumorales irregulares o indefinidos, señal heterogénea del tumor en secuencias en T2 y metástasis se asociaron a una supervivencia más corta.

El estudio inmunohistoquímico de la expresión de Tregs FOXP3+ en nuestra muestra de gliomas caninos reveló infiltración por estas células en todos los tipos y grados de tumor. Además, la acumulación de Tregs FOXP3+ fue más pronunciada en tumores astrocíticos que oligodendrogliales.

También demostramos que la PD-1 y PD-L1 se pueden detectar mediante inmunohistoquímica en gliomas caninos de diferentes tipos y grados. Observamos diferentes grados de expresión de PD-L1 en todas nuestras muestras de glioma y los astrocitomas se asociaron con un mayor nivel de expresión que los oligodendrogliomas.

Finalmente, la evaluación inmunohistoquímica del infiltrado de TILs en gliomas caninos incluyó la evaluación de los subconjuntos de TILs CD3+ y CD20+, correspondientes a linfocitos T y B respectivamente. Observamos TILs esparcidos por todo el tumor, sin embargo, solían acumularse a nivel perivascular en los márgenes del tumor y la zona de infiltración, y los TILs CD3+ positivos estaban presentes en mayor número que los CD20+. Adicionalmente, los subconjuntos de TILs FOXP3+ y PD-1+ se solapaban con los CD3+ en secciones tisulares adyacentes.

Los resultados de los estudios incluidos en esta tesis incrementan el conocimiento actual sobre el diagnóstico, respuesta al tratamiento y pronóstico en gliomas caninos, información esencial para la evaluación de terapias. Además, la caracterización de la acumulación intratumoral de Tregs FOXP3+ y la expresión de PD-L1 en gliomas caninos, demuestra que el glioma canino espontáneo comparte estos mecanismos de evasión del sistema inmune en su homólogo humano. Esto apoya el uso de gliomas caninos en estudios traslacionales para la evaluación y desarrollo de inmunoterapias para humanos.

INTRODUCTION

4. INTRODUCTION

This doctoral thesis was motivated by the current translational drive to validate canine glioma as a model for human glioma and the interest on the potential contribution of certain mechanisms of antitumor immune response escape to their complex pathophysiology.

Gliomas are a group of primary central nervous system (CNS) tumors with histological features of glial cells (predominantly astrocytes (astrocytomas), oligodendrocytes (oligodendrogliomas), or mixtures of glial cells).¹

Glioma is the most common of brain cancers in people, representing 81% of all malignant brain tumors in adults.² It is classified into four grades based on malignancy.¹ Glioblastoma, a grade IV astrocytoma, is the most common of all gliomas and is considered the most malignant, with a median survival of 14.6 months even after surgery and adjuvant radiotherapy and chemotherapy.²⁻⁵ Thus, novel treatment concepts based on biological insights are urgently needed to improve patient outcomes.

Although genetically engineered mice are frequently used to model human gliomas, such models are limited by the inbred nature of rodent strains, differences in mouse life span, size of brain and lack of spontaneous development of the disease.^{6,7} The consequence is that these models have failed to reliably predict which of the therapies that are efficacious in pre-clinical studies will be effective in the clinic. Similarly, orthotopic transplantation of tumor cells (TCs) into often immunodeficient mice fails to model the complexities of the immune system which, is known to play a central role in tumor biology. Hence why models that recapitulate human tumors with greater fidelity are necessary to test new treatment strategies.

Canine brain tumors are becoming established as naturally occurring models for human disease to advance diagnostic and therapeutic understanding.⁸ The incidence of adult canine brain tumors is 2.8-4.5% of all tumors diagnosed at necropsy, compared with a human

incidence of 1.3-2% of all cancers.⁹⁻¹³ Although individual studies vary, gliomas represent 36-70% of primary brain tumors in dogs.¹²⁻¹⁴ Thus, the dog presents a promising model for understanding human glioma and is also preferable to rodent models because of the closer evolutionary relationship to human compared to the mouse counterpart, the high incidence of spontaneous diffusely infiltrating gliomas representative of tumor true nature and behavior in humans, and the coexistence with an active immune system.⁷ Conversely, there are many gaps in knowledge related to canine glioma natural biology as well as molecular characteristics and immunologic profile that need to be addressed to validate the dog as a realistic animal model so new therapies can be tested and developed.

One of the principal recent advances in the understanding of human glioma has been characterization of the immune system's role in tumor biology. The immune system can recognize tumors and eliminates many early malignant cells.^{15,16} However, tumors evolve to evade immune attack by maintaining an immunosuppressive microenvironment.¹⁵ Human gliomas appear to exploit immune inhibitory mechanisms such as immune cell regulation and immune checkpoints.¹⁶

These observations and the promising results shown by immunotherapies as positive adjuvant treatments in other malignancies have prompted the intensive study of immunotherapeutic targeting of these immunomodulating pathways in human gliomas. However, preclinical promise in murine models of glioma has not translated into meaningful clinical responses.^{17,18}

Therefore, the aims of this thesis were 1) to validate canine glioma as an animal clinical model for human glioma by further characterizing its epidemiologic, clinicopathologic and diagnostic imaging features as well as outcome after treatment in correlation with their histological type and grade; and 2) to establish whether canine gliomas model immune evasion in the human counterpart.

4.1 Gliomas

4.1.1 Morphologic diagnosis and classification

By the start of this doctoral research in 2016, it was standard veterinary practice to use the 2007 World Health Organization (WHO) human glioma classification to grade canine gliomas.¹ The reason for this was to facilitate translational studies based on the histological similarities between human and canine gliomas, and because the veterinary WHO classification, dating from 1999, was hopelessly outdated.¹⁹

The 2007 WHO human glioma diagnostic scheme classified and graded tumors based on analysis of clinical outcome and survival relative to specific pathologic criteria such as increasing cell density, necrosis, nuclear atypia, and mitotic count.¹ However, information on tumor progression and outcome following treatment in canine gliomas was anecdotal at that stage, thus, little was known about whether histologic type and grade correlated with tumor biologic behavior.²⁰ Additionally, advances in molecular genetics and biology enhancing our understanding and subclassification of human gliomas were included in the 2016 edition of the WHO classification.²¹ Most relevantly, prognosis in human gliomas is currently guided by isocitrate dehydrogenase (IDH) mutation and 1p/19q status. In the setting of current standard of care in people, IDH-mutant gliomas may follow a less aggressive clinical course. Likewise, 1p and 19q loss in oligodendrogliomas may be associated with longer survival.

This, in conjunction with the translational drive to compare canine and human gliomas, led the Comparative Brain Tumor Consortium (CBTC) of the National Cancer Institute (NCI) to revise the diagnostic classification of canine gliomas in 2018.²²

This new diagnostic schema classified canine gliomas as oligodendroglioma if they contained $\geq 80\%$ neoplastic cells with oligodendroglial morphology, astrocytoma if contained $\geq 80\%$ neoplastic cells with astrocytic morphology, and undefined if neoplastic cells showed a

mixture of morphologies with no dominant one or primitive morphology that fitted neither category. Further to this, canine gliomas were classified as low- or high-grade based on the presence of one or more unequivocal features of malignancy consisting of microvascular proliferation, large tracts of necrosis with or without pseudopalisading and observation of >1 mitosis per 400X field.

The aim was to provide an updated canine-specific scheme for clinical and molecular data to be added into a morphologic diagnosis, to assist with prediction of tumor behavior. Table 1 summarizes the 2016 WHO guidelines for human glioma diagnosis and the CBTC canine glioma diagnostic scheme. These classify diffusely infiltrating gliomas, which are most common in both species. Other predominantly low-grade, well-circumscribed subtypes of astrocytic gliomas in humans and in dogs include subependymal giant cell astrocytoma, pilocytic astrocytoma, gemistocytic astrocytoma, pleomorphic xanthoastrocytoma.^{21,23}

Table 1. Summary of the 2016 WHO and CBTC diagnostic guidelines for human and canine diffuse gliomas, respectively.

2016 WHO classification ²¹		CBTC classification ²²	
Tumor type	Grade	Tumor type	Grade
Diffuse astrocytoma, IDH-mutant	II	Astrocytoma	Low-grade
Anaplastic astrocytoma, IDH-mutant	III		High-grade
Anaplastic astrocytoma, IDH-wildtype	III		
Glioblastoma, IDH-wildtype	IV		
Glioblastoma, IDH-mutant	IV		
Diffuse midline glioma, H3 K27M-mutant	IV	Oligodendroglioma	
Oligodendroglioma, IDH-mutant and 1p/19q-codeleted	II		Low-grade
Anaplastic oligodendroglioma, IDH-mutant and 1p/19q-codeleted	III		High-grade
Oligoastrocytoma, NOS	II	Undefined glioma	Low-grade
Anaplastic oligoastrocytoma, NOS	III		High-grade

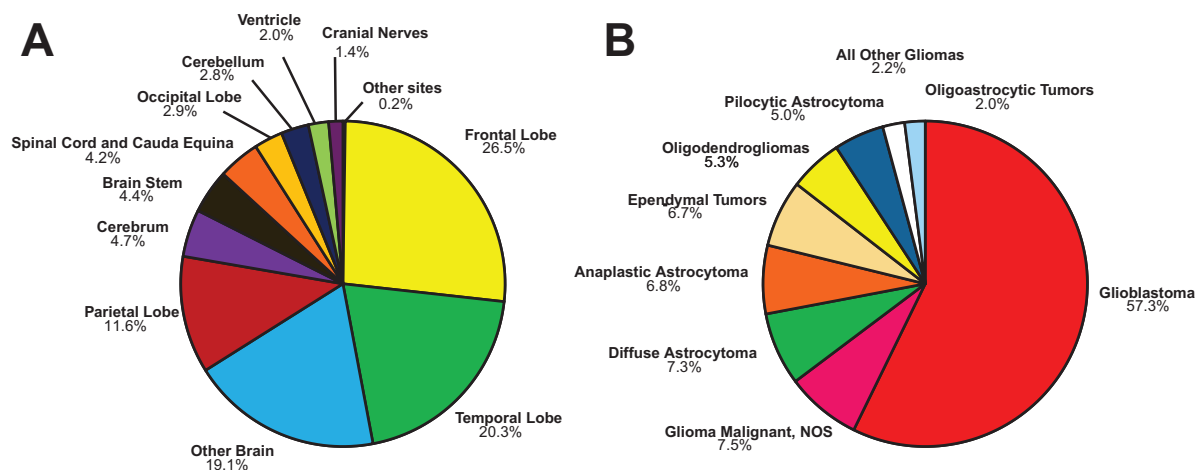
Abbreviations: IDH, isocitrate dehydrogenase; NOS, not otherwise specified.

This doctoral research is focused on diffusely infiltrating canine gliomas. These were classified according to the CBTC diagnostic scheme as we aimed to enhance this recently revised classification by further characterizing the epidemiologic, clinicopathologic, diagnostic imaging and outcome features of gliomas in dogs as well as unravelling their immunologic profile.

4.1.2 Epidemiology: tumor subtype distribution, anatomic location within the CNS and patient demographics

As stated above, gliomas are the most common malignant brain tumors in humans. Glioblastoma accounts for the majority of human gliomas (57.3%) and overall, astrocytomas add up to 76.4% of all glial tumors in people (Figure 1).³ Over 58% of human gliomas are located in the fronto-olfactory, temporal and parietal regions of the cerebral cortex (Figure 1).

Figure 1. Distribution of primary brain and other CNS gliomas in humans. **A**, Site and **B**, Histology subtypes.



From: CBTRUS Statistical Report: US Cancer Statistics, 2012–2016.³

Although gliomas can affect children and young adults, particularly certain subtypes (e.g., diffuse midline glioma), they are most commonly diagnosed in middle- to old-age patients.²¹ Median age at diagnosis of glioblastoma is 65 years.³ A male sex predilection with

significantly higher incidence ratios (1.25-1.58) for males/females is reported in all diffuse glioma subtypes.³

At the start of this doctoral research, descriptions of the epidemiologic features of canine gliomas were scarce and scattered across the veterinary literature. There was marked variability in the relative frequency of canine oligodendroglioma and astrocytoma and their subtypes between individual studies.^{13,14,23-25} Most reported tumor location was hemispheric and a significantly increased likelihood of histologic involvement of the diencephalon in astrocytomas had been described.^{14,26} Over 50% of all gliomas were reported in certain brachycephalic breeds.^{13,14,20,23} No sex predisposition had been found and median age for dogs with glioma was reported as 8 years although there were occasional descriptions in younger dogs.

Revision of 193 canine gliomas for validation of the abovementioned CBTC diagnostic scheme in 2018 yielded epidemiologic data on the largest cohort to date. That study identified 69.4% oligodendrogliomas (35 low-grade, 99 high-grade), 22.3% astrocytomas (19 low-grade, 24 high-grade), and 8.3% undefined gliomas (2 low-grade, 14 high-grade). Over 55% gliomas were in the fronto-olfactory, temporal, and parietal regions of the brain. A median age at diagnosis of 8 years and previously reported brachycephalic breed predilection in canine gliomas were confirmed. Furthermore, a significantly higher prevalence of oligodendrogliomas in the Boston Terrier, Bulldog and Boxer breeds as well as an incidence ratio of glioma of 1.53 for all males/females were found.

4.1.3 Clinical diagnosis

Gliomas result in space-occupying mass lesions that affect the surrounding CNS parenchyma by their expansion. The clinical consequences of gliomas depend upon their localization and size as well as secondary mass effect including peritumoral edema, hemorrhage and, in

intracranial tumors, obstructive hydrocephalus. As gliomas are most frequently located within the brain, clinical features in people may range from subtle abnormalities such as speech difficulties and changes in sensation or vision, to behavior or personality changes, pulsating headaches, aphasia, motor deficits (e.g., hemiparesis) and seizures. As many as half of all human patients are diagnosed after an inaugural seizure.²¹

By contrast, at the beginning of this project, little was known about the constellation of clinical signs associated with glioma in dogs, their frequency and their relationship with tumor type or grade. Most commonly reported clinical signs in dogs with glioma in the few descriptions available included mentation changes, seizures, and visual deficits.^{14,23,27}

Provisional tumor diagnosis in canine glioma depends on many factors, including signalment (age, breed, and more recently, sex) and neuroanatomical localization but ultimately, advanced imaging such as computed tomography (CT) or magnetic resonance imaging (MRI) is required for a tentative diagnosis. Typically, canine intracranial gliomas are described as intra-axial, T1-weighted iso- to hypointense and T2-weighted iso- to hyperintense mass lesions with varying degrees of perilesional edema and contrast enhancement (CE) on conventional MRI.^{14,26,28-30}

Although definitive diagnosis of glioma requires histopathologic analysis of tumor tissue, biopsy or resection of tumors is not always possible in veterinary medicine due to its high cost and risks of the procedure. Therefore, the ability to predict intracranial glioma type and grade in dogs based on MRI characteristics has been investigated over recent years.^{26,30,31}

Two independent studies including 30 and 31 dogs with glioma, respectively, evaluated the relationship between MRI features and tumor type and grade in histologically confirmed tumors.^{26,30} Whilst the first found oligodendrogliomas were significantly more likely to contact the brain surface and meninges than astrocytomas, the second described astrocytomas were associated with the presence of moderate to extensive peritumoral edema, lack of

ventricular distortion, and iso- to hyperintense T1-weighted signal.^{26,30} Finally, one study found CE was significantly more common in high-grade gliomas whereas the other found mild to no CE, absence of cystic structures, and tumor location other than the thalamo-capsular region were associated with low-grade gliomas compared to high-grade gliomas. Many of those features coincided with observations in human glioma. In humans, CE correlates with grade of glioma, with central non-enhancing portions being typical of glioblastoma.³² Cystic regions or necrosis also correlate to glioma grade.^{33,34} Human oligodendrogliomas also typically display absent to mild peritumoral edema and are largely T1-weighted hypointense.^{35,36} However, a study evaluating the predictability of grade and type of histologically confirmed canine intracranial gliomas using the above MRI predictors found an accuracy of 53.3% for tumor grade and 60% for predicted tumor type.³¹ This indicated further analysis of MRI features of canine gliomas in relation to their type and grade as well as other MRI techniques was necessary to enhance clinical diagnosis of glioma type and grade in dogs.

4.1.4 Treatment and outcome

While prognosis and survival rates for each subtype of glioma are well-established in people,²¹ when we started this research, information on outcome following treatment in canine gliomas was anecdotal.

Meaningful statements regarding the natural biology and behavior in light of therapy of canine gliomas were difficult to make due to the limitations of most studies: small case numbers, retrospective study design and most importantly, lack of histologic diagnosis including tumor typing and grading.

Case series with palliative treatment outcome information relating to canine glioma type or grade were lacking. No conclusions could be made from published data relating to surgery

for canine gliomas either, other than that anecdotally it could be beneficial with some animals surviving for several months with or without adjunctive treatments.^{37,38} Similarly, there was very little meaningful information available relating to the efficacy of chemotherapeutic agents or radiotherapy for gliomas in dogs, as most reports included cases with just presumptive diagnoses.^{20,39}

Thus, for the first study of this thesis, we set out to increase the available knowledge on canine glioma epidemiologic, clinicopathologic, diagnostic imaging and outcome features in relation with tumor type and grade so further comparisons with human glioma could be made. To achieve this, multicentric collaboration was sought to include more cases in our research and increase its relevance. As a result, seven European veterinary neurology specialist referral services contributed cases of dogs with glioma for their study. Finally, as the CBTC classification of canine glioma was proposed shortly after we started our research, we decided to add the resulting evidence of our series to this canine-specific diagnostic scheme.

4.2 The mechanisms of tumor immune evasion in gliomas

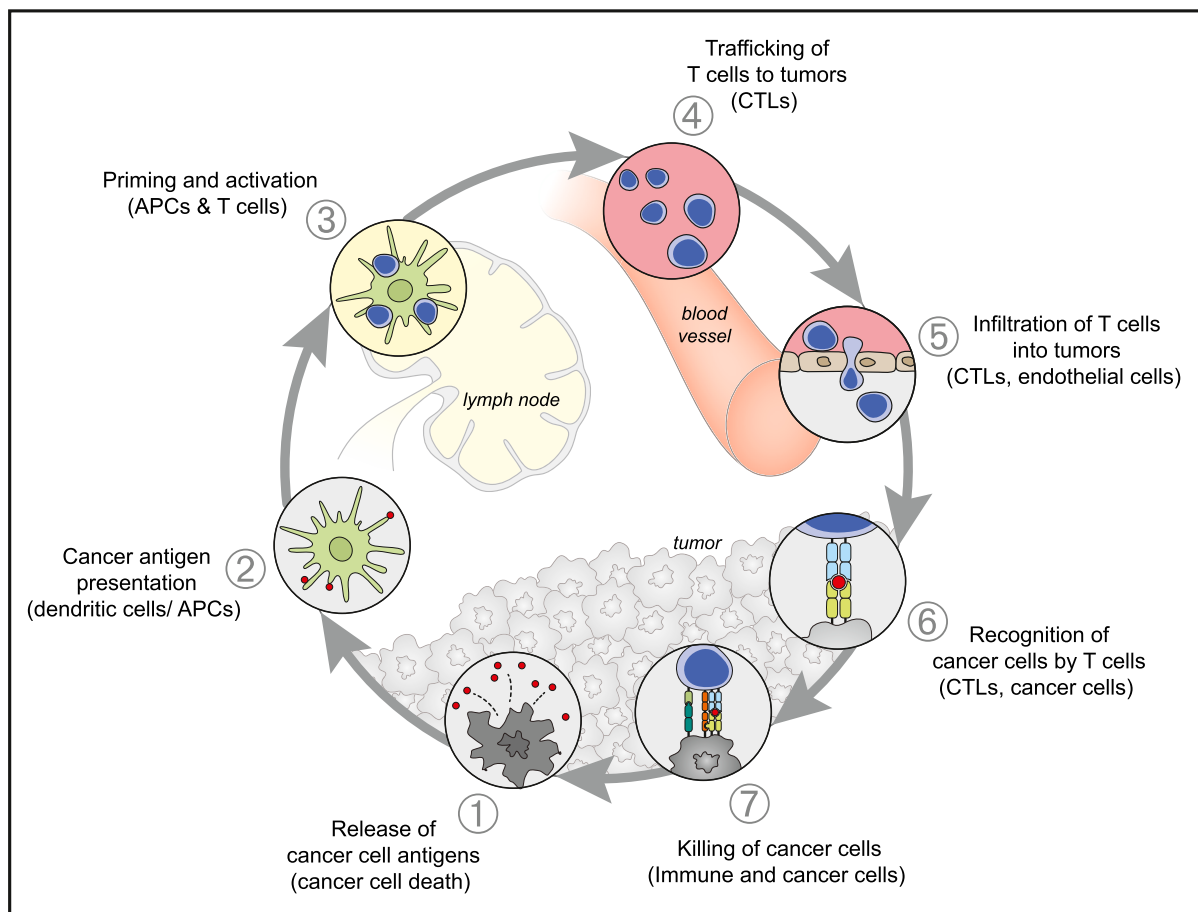
4.2.1 Interaction of tumor cells with the immune system

A major determinant of cancer pathogenesis is the interaction of TCs with the immune system. Cancer is a multistep process characterized by the accumulation of genetic and epigenetic alterations that drive or reflect tumor progression. These changes distinguish cancer cells from their normal counterparts, allowing tumors to be recognized as foreign by the immune system.^{15,40}

Thus, the immune system recognizes and even eliminates many early malignant cells via the anticancer or antitumor immune response. As TCs start to develop and cancer begins to progress, release of cancer cell antigens initiates a series of stepwise events beginning with

tumor antigen presentation by antigen-presenting cells (APCs) and progressing through priming and activation of T-cells, trafficking of cytotoxic T-cells to tumors and infiltration into these, and ultimately, the recognition and killing of TCs. This goes on on a cycle (Figure 2) that can be self-propagating, leading to an accumulation of immune-stimulatory factors that, in principle, should amplify and broaden T-cell responses.⁴⁰

Figure 2. The cancer-immunity cycle.



From: Chen DS, Mellman I. Oncology meets immunology: the cancer-immunity cycle. *Immunity* 2013; 39:1-10.
Abbreviations: APCs, antigen presenting cells; CTLs, cytotoxic T-lymphocytes.

However, tumors are rarely rejected spontaneously. This is because the above cycle is also characterized by inhibitory factors that lead to immune regulatory feedback mechanisms, which can halt or limit immunity.⁴⁰

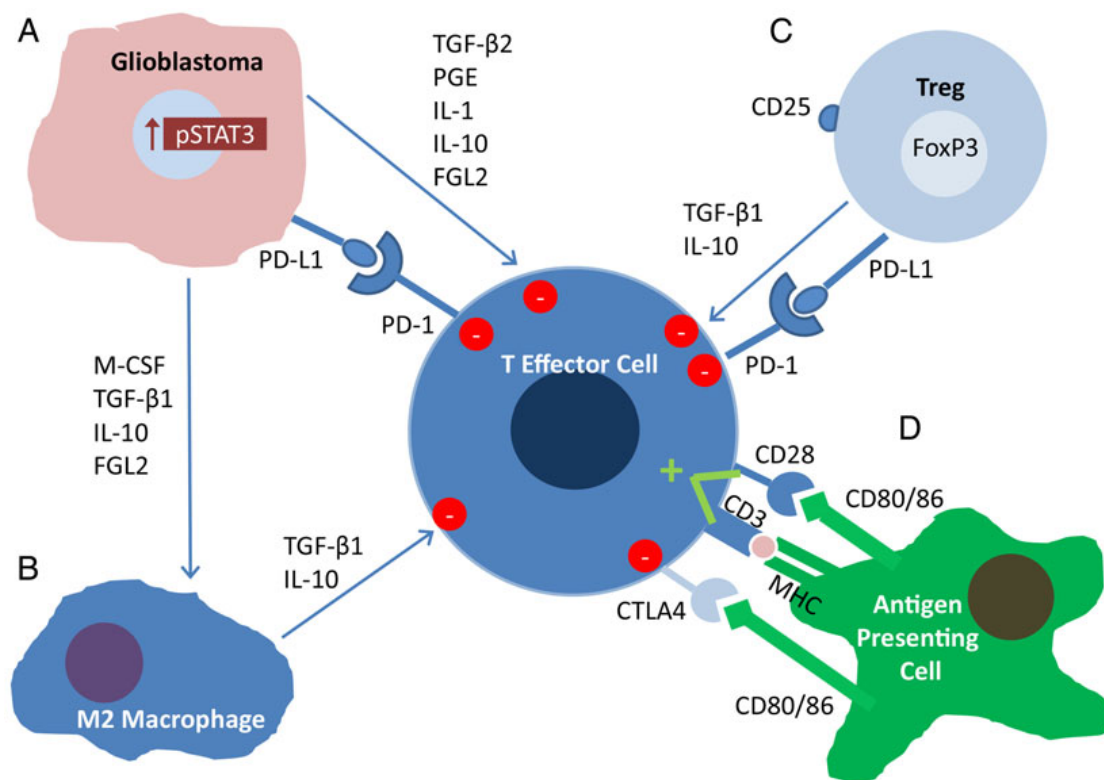
Tumors develop multiple mechanisms to maintain an immunosuppressive microenvironment and evade immune eradication including regulation of immune cells, chemokines, and immunosuppressing cytokines, as well as pathways modulating and decreasing immune function, known as immune checkpoints.¹⁵ This applies to gliomas too, an several mechanisms of immunosuppression have been described in these tumors with a focus on those utilized in the setting of glioblastoma.¹⁶

4.2.2 Mechanisms of glioma immune escape

Human gliomas, in particular, glioblastoma, have multiple operational mechanisms to prevent immune detection and eradication (Figure 3).¹⁶ They can trigger trafficking of regulatory T-cells (Tregs) to the tumor microenvironment or express immune checkpoints such as cytotoxic T-lymphocyte-associated protein 4 (CTLA4), a surface receptor that induces activated effector T-cell anergy, or programmed cell death protein 1 (PD-1) that, in binding with its ligand, programmed death ligand 1 (PD-L1), provides another signal to suppress activated T-cells. Also, many secreted cytokines in the glioblastoma microenvironment have been discovered, all of which have some varying level of effect on the immune response to glioblastoma. For example, tumor growth factor beta (TGF β) 1 and 2, and interleukins 1 and 10 (IL-1 and IL-10) that suppress effector lymphocyte activity. Furthermore, colony stimulating factor 1 (CSF-1), produced by gliomas, has been shown to polarize the macrophage infiltrate from an M1 phenotype, associated with a pro-inflammatory state, to a glioma-supportive M2 phenotype, which is associated with an anti-inflammatory state and enhances immunosuppression.^{41,42}

Figure 3. Immunosuppression in the glioblastoma microenvironment. **A**, Partially driven by increased STAT3 expression, glioblastoma cells secrete immunosuppressive factors such as TGF β -2, PGE, IL-1, IL-10, FGL2, all of which suppress the activity of effector cells. PD-L1

expressed on its surface also engages PD-1 to suppress effector activity. CSF-1, TGF β -1 and IL-10 skew tumor-associated macrophages to the immunosuppressive M2 phenotype. **B**, M2 macrophages secrete TGF β -1 and IL-10, suppressing effector cells further. **C**, Regulatory T-cells secrete TGF β -1 and IL-10 as well, further suppressing immune reactivity, while also expressing PD-L1. **D**, Antigen is presented to T-cells by APCs within an MHC molecule, but a costimulatory signal from CD80/86 to CD28 is required for activation. CD80/86 can also suppress activity by engaging the CTLA4 receptor on the activated T-cell.



From: Nduom EK, Weller M, Heimberger AB. Immunosuppressive mechanisms in glioblastoma. *Neuro Oncol* 2015;17(suppl.7): vii9-vii14.

Abbreviations: APCs, antigen presenting cells; CSF, colony stimulating factor; CTLA4, cytotoxic T-lymphocyte-associated protein 4; FGL2, fibrinogen-like protein 2; IL-1, interleukin 1; IL-10 interleukin 10; MHC, major histocompatibility complex; PD-1, programmed cell death protein 1; PD-L1, programmed death ligand 1; PGE, prostaglandin E; STAT3; signal transducer and activator of transcription 3; TGF β , tumor growth factor beta.

For this doctoral thesis, we focused our research on investigating whether canine gliomas model expression of Tregs and the PD-1-PD-L1 immune checkpoint, two of the most studied immunomodulating pathways in human disease, as mechanisms of immune evasion.

4.2.3 Regulatory T-cells

Regulatory T-cells are a subtype of T-lymphocytes with CD4⁺/CD25⁺/FOXP3⁺ immunophenotype. The activity of Tregs is associated with the nuclear expression of forkhead box P3 (FOXP3), a member of the forkhead/winged-helix family of transcriptional regulators that is involved in Tregs development and function.⁴³⁻⁴⁵

The main role of Tregs is to suppress effector T-cells and APCs activity.^{46,47} Therefore, they are essential to maintain self-tolerance and immune system homeostasis.⁴⁷ The association between Tregs and cancer has been widely documented and an increment in the number of systemic and intratumoral Tregs is correlated with an increased immunosuppressive state and decreased antitumor immune response in many affected patients.^{43,44,46,48} Regulatory T-cells hyperactivity and expansion results in effector T-cell inhibition, contributing to a tumor immunosuppressive microenvironment. This has been correlated with glioma development in both murine models and human patients.⁴⁹

In healthy humans, Tregs represent approximately 5-15% of the total circulating CD4⁺ T-lymphocytes; this fraction increases up to 40-60% in glioma patients, with the subsequent reduction in conventional CD4⁺ and CD8⁺ T-cells.^{49,50} Additionally, there is selective accumulation of Tregs in the tumor microenvironment, which seems directed by tumor cytokines secretion and results in tumor immune tolerance.^{47,51} An increased proportion of Tregs within the usually recognized T-cell infiltrate in human gliomas correlates positively with a higher tumor grade and, although expression of FOXP3⁺ Tregs seems higher in astrocytic than oligodendroglial tumors, increased proportion of these cells infiltrate has a negative correlation with survival in all glioma subtypes.^{49,52,53} Actually, accumulation of CD4⁺/CD25⁺/FOXP3⁺ Tregs is one of the hallmark features of human glioblastoma and several approaches to therapeutically target these cells are currently under study.^{47,51}

However, despite several targeted immunotherapies showing promise in preclinical studies

with murine models of glioma, no meaningful clinical responses have been obtained in human patients.^{18,47}

Studies evaluating Tregs and tumor immune evasion in dogs are scarce; however, increased CD4⁺/CD25⁺/FOXP3⁺ Tregs proportion has been observed in peripheral blood, adjacent lymphnodes and intratumorally in a series of neoplastic diseases.^{45,54} In canine oral malignant melanoma, an increment of CD4⁺/CD25⁺/FOXP3⁺ Tregs in peripheral blood has been correlated with increased malignancy and decreased percentage of cytotoxic T-cells.⁵⁵ Moreover, the presence of metastatic disease has been associated with increased percentage of CD4⁺/CD25⁺/FOXP3⁺ Tregs in peripheral blood in several types of cancer.^{45,55} Finally, immunohistochemical study of FOXP3⁺ Tregs in canine mammary carcinoma has demonstrated an association of abundant Treg cells with high histological grade and lymphatic invasion.⁵⁶ The numbers of Tregs infiltrating intratumoral areas markedly increased in tumors with poor prognostic factors, such as high histological grade, lymphatic invasion, and necrosis. These findings suggested that Tregs play a role in canine mammary carcinoma progression, and that they might represent a prognostic factor as well as a potential therapeutic target.

FOXP3 is considered the most reliable marker to identify Tregs phenotype *in vivo* and studies on its expression in canine gliomas were lacking.^{50,56,57} Thus, for the second study included in this thesis, we proceeded to immunohistochemically characterize the tumoral Treg infiltrate in dogs with glioma to assess for associations with tumor type and grade and compare our observations with the human counterpart.

4.2.4 PD-1-PD-L1 immune checkpoint

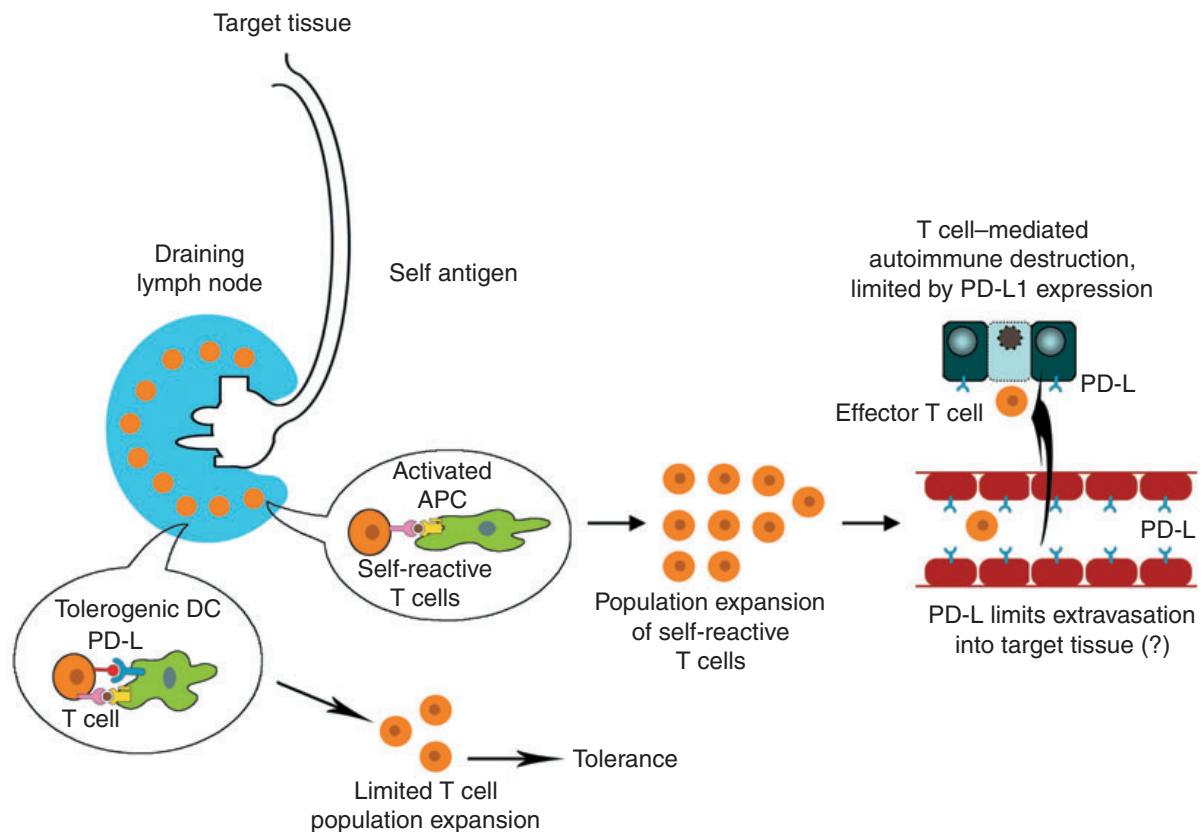
PD-1 and its ligand PD-L1 play a pivotal role in the ability of TCs to evade the host's immune system.⁵⁸ PD-1 (also called CD279) is a transmembrane receptor that functions as a

major negative immune regulator, controlling T-cell activation, T-cell exhaustion, T-cell tolerance, and resolution of inflammation.⁵⁸⁻⁶¹ PD-1 binds to two ligands that differ in their expression patterns, with expression of PD-L2 being much more restricted than PD-L1 expression.⁶⁰⁻⁶² PD-L1 (also named B7-H1 or CD274) is expressed on T-cells, B-cells, monocytes, dendritic cells (DCs), and macrophages in addition to a wide variety of non-hematopoietic cell types, including vascular endothelial cells, epithelial cells, muscle cells, hepatocytes, pancreatic islet cells and astrocytes in the brain, as well as at sites of immune privilege, including the placenta and the eye.^{63,64}

The PD-1-PD-L pathway acts as an immune checkpoint to control autoimmunity.⁶³ PD-L proteins on tolerogenic DCs can induce T-cell tolerance limiting the T-cell population expansion. PD-L1 is constitutively expressed on APCs and T-cells and is further upregulated by proinflammatory cytokines. PD-1 is upregulated on T-cells after they are activated. After initial T-cell activation, PD-1-PD-L interactions can trigger self-reactive T-cell functional exhaustion, limiting proliferation and cytokine production. Effector functions of self-reactive T-cells that migrate to the target tissue may be limited too by PD-L1 expressed on non-hematopoietic tissue cells such as vascular endothelial cells or perivascular astrocytes (*glia limitans interna*), restricting T-cell extravasation, and on target tissue, decreasing T-cell-mediated autoimmune destruction (Figure 4).

Tumor cells acquire mutations that can be targeted by lymphocytes and accumulating lines of evidence suggest that TCs evade host's immune attack by expressing physiological PD-1 ligands and stimulating PD-1 expression on the lymphocytes.⁶³⁻⁶⁵ Early studies have shown that PD-L1 is frequently expressed on human cancer cells. Many groups have reported separately that the level of PD-L1 and/or PD-1 expression significantly correlates with the poor prognosis of patients with various kinds of solid and haematological malignancies.⁶⁶⁻⁸⁴

Figure 4. The PD-1-PD-L pathway controls autoimmunity.



From: Sharpe AH, Wherry EJ, Ahmed R, et al. The function of programmed cell death 1 and its ligands in regulating autoimmunity and infection. *Nat immunol* 2007; 8:239-245.

Abbreviations: APC, antigen presenting cell; DC, dendritic cell; PD-L1, programmed death ligand 1.

In mice, ectopic expression of PD-L1 on a murine myeloma cell line inhibited the cytotoxic activity of killer T-cells through PD-1 ligation.⁸⁵ These observations led to the idea that PD-L1 on cancer cells triggers PD-1 on the attacking T-cells, prevents their activation, and contributes to the induction of cancer immune tolerance. Researchers successfully confirmed this hypothesis by therapeutic administration of mice bearing TC lines with anti-PD-1 and/or anti-PD-L1 antibodies.^{85,86} In 2012, data from a large-scale clinical study (~300 patients) was reported, demonstrating that monotherapy with PD-1 monoclonal antibodies produced objective durable responses in up to 25% patients with non-small-cell lung cancer, melanoma or renal-cell cancer.⁸⁷ The same group also demonstrated antibody-mediated blockade of PD-L1 induced both durable tumor regression (objective response rate of 6 to 17%) and

prolonged (≥ 24 weeks) disease stabilization in patients with metastatic disease in the aforementioned cancers.⁸⁸

Additionally, a subsequent study showed that murine and human melanomas frequently contain PD-1-expressing cancer cell subpopulations and demonstrated that melanoma cell-intrinsic PD-1 overexpression and melanoma-PD-1-PD-L1 interactions promote tumorigenesis.⁸⁹ Inhibition of melanoma-PD-1 in mice in that study reduced tumor growth independently of adaptive immunity, suggesting that blocking melanoma-PD-1 might contribute to the reported striking clinical efficacy of anti-PD-1 therapy.

The functions of the PD-1-PD-L1 axis in tumor-associated immunosuppression have also been investigated in human brain tumors. Subsequently, PD-L1 expression has been demonstrated in human gliomas with some studies showing higher expression in high-grade gliomas than in low-grade tumors.⁹⁰⁻⁹⁹ As with other malignancies, PD-L1 positive expression has been associated with poor prognosis in human gliomas,⁹⁷⁻⁹⁹ and the PD-1-PD-L1 pathway has been postulated as a potential immunotherapy target. In support of this, a recent study systematically evaluated the antitumor efficacy of murine antibodies targeting PD-1 and PD-L1 in an orthotopic, immunocompetent murine glioblastoma model, and long-term tumor-free survival following single-agent anti-PD-1 and anti-PD-L1 therapy was observed in 50% and 20% of treated animals, respectively.¹⁷

In dogs, only limited information on PD-1 and PD-L1 expression is available. Initial studies have shown that most canine tumors express PD-L1 and that the PD-1-PD-L1 pathway is associated with tumor immune regulation.^{100,101} In addition, PD-1 was highly expressed on tumor-infiltrating lymphocytes obtained from oral melanoma.¹⁰² More recently, in a study evaluating PD-L1 expression in several haematological malignancies, high endogenous expression was observed on canine B lymphoma cells and its inhibition by mitogen-activated protein kinase kinase 1/2 suggested a possible treatment strategy using targeted drugs which

could likely enhance anti-tumor immune response.¹⁰³ Another study assessed T-cell binding of monoclonal antibodies specific for canine PD-1, characterizing T-cell PD-1 expression in healthy dogs and demonstrating upregulated expression in dogs with cancer.¹⁰⁴ Functionally, PD-1 antibodies significantly enhanced T-cell activation, as assessed by proliferation and interferon-gamma (IFN- γ) production. These findings indicated that PD-1 antibodies have potential for use in cancer immunotherapy in dogs.

In view of the above and the lack of systematic studies on the expression of PD-L1 in canine gliomas, we aimed to characterize immunohistochemical expression of PD-L1 and its association with PD-1 expression in tumor-infiltrating lymphocytes (TILs) in canine gliomas of different types and grades as the final study of this doctoral thesis.

Overall, we hypothesized that 1) canine gliomas share remarkable epidemiologic, clinicopathologic and prognosis similarities with their human counterparts and thus, from a comparative neuro-oncology viewpoint, are the best spontaneous tumor model for translational studies; and 2) canine gliomas are able to induce a tolerant immune state through manipulation of the microenvironment and by modifying immune function through disruption of immunomodulating pathways in a similar fashion to human gliomas.

OBJECTIVES

5. OBJECTIVES

The main objective of this doctoral thesis research was to further validate canine glioma as an animal model for human glioma and, most particularly, as a model for immune evasion in the human counterpart. Ultimately, we aimed to support the use of canine gliomas in translational human studies, so targeted immunotherapies can be tested and developed.

The specific objectives of this doctoral thesis were:




1. To evaluate associations between the epidemiologic, clinicopathologic, imaging and outcome features of a large sample of canine gliomas and their histological type and grade, applying the new diagnostic classification for dogs.
2. To characterize the immunohistochemical expression of regulatory T-cells and the PD-1-PD-L1 immune checkpoint in canine gliomas.
3. To compare the above findings with corresponding observations in human gliomas.

MATERIALS, METHODS AND RESULTS

ARTICLE 1

STANDARD ARTICLE

Clinical features, diagnosis, and survival analysis of dogs with glioma

Roberto José-López^{1,2}  | Rodrigo Gutierrez-Quintana¹  | Cristian de la Fuente² | Edgar G. Manzanilla^{3,4} | Anna Suñol⁵ | Dolors Pi Castro^{2,6} | Sonia Añor²  | Daniel Sánchez-Masian⁷ | Francisco Fernández-Flores⁷ | Emanuele Ricci⁷ | Katia Marioni-Henry⁸ | Joan Mascort⁵ | Lara A. Matiassek⁹ | Kaspar Matiassek¹⁰ | Paul M. Brennan¹¹ | Martí Pumarola^{2,6}

¹School of Veterinary Medicine, College of Medical, Veterinary and Life Sciences, University of Glasgow, Glasgow, UK

²Department of Animal Medicine and Surgery, Veterinary Faculty, Universitat Autònoma de Barcelona, Barcelona, Spain

³School of Veterinary Medicine, University College Dublin, Dublin, Ireland

⁴TEAGASC, The Irish Food and Agriculture Authority, Cork, Ireland

⁵ARS Veterinaria, Barcelona, Spain

⁶Networking Research Center on Bioengineering, Biomaterials and Nanomedicine (CIBER-BBN), Universitat Autònoma de Barcelona, Barcelona, Spain

⁷Institute of Veterinary Science, University of Liverpool, Neston, UK

⁸Royal (Dick) School of Veterinary Studies and Roslin Institute, University of Edinburgh, Edinburgh, UK

⁹Tierklinik Haar, Haar, Germany

¹⁰Centre for Clinical Veterinary Medicine, Ludwig-Maximilians-Universitaet, Munich, Germany

¹¹Translational Neurosurgery, Centre for Clinical Brain Sciences, University of Edinburgh, Edinburgh, UK

Correspondence

Roberto José-López, School of Veterinary Medicine, University of Glasgow, Bearsden Road, Glasgow, G61 1QH, UK.
 Email: roberto.jose-lopez@glasgow.ac.uk

Present address

Anna Suñol, Royal (Dick) School of Veterinary Studies, University of Edinburgh, Edinburgh, UK

Dolors Pi Castro, Anicura Arvivet Hospital Veterinari, Barcelona, Spain

Daniel Sánchez-Masian, Anderson Moores Veterinary Specialists, Winchester, UK

Lara A. Matiassek, Anicura Small Animal Clinic, Babenhausen, Germany

Abstract

Background: Gliomas in dogs remain poorly understood.

Objectives: To characterize the clinicopathologic findings, diagnostic imaging features and survival of a large sample of dogs with glioma using the Comparative Brain Tumor Consortium diagnostic classification.

Animals: Ninety-one dogs with histopathological diagnosis of glioma.

Methods: Multicentric retrospective case series. Signalment, clinicopathologic findings, diagnostic imaging characteristics, treatment, and outcome were used. Tumors were reclassified according to the new canine glioma diagnostic scheme.

Results: No associations were found between clinicopathologic findings or survival and tumor type or grade. However, definitive treatments provided significantly ($P = .03$) improved median survival time (84 days; 95% confidence interval [CI], 45–190)

Abbreviations: CBTC, Comparative Brain Tumor Consortium; CE, contrast enhancement; CI, confidence interval; CNS, central nervous system; CSF, cerebrospinal fluid; CT, computed tomography; FLAIR, fluid-attenuation inversion recovery; GFAP, glial fibrillary acidic protein; GRE, gradient-recalled echo; HA, high-grade astrocytoma; HO, high-grade oligodendroglioma; HU, high-grade undefined glioma; LA, low-grade astrocytoma; LO, low-grade oligodendroglioma; MRI, magnetic resonance imaging; MST, median survival time; OR, odds ratio; WHO, World Health Organization.

This is an open access article under the terms of the Creative Commons Attribution-NonCommercial License, which permits use, distribution and reproduction in any medium, provided the original work is properly cited and is not used for commercial purposes.

© 2021 The Authors. *Journal of Veterinary Internal Medicine* published by Wiley Periodicals LLC on behalf of American College of Veterinary Internal Medicine.

Funding information

University of Glasgow, Small Animal Hospital
Fund Postgraduate Research Grant, Grant/
Award Number: 145973-02

compared to palliative treatment (26 days; 95% CI, 11-54). On magnetic resonance imaging (MRI), oligodendrogliomas were associated with smooth margins and T1-weighted hypointensity compared to astrocytomas (odds ratio [OR], 42.5; 95% CI, 2.42-744.97; $P = .04$; OR, 45.5; 95% CI, 5.78-333.33; $P < .001$, respectively) and undefined gliomas (OR, 84; 95% CI, 3.43-999.99; $P = .02$; OR, 32.3; 95% CI, 2.51-500.00; $P = .008$, respectively) and were more commonly in contact with the ventricles than astrocytomas (OR, 7.47; 95% CI, 1.03-53.95; $P = .049$). Tumor spread to neighboring brain structures was associated with high-grade glioma (OR, 6.02; 95% CI, 1.06-34.48; $P = .04$).

Conclusions and Clinical Importance: Dogs with gliomas have poor outcomes, but risk factors identified in survival analysis inform prognosis and the newly identified MRI characteristics could refine diagnosis of tumor type and grade.

KEYWORDS

astrocytoma, dog, magnetic resonance imaging, oligodendroglioma, prognosis, tumor grade, undefined glioma

1 | INTRODUCTION

The incidence of brain tumors in adult dogs is 2.8% to 4.5% and, although individual studies vary, gliomas represent 36% to 70% of primary brain tumors in dogs.¹⁻⁵ Consequently, glioma in dogs is increasingly recognized as a naturally occurring model for understanding human glioma. The benefits include the size and structure of the canine brain, the incidence of spontaneous gliomas, and the coexistence with an active immune system.^{6,7} Nevertheless, there are many gaps in knowledge related to the natural biology of glioma in dogs as well as its molecular characteristics.

Epidemiologic data on glioma in dogs indicates a median age at diagnosis of 8 years, a male predilection (incidence ratio of 1.53 for males/females), and predominant lesion location within the fronto-olfactory, temporal, and parietal lobes of the brain.^{3,5,8} Over 50% of all gliomas in dogs occur in certain brachycephalic breeds^{3,5,8-10} and the Boston Terrier, Bulldog, and Boxer breeds have a higher prevalence of oligodendroglioma.⁸ On magnetic resonance imaging (MRI), intracranial gliomas in dogs are typically described as intra-axial, T1-weighted iso- to hypointense and T2-weighted iso- to hyperintense mass lesions with varying degrees of contrast enhancement (CE).^{5,11-14} Oligodendrogliomas are reported to contact the brain surface more commonly, whereas astrocytomas have been associated with more peritumoral edema, lack of ventricular distortion, and iso- to hyperintense T1-weighted signal.^{13,14} Tumors with mild to no CE, absent cystic structures, and tumor location other than the thalamo-capsular region have been associated with low-grade gliomas.¹⁴ Grade and type of histologically confirmed intracranial gliomas in dogs using these MRI features found an accuracy of 53.3% and 60% for predicted tumor grade and type, respectively.¹⁵

Standard veterinary practice in recent years has been to use the 2007 World Health Organization (WHO) human glioma classification to grade canine gliomas.^{16,17} This classified and graded human tumors based on analysis of clinical outcome and survival relative to specific pathologic

criteria. However, little is known about whether histologic tumor type and grade correlates with biologic behavior in canine gliomas. To date, information on tumor progression and outcome after treatment is anecdotal.¹⁸ Since 2007, advances in molecular genetics and biology have enhanced our understanding and subclassification of human gliomas, which led in 2016 to an updated edition of the WHO brain tumor classification.¹⁹ Subsequently, the Comparative Brain Tumor Consortium (CBTC) of the National Cancer Institute proposed a revised diagnostic classification of canine gliomas.⁸ Their aim was to provide an updated canine-specific scheme for clinical and molecular data to be added into a morphologic diagnosis, to assist with prediction of tumor behavior.

The aims of this study were to enhance this revised diagnostic classification by further characterizing the epidemiologic, clinicopathologic, diagnostic imaging, and outcome features of gliomas in dogs in a large sample. We assess the relationship between these features and tumor histological type and grade, based on the new diagnostic classification for dogs.

2 | MATERIALS AND METHODS

This study was approved by the Research Ethics Committee of the School of Veterinary Medicine of the University of Glasgow (Ref33a/17). The clinical records of dogs presented to 7 European referral centers between 2005 and 2018 were retrospectively analyzed. Dogs were included if they had a histopathologic diagnosis of glioma. Samples were obtained by means of surgical biopsy or at necropsy within 24 hours from death.

2.1 | Morphologic diagnosis

All samples were fixed in 10% neutral buffered formalin. Fixation times varied because of the multicentric and retrospective nature of the study;

however, this was always <5 days. After fixation, transverse sections of the brain or spinal cord were made and samples including the tumor area were routinely processed. Morphologic evaluation was performed on 4 µm paraffin-embedded sections stained with hematoxylin and eosin.

All gliomas were reviewed and classified by a board-certified pathologist (M. Pumarola) using the CBTC diagnostic scheme.⁸ When available, samples were further evaluated by immunohistochemistry for glial fibrillary acidic protein (GFAP) (Z0334; Dako; Glostrup; Denmark; 30-minute incubation at a dilution of 1:500), and Olig2 protein (AB 9610; Merck Millipore; Darmstadt; Germany; 30-minute incubation at a dilution of 1:100). For both markers, slides were scored on a scale of 0 to 4 as previously described.²⁰ Immunohistochemical characterization of 16 cases (dogs 10-20, 76-80; Supplementary Table 1) was reported previously.²⁰⁻²²

Histopathology reports and available tissue were reviewed for features of infiltrative spread consisting of invasion of adjacent central nervous system (CNS) regions as well as presence of secondary structures of Scherer, including perineuronal and perivascular satellitosis, subpial and subependymal tumor cell condensation, and invasion along white matter tracts.^{8,17,19,23} Extension through the corpus callosum into the contralateral hemisphere was documented as butterfly glioma.^{19,24} Gliomatosis cerebri growth pattern was recorded as recently defined.^{19,25}

Evidence of extension into the subarachnoid space (tumor spread through the pia mater with or without proliferation within the leptomeninges), ventricular invasion or drop metastases was noted.²⁶⁻²⁹ Penetration of the bone²¹ or infiltration of other non-CNS structures were also recorded. Finally, postmortem examination reports were reviewed for the presence of metastases elsewhere in the body.⁵

2.2 | Anatomic location of tumors

Gliomas were allocated into 1 of 4 main anatomic locations: hemispheric (cerebral hemispheres including deep gray matter), diencephalon, infratentorial, and spinal cord. Within these regions, the specific location of the largest portion of the tumor was recorded as fronto-olfactory, parietal lobe (including the adjacent corpus callosum), temporal lobe (including the piriform lobe), occipital lobe, ventricles, diencephalon, cerebellum, brainstem, and spinal cord segment corresponding with the overlying vertebrae.^{8,14,30} Furthermore, any degree of involvement of the diencephalon was noted.^{5,13}

2.3 | Dog demographics, clinicopathologic data, and staging

Demographic data (age, sex, and breed), presenting clinical signs, and physical and neurologic examination findings were recorded for each case. Clinical signs were annotated as summarized on Table 1.

Cerebrospinal fluid (CSF) analysis results, when available before treatment, were noted.

Reports of cases that underwent diagnostic imaging of the thorax, abdomen, or both for staging were reviewed for the presence of metastases.⁵

2.4 | Magnetic resonance imaging

Magnetic resonance imaging studies were performed with scanners of variable field strength (0.2-1.5 T). All studies included T2-weighted sagittal and transverse sequences and both, precontrast and postcontrast (gadopentate dimeglumine; Magnevist, Bayer Schering Pharma AG, Berlin, Germany) T1-weighted transverse sequences. When available, additional fluid-attenuation inversion recovery (FLAIR) dorsal or transverse sequences, gradient-recalled echo (GRE) transverse sequences, T2-weighted dorsal views, and precontrast and postcontrast T1-weighted dorsal and sagittal views were evaluated.

Magnetic resonance imaging features were independently evaluated by 2 board-certified neurologists (R. Gutierrez-Quintana, R. José-López) and classified based on the consensus opinion. Both observers were aware that lesions were gliomas but were blinded to the histopathologic type and grade and provided with standardized grading instructions. The MRIs were classified on the basis of 20 criteria adapted from a recent study.¹⁴ For each criterion, observers chose 1 option from those specified in Table 2. Spinal cord located gliomas were excluded from the analysis.

Observers were provided with specific instructions for some MRI criteria. If the tumor margins were clear, they were divided into smooth and irregular whereas if they were indistinct, they were considered poorly defined. Each glioma was classified on the basis of signal intensity relative to cortical gray matter and signal uniformity on T1-weighted, T2-weighted, and FLAIR images. Interpretation was based on the majority of the tumor area. Similarly, on T1-weighted postcontrast images, degree of CE was evaluated and classified based on the pattern of the largest portion of the tumor. Peritumoral edema was graded and cystic structures noted according to a previous study.³¹ Subarachnoid CSF signal loss, midline shift, ventricular distortion, brain herniations, and syringohydromyelia were all categorized

TABLE 1 Summary of clinical signs annotation

Clinical finding	Descriptions used in this study (total number of cases for each criterion)
Seizures	None (35); isolated (32); cluster seizures (24)
Mentation	Normal (28); lethargy/disorientation (14); depression (48)
Behavior	Normal (44); behavioral abnormalities (46)
Posture	Normal (69); head tilt (11); head turn (2); low-head carriage (6); kyphosis (1)
Gait	Normal (37); ataxia, paresis, or both (53)
Proprioception	Normal (23); deficits (67)
Vision	Normal (41); unilateral deficits (34); bilateral deficits (15)
Facial/nasal sensation	Normal (81); deficits (9)
Brainstem signs	Yes (facial asymmetry (3); abnormal eye movements/position (10); anisocoria (3); pupillary light reflex deficits (3)); no (75)
Hyperesthesia	Yes (14); no (76)

TABLE 2 Standardized MRI interpretation criteria for intracranial gliomas included in this study (n = 74)

MRI criteria	Descriptions used in this study (total number of cases for each criterion)
Origin	Intra-axial (72); extra-axial (2)
Margins	Poorly defined (25); smooth (44); irregular (5)
Shape	Spherical or ovoid/elongate (47); amorphous (24); lobulated (3)
Signal	
T2-intensity	Hypointense (3); isointense (0); hyperintense (71)
T2-uniformity	Homogeneous (22); heterogeneous (52)
T1-intensity	Hypointense (60); isointense (14); hyperintense (0)
T1-uniformity	Homogeneous (15); heterogeneous (59)
FLAIR intensity	Hypointense (11); isointense (0); hyperintense (63)
FLAIR uniformity	Homogeneous (16); heterogeneous (58)
GRE signal voids ^a	None (25); single (6); multiple (6); diffuse (majority of tumor) (4)
Degree of CE	None (19); mild (20); moderate (19); severe (16)
CE pattern	None (19); focal (1); nonuniform (28); uniform (entire tumor) (8); partial ring (7); complete ring (11)
Cystic structures	None (44); cyst (16); ITFs (14)
Peritumoral edema	None (7); peritumoral (≤ 10 mm beyond tumor margins) (47); extensive (> 10 mm beyond tumor margins) (20)
Mass effect	None (3); mild (16); moderate (29); severe (26)
Subarachnoid CSF signal loss	Yes (63); no (11)
Midline shift	Yes (54); no (20)
Ventricular distortion	Yes (68); no (6)
Brain herniations ^b	None (31); subfalcine (2); transtentorial (24); foramen magnum (19)
Syringohydromyelia	Yes (24); no (50)
Spread	
Adjacent brain structures	None (22); butterfly glioma (3); gliomatosis cerebri growth pattern (5); freehand description (44)
Brain surface contact	Yes (56); no (18)
Leptomeningeal CE	Yes (25); no (49)
Ventricular contact	Yes (62); no (12)
CSF pathways ^b	None (26); subarachnoid space (25); ventricular invasion (33); drop metastases (8)
Other structures ^b	None (60); penetration of bone (9); other (freehand description) (6)

Abbreviations: CE, contrast enhancement; CSF, cerebrospinal fluid; FLAIR, fluid-attenuation inversion recovery; GRE, gradient-recalled echo; ITFs, intratumoral accumulations of fluid; MRI, magnetic resonance imaging; T1, T1-weighted; T2, T2-weighted.

^aGRE images were only obtained in 41 gliomas.

^bMore than 1 criterion could be observed for a single case.

independently and subsequently considered for mass effect grading.^{14,32}

Additionally, brain MRIs were evaluated for features of tumor spread, categorized as specified in Table 2. For spread from the anatomic location containing the largest fraction of the tumor to neighboring brain structures or distant foci, observers were instructed to provide a freehand description of the anatomic region/s tumors were extending to. Tumor growth patterns consistent with butterfly glioma or gliomatosis cerebri were recorded.^{19,24,25} Leptomeningeal CE with associated FLAIR hyperintensity within the sulci was recorded as well.^{25,26} When present, this was also annotated as extension into the subarachnoid space as was tumor invasion of the subarachnoid space without associated meningeal MRI changes. Spread along the CSF pathways including ventricular invasion and drop metastases was noted too.²⁶⁻²⁹ Similarly, propagation to non-CNS structures was recorded.

Finally, based on the observations of published MRI predictors of canine glioma type and grade (summarized in Supplementary Table 2), investigators predicted the grade (high or low) and type (astrocytoma or oligodendroglioma) for each tumor.¹³⁻¹⁵ Accuracy for predicting the lesion grade and type on MRI compared to histopathologic diagnosis was performed using the consensus opinion of both observers.

2.5 | Treatment and outcome

Treatment groups were defined as definitive if specific treatment modalities including surgical resection, radiotherapy, or chemotherapy were used in any combination, and palliative if corticosteroid, anti-epileptic, or analgesic medications were the only therapeutic

interventions.³³ Survival was defined for all cases from time of MRI diagnosis, and only for cases with survival times >1 day to exclude animals euthanized at the time of diagnosis.³³

2.6 | Statistical analyses

All analyses were carried out using SAS 9.4 (SAS Institute Inc, Cary, North Carolina) and R 4.0.2 (R Foundation for Statistical Computing, Vienna, Austria). When not specified, alpha level for determination of significance was .05 and trends were discussed for alpha .1.

Interobserver agreement for each MRI criterion was assessed using Cohen's kappa. Values of 0.81-1.00 were considered to indicate excellent agreement; 0.61-0.80, good agreement; 0.41-0.60, moderate agreement; 0.21-0.40, fair agreement; 0.01-0.20, poor agreement, and 0.00, chance agreement.

Agreement between histopathologic diagnosis (reference test) of type and grade and classification of glioma type and grade following previously published MRI criteria^{13,14} was analyzed using specificity and sensitivity for detection of astrocytoma for type and high for grade.

Associations between tumor location, patient demographics, clinical signs, MRI criteria, and tumor type and grade were performed in 2 stages, first univariate analysis, and then multivariable analysis. Univariate analysis was done using contingency tables and Fisher's exact test. Variables with *P* value <.25 were used for the multivariable model. For multivariable analysis, forward stepwise logistic regression was used. A *P*-value to enter the model of <.20 and to remain of <.05 was used. Final logistic regression model fit was evaluated using the Hosmer-Lemeshow goodness-of-fit test.

Associations between all risk factors and hazard of death was performed for dogs with survival of >1 day and available MRI for revision using univariable followed by multivariable Cox proportional hazard modeling. All risk factors with a *P* value <.25 in the univariate analysis were used in the multivariable analysis. A forward stepwise manual approach was used to build the multivariable model. Risk factors were kept in the final model after assessing for confounding with a *P* value of .05. The proportional hazards assumption was tested by visual inspection of log-minus-log survival plots and statistical assessment of residuals.

3 | RESULTS

3.1 | Morphologic diagnosis

Ninety-one dogs with histopathological diagnosis of glioma were identified. Ten cases were identified by surgical biopsy and 81 cases were diagnosed at necropsy. Of these, 68.1% were classified as oligodendroglioma (52 high-grade and 10 low-grade), 18.7% as astrocytoma (16 high-grade and 1 low-grade), and 13.2% as undefined glioma (12, all high-grade).

Immunohistochemistry results for GFAP were available for 60 cases with a mean immunoreactivity score of 0.32/4 (range, 0-2/4) on 35 oligodendrogliomas, 1.71/4 (range, 0-4/4) on 14 astrocytomas, and 1.55/4 (range, 0-4/4) on 11 high-grade undefined gliomas (HUs). Olig2 immunoreactivity results were available for 57 cases with mean scores of 2.67/4 (range, 1-4/4) on 36 oligodendrogliomas, 1.85/4 (range, 0-4/4) on 13 astrocytomas, and 2/4 (range, 1-3/4) on 8 HUs.

Information on histopathologically confirmed infiltrative spread was available for 75 cases. Invasion of neighboring brain structures was observed in 51/75 cases including 35 oligodendrogliomas (32 high-grade and 3 low-grade), 10 high-grade astrocytomas (HAs), and 6 HUs. Secondary structures of Scherer were noted in 28/75 cases: 19 oligodendrogliomas (18 high-grade and 1 low-grade), 6 HAs, and 3 HUs. These consisted of perivascular satellitosis and subpial tumor cell condensation (9 cases, respectively), and perineuronal satellitosis, subependymal tumor cell condensation, and white matter tract invasion (7 cases, respectively) in any combination. Three high-grade oligodendrogliomas (HOs) presented as butterfly gliomas (Figure 1A-C) whereas gliomatosis cerebri growth pattern was seen in 3 HAs and 1 HU.

Ventricular invasion was confirmed in 24/75 cases (18 HOs, 4 HAs, 1 HU, and the only low-grade astrocytoma [LA]). Subarachnoid spread with or without proliferation within the leptomeninges was noted in 22/75 gliomas (16 HOs, 4 HAs, and 2 HUs). Drop metastases were found in 9 HOs and 1 HA. Additionally, 1 HA presented 2 independent foci (Figure 1D-G).

Information on spread to non-CNS structures and extraneural metastases was available in 50 cases. Penetration of the cribriform plate and infiltration of the ethmoturbinates and nasal mucosa was confirmed in 3 HOs whereas osteolytic calvarial invasion was noted on a previously reported HA.²¹ Pituitary gland infiltration (Figure 1H-J) was found in 1 of each of HA, HO, and low-grade oligodendroglioma (LO). No metastases were found elsewhere in the body.

3.2 | Location of gliomas within the CNS

There were 69/91 (76%) hemispheric gliomas, 14/91 (15%) diencephalic, 5/91 (6%) infratentorial, and 3/91 (3%) in the spinal cord. Geographic distribution within the brain of type and grade of glioma is summarized in Figure 2A. Within the cerebral hemispheres (Figure 2B), 29/69 tumors (42%) had a fronto-olfactory location, 25/69 (36%) were in the temporal lobe, 11/69 (16%) in the parietal lobe, and 4/69 (6%) were primarily intraventricular. All of the latter were located within the lateral ventricles and consisted of HOs. In addition to the 14 primarily diencephalic gliomas, another 16 gliomas involved the diencephalon to some extent (diencephalic involvement by tumor type and grade is presented in Table 3). Infratentorial gliomas included 4 HAs (brainstem, 3; cerebellum, 1) and 1 HO (brainstem). Spinal cord gliomas consisted of 2 HOs located at the level of C1 and T11 vertebrae, respectively, and 1 LO extending from C7 to T5 vertebral bodies.

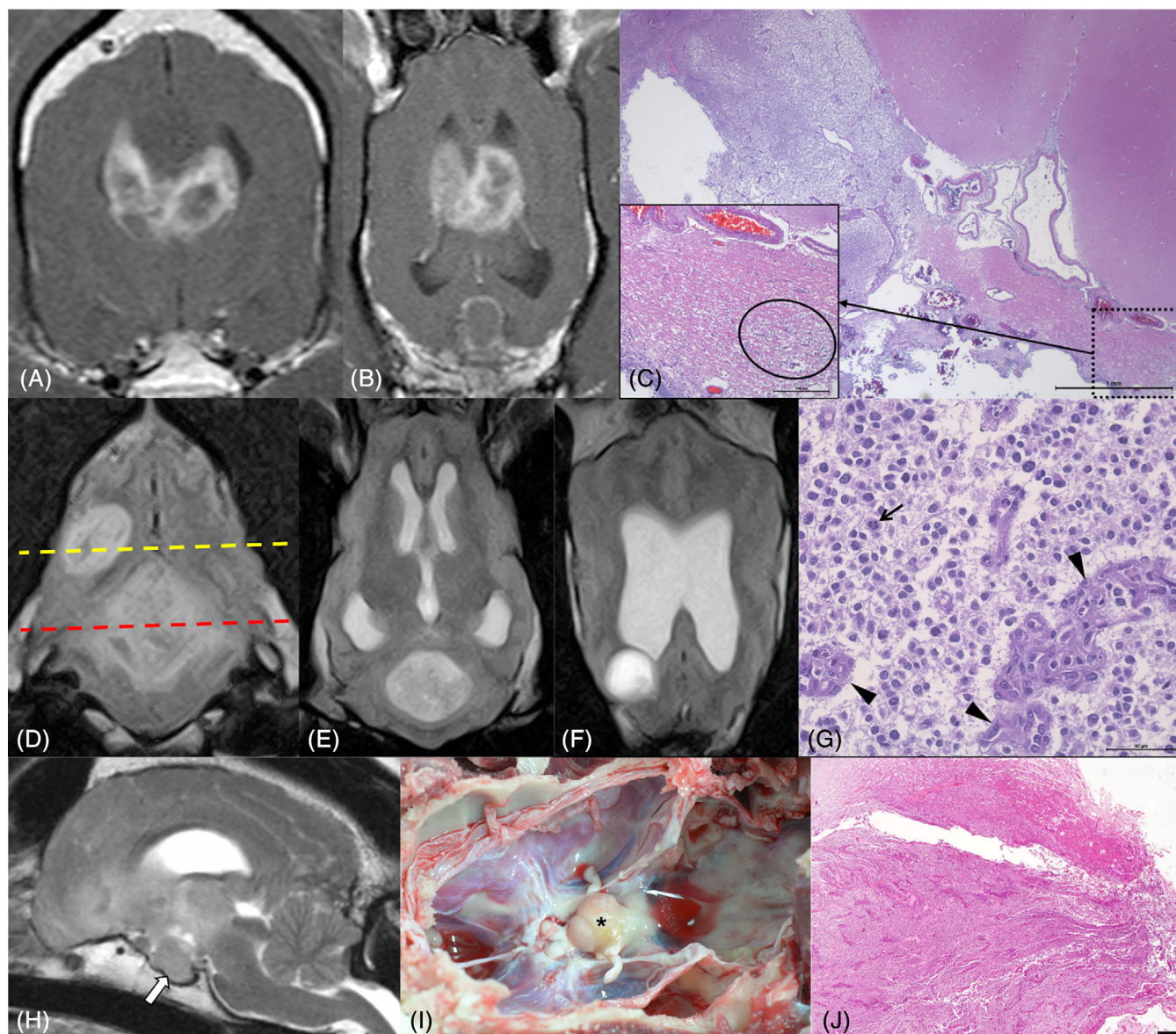


FIGURE 1 Transverse (A) and dorsal (B) T1-weighted postcontrast magnetic resonance (MR) images of a ring-enhancing high-grade oligodendroglioma (HO) showing the typical features of butterfly glioma with extensive involvement of the corpus callosum leading to bihemispheric spread. Photomicrograph of the same HO as in (A) and (B) occupying the lumen of the lateral ventricle and infiltrating the cingulate gyrus (top of the figure) and the corpus callosum (bottom of the figure) (C). The inset shows neoplastic cells invading the corpus callosum towards the contralateral ventricle (the oval represents an area of higher neoplastic cell density). HE stain. Scale bar = 1 mm (inset 200 μ m). Transverse fluid-attenuation inversion recovery MR image at the level of the tentorium cerebelli demonstrating 2 heterogeneously hyperintense independent foci of a high-grade astrocytoma (D). Dorsal T2-weighted images obtained at the level of the red (E) and the yellow (F) dotted lines show the largest tumor in the cerebellum and a second focus in the right occipital lobe, respectively. Both foci were characterized by large sized anisokaryotic cell populations with scant cytoplasm growing in a solid pattern (G). A mitotic figure is present (arrow) as well as glomeruloid-like vessels (arrowheads). HE stain. Scale bar = 50 μ m. Midsagittal T2-weighted images of a poorly defined, heterogeneously hyperintense HO extending from the fronto-olfactory area to the diencephalon (H). Note the enlarged and hyperintense pituitary gland (arrow). Severe nonuniform enhancement of the pituitary gland was noted on T1-weighted postcontrast images whereas this was mild for the intra-axial tumor. Dorsal view of the unfixed base of the neurocranium in the same dog as (H) demonstrating an expanded pituitary gland (asterisk) (I). Photomicrograph of the pituitary gland of the dog in (H) and (I) revealing severe infiltration of the hypophyseal lobules by the neoplastic cell population (J). HE stain. Scale bar = 500 μ m

3.3 | Demographics, clinicopathologic features, and staging

Median age of dogs at diagnosis of glioma was 7.9 years (range, 1.5-13.0 years). There were 40/91 (44%) intact males, 11/91 (12%)

castrated males, 21/91 (23%) intact females, and 19/91 (21%) spayed females. The ratio for all males/females was 1.28, and 1.9 for intact males/females. Seventy-eight percent of the cases (71/91) belonged to brachycephalic dog breeds including 40/91 (44%) Boxers, 26/91 (29%) Bulldogs (French, 23; English, 1; and not otherwise specified, 2),

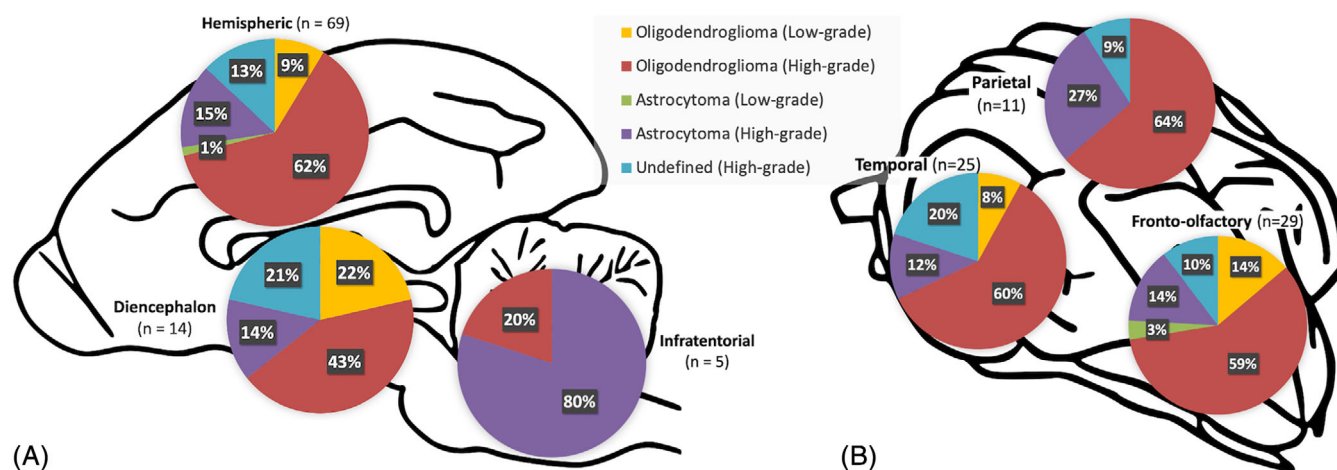


FIGURE 2 Anatomic distribution of intracranial gliomas in 88 dogs classified according to the Comparative Brain Tumor Consortium diagnostic scheme (A). Specific location of 65 hemispheric gliomas (B). Note there were an additional 4 high-grade oligodendrogliomas primarily located within the lateral ventricles

3/91 (3%) Dogues de Bordeaux, and 2/91 (2%) Staffordshire Bull Terriers. The breeds of the remaining 22% of dogs are captured on Supplementary Table 1.

Time between onset of clinical signs and presentation ranged between <1 and 180 days (median 14 days) for all gliomas. The main presenting complaint in 62% (56/91) of the cases was seizures either isolated (32 dogs) or in clusters (24). Of these, 5/56 (9%) presented with a normal interictal neurologic examination and seizures as the only clinical sign. In addition to seizures, the most common presenting neurologic signs included proprioceptive deficits (67/90 cases, 74%), mentation changes (62/90 cases, 69%), gait abnormalities (53/90 cases, 59%), visual deficits (49/90 cases, 54%), and behavioral changes (46/90 cases, 51%). The remaining clinical signs are outlined in Table 1 and most common neurologic signs by tumor type and grade are presented in Table 3.

Cerebrospinal fluid was collected in 23 dogs. The results are summarized in Table 4. These were within reference limits in 31.6% (6/19), consistent with albuminocytologic dissociation in 36.8% (7/19) and with an elevated total nucleated cell count in 34.8% (8/23) cases. Mixed cell pleocytosis was the most common cytologic abnormality. No neoplastic cells were detected. Thoracic radiographs (40 cases) and CT (8), as well as abdominal ultrasonography (40 cases) or CT (3), failed to reveal abnormalities suggestive of metastatic disease.

3.4 | Magnetic resonance imaging

Magnetic resonance imaging was obtained for diagnosis in 87 dogs. The remaining 4 dogs were euthanized on presentation at their owners request in view of the clinical suspicion and severity of clinical signs. The MRI studies of 77 cases were available for review, including 74 brain and 3 spinal cord gliomas. Median time between MRI and postmortem examination was 1 day (range, <1-1104 days). All brain studies included FLAIR sequences whereas GRE images were attained on 41.

Magnetic resonance imaging features of spinal cord gliomas consisted of T2-weighted hyperintense, T1-weighted isointense focal, or diffuse mass lesions with none to severe CE located intramedullary except for the HO at C1 that appeared intradural extramedullary (Figures 3A-C).

The MRI features of intracranial gliomas are captured in Table 2. All intracranial gliomas in this study were intra-axial except for a HA (Figures 3D-F) and a previously reported case of leptomeningeal oligodendrogliomatosis reclassified as HO.²² Spread to adjacent brain structures was detected in 52/74 (70%) gliomas and further characterized as butterfly glioma in 3 HOs and as gliomatosis cerebri growth pattern in 4 HAs and 1 HU. Extension outside the CNS including penetration into the bone and invasion of the pituitary gland was suspected in 9/74 and 6/74 gliomas, respectively. The MRI findings by tumor type and grade are presented in Table 5.

Supplementary Figure 1 shows the interobserver agreement for all the MRI variables studied. Kappa values were excellent or good in most cases except for predicted tumor grade and spread to bone structures that showed moderate agreement, and poor for predicted tumor type.

Evaluation of previously published criteria^{13,14} for prediction of intracranial glioma type and grade demonstrated a sensitivity of 58.8% (95% confidence interval [CI], 35.4%-82.2%) and specificity of 68.8% (95% CI, 55.6%-81.8%) for the diagnosis of astrocytoma, and a sensitivity of 67.2% (95% CI, 55.2%-79.3%) and specificity 57.1% (95% CI, 20.5%-93.8%) for the diagnosis of high-grade.

3.5 | Associations among tumor location, demographics, clinical signs, MRI features, and glioma type and grade

The preliminary univariate analysis (Tables 3 and 5) showed associations between glioma type and presence of facial or nasal sensation

TABLE 3 Univariate analysis of tumor location, patient demographics, and clinical features of 91 gliomas based on type and grade. Table shows percentage of each criterion within each type or grade (total number of cases for each criterion)

	Type				Grade		
	Astrocytoma (n = 17)	Oligodendroglioma (n = 62)	Undefined (n = 12)	P value	High (n = 80)	Low (n = 11)	P value
Location							
Diencephalon	11.8 (2)	14.5 (9)	25.0 (3)	.07	13.8 (11)	27.3 (3)	.28
Hemispheric	64.7 (11)	79.0 (49)	75.0 (9)		77.5 (62)	63.6 (7)	
Infratentorial	23.5 (4)	1.6 (1)	0 (0)		6.3 (5)	0 (0)	
Spinal cord	0 (0)	4.9 (3)	0 (0)		2.5 (2)	9.1 (1)	
Diencephalic involvement	29.4 (5)	33.9 (21)	33.3 (4)	.99	33.8 (27)	27.3 (3)	.99
Demographics							
Age (>96 months)	53.0 (9)	46.8 (29)	58.3 (7)	.73	50.0 (37)	45.5 (4)	.78
Sex							
F	11.8 (2)	25.8 (16)	25.0 (3)	.86	26.3 (21)	0 (0)	.06
FN	29.4 (5)	19.4 (12)	16.7 (2)		20.0 (16)	27.3 (3)	
M	41.2 (7)	43.6 (27)	50.0 (6)		40.0 (32)	72.7 (8)	
MN	17.7 (3)	11.3 (7)	8.33 (1)		13.8 (11)	0 (0)	
Boxer breed	41.2 (7)	46.8 (29)	33.3 (4)	.66	43.8 (35)	45.5 (5)	.99
Bulldog breed	35.3 (6)	25.8 (16)	33.3 (4)	.68	31.3 (25)	9.1 (1)	.17
Boxer's phylogenetic clade ³⁴	82.4 (14)	79.0 (49)	66.7 (8)	.64	78.7 (63)	72.7 (8)	.7
Clinical features							
Duration of signs (>3 days)	86.7 (15)	81.4 (50)	81.8 (10)	.99	79.7 (64)	100.0 (11)	.2
Seizures							
None	41.2 (7)	37.1 (23)	41.7 (5)	.87	38.8 (31)	36.4 (4)	.99
Isolated	29.4 (5)	38.7 (24)	25.0 (3)		35.0 (28)	36.4 (4)	
Cluster seizures	29.4 (5)	24.2 (15)	33.3 (4)		26.3 (21)	27.3 (3)	
Mentation							
Normal	11.8 (2)	36.1 (22)	33.3 (4)	.21	27.9 (22)	54.6 (6)	.08
Lethargy/disorientation	11.8 (2)	14.8 (9)	25.0 (3)		15.2 (12)	18.2 (2)	
Depression	76.5 (13)	49.2 (30)	41.7 (5)		57.0 (45)	27.3 (3)	
Behavioral abnormalities	58.8 (10)	47.5 (29)	58.3 (7)	.62	51.9 (41)	45.5 (5)	.76
Kyphosis/low-head carriage	5.9 (1)	8.2 (5)	8.3 (1)	.99	7.6 (6)	9.1 (1)	.99
Head tilt or turn	29.4 (5)	11.5 (7)	8.3 (1)	.21	16.5 (13)	0 (0)	.36
Gait abnormalities	47.1 (8)	62.3 (39)	50.0 (6)	.42	58.2 (47)	54.6 (6)	.99
Proprioceptive deficits	70.6 (12)	70.5 (44)	91.7 (11)	.36	74.7 (60)	63.6 (7)	.48
Vision							
Normal	64.7 (11)	44.3 (27)	25.0 (3)	.29	43.0 (34)	63.6 (7)	.27
Unilateral deficits	29.4 (5)	37.7 (23)	50.0 (6)		38.0 (30)	36.4 (4)	
Bilateral deficits	5.9 (1)	18.0 (11)	25.0 (3)		19.0 (15)	0 (0)	
Facial/nasal sensation deficits	11.8 (2)	4.9 (3)	33.3 (4)	.01	10.1 (8)	9.1 (1)	.99
Facial asymmetry	0 (0)	4.9 (3)	0 (0)	.99	3.8 (3)	0 (0)	.99
Abnormal eye movements/position	11.8 (2)	13.1 (8)	0 (0)	.52	11.4 (9)	9.1 (1)	.99
Anisocoria/PLR deficits	11.8 (2)	6.6 (4)	0 (0)	.55	7.6 (6)	0 (0)	.99
Hyperesthesia	17.7 (3)	14.8 (9)	16.7 (2)	.91	17.7 (14)	0 (0)	.2

Abbreviations: F, female; FN, female neutered; M, male; MN, male neutered; PLR, pupillary light reflex.

TABLE 4 CSF analysis results by tumor type and grade in dogs with glioma⁵

Tumor type and grade ^a	Elevated TP concentration ^b	Elevated TNCC ^c	ACD ^d	Normal CSF ^a	Mean TP concentration and range (mg/dL)	Mean TNCC and range (cells/ μ L)	Differential cytology
LO (3)	1 (2)	1 (3)	1 (2)	1 (2)	23.3 (20-26.5)	28 (1-81)	Eosinophilic pleocytosis, 1 ^e
HO (13)	8 (11)	3 (13)	6 (11)	3 (11)	143.0 (10.1-780)	38 (0-460)	Increased percentage of neutrophils (62%), 1 ^f ; Mixed cell pleocytosis, 3 ^g
HA (4)	3 (4)	3 (4)	0 (4)	1 (4)	206.1 (22.5-736)	15 (0-27)	Mixed cell pleocytosis, 3
HU (3)	1 (2)	1 (3)	0 (2)	1 (2)	75.1 (20-130.2)	10 (0-27)	Neutrophilic pleocytosis, 1 ^h

Abbreviations: ACD, albuminocytologic dissociation; CSF, cerebrospinal fluid; HA, high-grade astrocytoma; HO, high-grade oligodendroglioma; HU, high-grade undefined glioma; LO, low-grade oligodendroglioma; TNCC, total nucleated cell count; TP, total protein.

^aNumber of cases in which CSF information was available.

^bNumber of cases with >25 mg/dL TP concentration (number of cases with available information).

^cNumber of cases with >5 cells/ μ L (number of cases with available information).

^dNumber of cases with >25 mg/dL TP concentration and <5 cells/ μ L (number of cases with available information).

^eDefined as CSF with >50% eosinophils.

^fDefined as CSF >2% nondegenerated neutrophils.³⁵

^gDefined as CSF with a mixture of mostly lymphocytes and large mononuclear cells and >20% contribution of neutrophils and, occasionally, eosinophils.³⁵

^hDefined as CSF with >75% neutrophils.

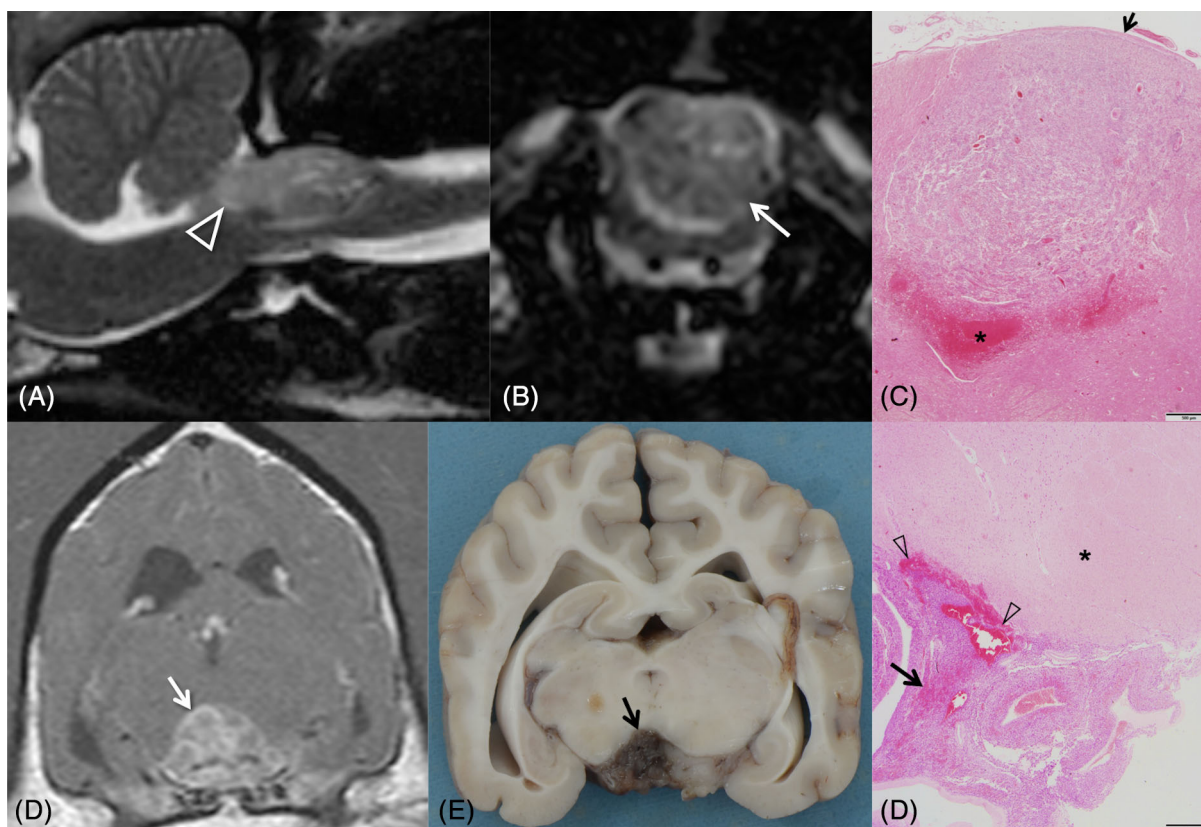


FIGURE 3 Midsagittal (A) and transverse (B) T2-weighted magnetic resonance (MR) images of a heterogeneously hyperintense high-grade oligodendroglioma at the level of C1 vertebra (arrow) identified as intradural-extramedullary by both observers. Note the mass extension into the foramen magnum (arrowhead). Photomicrograph of the same tumor as (A) and (B) demonstrating a highly cellular proliferation in direct contact with the thickened pia mater (arrow) in the dorsal aspect of the spinal cord (C). Note the severe hemorrhages ventrally where the mass is compressing the spinal cord parenchyma (asterisk). HE stain. Scale bar = 500 μ m. Transverse T1-weighted postcontrast MR image of an extra-axial nonuniformly contrast-enhancing high-grade astrocytoma ventral to the mesencephalon (arrow) (D). Formalin-fixed transverse section of the brain at the level of (D) demonstrating the extra-axial appearance of the tumor (arrow) (E). Photomicrograph of the paraffin-embedded tumor in (D) and (E) showing a highly cellular proliferation spreading through the subarachnoid space ventral to the mesencephalon (asterisk) with multiple foci of hemorrhage (arrowheads) and necrosis (arrow) (F). HE stain. Scale bar = 500 μ m

TABLE 5 Univariate analysis of MRI criteria of 74 intracranial gliomas based on type and grade. Table shows percentage of each criterion within each type or grade (total number of cases for each criterion)

	Type			P value	Grade		
	Astrocytoma (n = 17)	Oligodendroglioma (n = 49)	Undefined (n = 8)		High (n = 67)	Low (n = 7)	P value
Margins							
Smooth	47.1 (8)	69.4 (34)	25.0 (2)	.02	56.7 (38)	85.7 (6)	.53
Irregular	11.8 (2)	2.0 (1)	25.0 (2)		7.5 (5)	0 (0)	
Poorly defined	41.2 (7)	28.6 (14)	50.0 (4)		35.8 (24)	14.3 (1)	
Shape							
Amorphous	29.4 (5)	28.6 (14)	62.5 (5)	.09	34.3 (23)	14.3 (1)	.24
Lobulated	5.9 (1)	2.0 (1)	12.5 (1)		3.0 (2)	14.3 (1)	
Spherical or ovoid/elongate	64.7 (11)	69.4 (34)	25.0 (2)		62.7 (42)	71.4 (5)	
Signal							
T2-hypointensity ^a	11.8 (2)	2.0 (1)	0 (0)	.26	4.5 (3)	0 (0)	.99
T2-homogeneity	29.4 (5)	32.7 (16)	12.5 (1)	.63	28.4 (19)	42.9 (3)	.42
T1-hypointensity ^b	47.1 (8)	95.9 (47)	62.5 (5)	<.001	80.6 (54)	85.7 (6)	.99
T1-homogeneity	29.4 (5)	14.3 (7)	37.5 (3)	.15	19.4 (13)	28.6 (2)	.62
FLAIR hypointensity ^c	11.8 (2)	16.3 (8)	12.5 (1)	.99	14.9 (10)	14.3 (1)	.99
FLAIR homogeneity	29.4 (5)	16.3 (8)	37.5 (3)	.23	22.4 (15)	14.3 (1)	.99
GRE signal voids ^d	50.0 (5)	37.0 (10)	25.0 (1)	.7	41.0 (16)	0 (0)	.51
Contrast enhancement							
Moderate to severe ^e	58.8 (10)	44.9 (22)	37.5 (3)	.56	49.3 (33)	28.6 (2)	.43
CE pattern							
No CE	17.7 (3)	27.5 (14)	25.0 (2)	.42	22.1 (15)	50.0 (4)	.37
Partial or complete ring	23.5 (4)	27.5 (14)	0 (0)		25.0 (17)	12.5 (1)	
Other patterns	58.8 (10)	42.9 (21)	75.0 (6)		50.7 (34)	37.5 (3)	
Tumor characteristics							
Cystic structures	41.2 (7)	42.9 (21)	25.0 (2)	.72	40.3 (27)	42.9 (3)	.99
Peritumoral edema							
None	5.9 (1)	12.2 (6)	0 (0)	.28	9.0 (6)	14.3 (1)	.84
Peritumoral	47.1 (8)	67.4 (33)	75.0 (6)		64.2 (43)	57.1 (4)	
Extensive	47.1 (8)	20.4 (10)	25.0 (2)		26.9 (18)	28.6 (2)	
Mass effect							
None	11.8 (2)	2.0 (1)	0 (0)	.11	4.5 (3)	0 (0)	.11
Mild	17.7 (3)	26.5 (13)	0 (0)		20.9 (14)	28.6 (2)	
Moderate	23.5 (4)	44.9 (22)	37.5 (3)		35.8 (24)	71.4 (5)	
Severe	47.1 (8)	26.5 (13)	62.5 (5)		38.8 (26)	0 (0)	
Subarachnoid CSF signal loss	88.2 (15)	81.6 (40)	100.0 (8)	.62	85.1 (57)	85.7 (6)	.99
Midline shift	64.7 (11)	73.5 (36)	87.5 (7)	.52	71.6 (48)	85.7 (6)	.66
Ventricular distortion	88.2 (15)	91.8 (45)	100.0 (8)	.82	91.0 (61)	100.0 (7)	.99
Brain herniations							
None	35.3 (6)	44.9 (22)	37.5 (3)	.09	41.8 (28)	42.8 (3)	.21
Transtentorial or subfalcine	41.2 (7)	34.7 (17)	0 (0)		29.9 (20)	57.1 (4)	
Foramen magnum	23.5 (4)	20.4 (10)	62.5 (5)		28.4 (19)	0 (0)	
SHM	35.3 (6)	30.6 (15)	37.5 (3)	.8	35.8 (24)	0 (0)	.09
Spread							
Adjacent brain structures	58.8 (10)	69.4 (34)	100.0 (8)	.09	74.6 (50)	28.6 (2)	.02

(Continues)

TABLE 5 (Continued)

	Type			P value	Grade		
	Astrocytoma (n = 17)	Oligodendroglioma (n = 49)	Undefined (n = 8)		High (n = 67)	Low (n = 7)	P value
Brain surface contact	76.5 (13)	77.6 (38)	62.5 (5)	.65	74.6 (50)	85.7 (6)	.99
Leptomeningeal CE	47.1 (8)	28.6 (14)	37.5 (3)	.34	35.8 (24)	14.3 (1)	.26
Ventricular contact	64.7 (11)	87.8 (43)	100.0 (8)	.05	83.6 (56)	85.7 (6)	.99
CSF pathways							
Subarachnoid space	47.1 (8)	28.6 (14)	37.5 (3)	.34	35.8 (24)	14.3 (1)	.41
Ventricular invasion	23.5 (4)	49.0 (24)	62.5 (5)	.09	46.3 (31)	28.6 (2)	.45
Drop metastases	0 (0)	16.3 (8)	0 (0)	.16	11.9 (8)	0 (0)	.99
Other structures							
Pituitary gland	5.9 (1)	8.2 (4)	12.5 (1)	.82	7.5 (5)	14.3 (1)	.46
Penetration of bone	17.7 (3)	12.2 (6)	0 (0)	.56	13.4 (9)	0 (0)	.59

Abbreviations: CE, contrast enhancement; CSF, cerebrospinal fluid; FLAIR, fluid-attenuation inversion recovery; GRE, gradient-recalled echo; MRI, magnetic resonance imaging; SHM, syringohydromyelia; T1, T1-weighted; T2, T2-weighted.

^aAs opposed to T2-weighted hyperintensity seen in 88.2% (15) astrocytomas, 98% (48) oligodendrogliomas, and all undefined gliomas; 95.5% (64) high-grade gliomas and all low-grade gliomas.

^bAs opposed to T1-weighted isointensity seen in 52.9% (9) astrocytomas, 4.1% (2) oligodendrogliomas, and 37.5% (3) undefined gliomas; 19.4% (13) high-grade gliomas and 14.3% (1) low-grade gliomas.

^cAs opposed to FLAIR hyperintensity seen in 88.2% (15) astrocytomas, 83.7% (41) oligodendrogliomas, and 87.5% (7) undefined gliomas; 85.1% (57) high-grade gliomas and 85.7% (6) low-grade gliomas.

^dPercentages and total number of cases with signal voids out of 41 gliomas where GRE images were obtained.

^eAs opposed to none to mild CE seen in 41.2% (7) astrocytomas, 55.1% (27) oligodendrogliomas, and 62.5% (5) undefined gliomas; 50.7% (34) high-grade gliomas and 71.4% (5) low-grade gliomas.

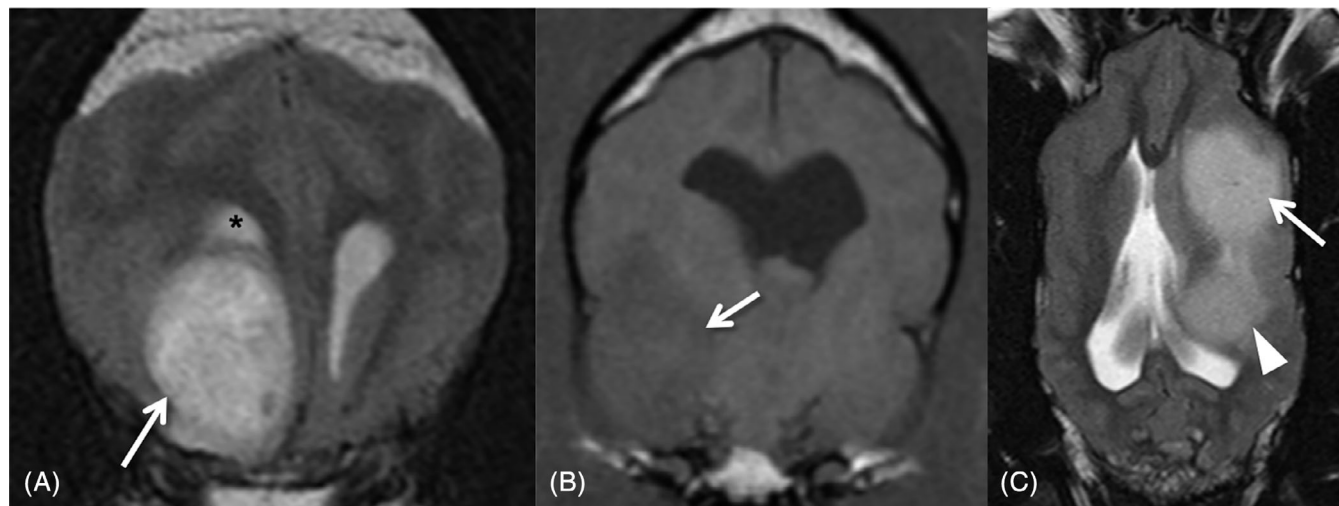


FIGURE 4 Transverse T2-weighted magnetic resonance (MR) image of a high-grade oligodendroglioma (HO) in the right frontal lobe (arrow) with smooth margins and in close contact with the lateral ventricle (asterisk) (A). Transverse T1-weighted image of a hypointense to gray matter HO in the right temporal lobe (arrow) (B). Dorsal T2-weighted MR image showing a high-grade undefined glioma extending from the frontal (arrow) to the temporal lobe (arrowhead) (C). Involvement of the parietal lobe and hippocampus were also noted and gliomatosis cerebri growth pattern was subsequently confirmed on histopathology

deficits ($P = .01$), tumor margins ($P = .02$) on MRI, T1-weighted signal intensity ($P < .001$), and ventricular contact ($P = .04$).

Multivariable logistic regression analysis indicated that oligodendrogliomas were more often associated with smooth margins

(Figure 4A) than astrocytomas (odds ratio [OR], 42.5; 95% CI, 2.42–744.97; $P = .04$) or undefined gliomas (OR, 84; 95% CI, 3.43–999.99; $P = .02$). Oligodendrogliomas were also associated with T1-weighted hypointensity (Figure 4B) in comparison with astrocytomas (OR, 45.5;

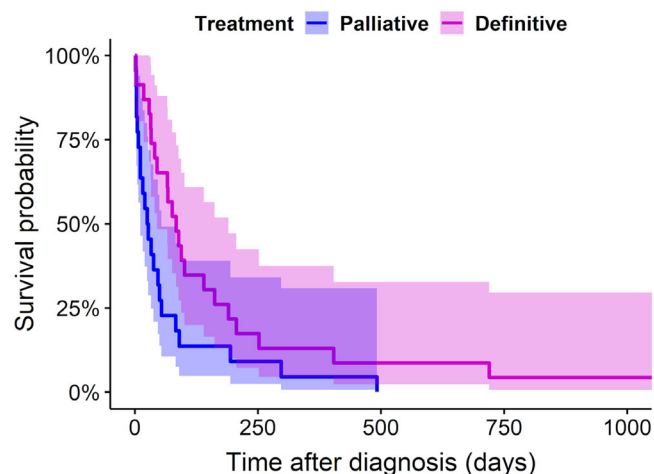


FIGURE 5 Kaplan-Meier survival curve for definitively and palliatively treated dogs with intracranial glioma that survived >1 day ($n = 45$). Dogs receiving definitive treatment survived significantly longer ($P = .03$) than did dogs with palliative treatment. Survival time represents the time from diagnosis to death or euthanasia. Shadow areas represent 95% confidence intervals

TABLE 6 Multivariable Cox proportional hazard ratios for the survival analysis of 36 dogs surviving >1 day after imaging diagnosis and available MRI study for evaluation

Clinical or MRI variable	P value	Hazard ratio	95% confidence interval
Seizures	<.001	0.044	0.011-0.173
Margins ^a			
Irregular	.001	31.69	4.23-237.28
Poorly defined	.003	7.57	2.04-22.18
Drop metastases	<.001	53.15	6.25-452.22
T2-heterogeneity	.001	6.93	2.21-21.73

Abbreviations: MRI, magnetic resonance imaging; T2-heterogeneity, T2-weighted heterogeneity.

^aReference category: smooth margins.

95% CI, 5.78-333.33; $P < .001$) or undefined gliomas (OR, 32.3; 95% CI, 2.51-500.00; $P = .008$). Finally, oligodendrogliomas were more often in contact with the ventricles (Figure 4A) than astrocytomas (OR, 7.47; 95% CI, 1.03-53.95; $P = .049$).

For tumor grade, the univariate analysis (Tables 3 and 5) showed associations with spread to adjacent brain structures ($P = .02$).

The multivariable logistic regression analysis indicated that spread to neighboring brain structures (Figure 4C) was more often associated with high-grade gliomas (OR, 6.02; 95% CI, 1.06-34.48; $P = .04$).

3.6 | Treatment and outcome

Survival time was available for all 87 dogs undergoing MRI for diagnosis. Forty-two dogs survived <1 day (euthanized at diagnosis) and were excluded from further analysis to remove cases without intent to treat. Of the 45 dogs that survived >1 day, 22 received palliative treatment (10 HOs, 6 HAs, 3 HUs, and 3 LOs), and 23 received definitive treatment (11 HOs, 5 HUs, 3 HAs, 3 LOs, and 1 LA). Treatment modalities and survival data are outlined in Supplementary Table 1.

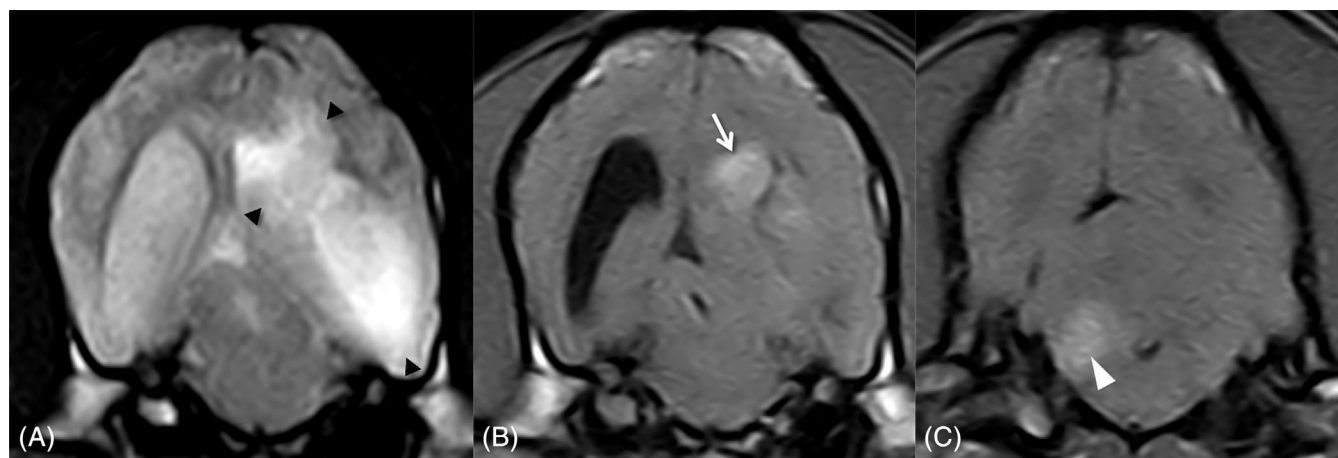


FIGURE 6 Transverse T2-weighted magnetic resonance (MR) image of a left temporal lobe high-grade oligodendroglioma (arrowheads) with poorly defined margins and heterogeneously hyperintense signal extending to the parietal lobe and invading the adjacent lateral ventricle (A). Transverse T1-weighted postcontrast image at the same level demonstrating moderate non-uniform contrast enhancement of the parietal portion of the tumor (arrow) (B). Transverse T1-weighted postcontrast image of the same dog demonstrating a contrast-enhancing drop metastasis in the right cerebellum (arrowhead), just dorsal to the lateral aperture of the fourth ventricle (C)

Among the >1-day survivors, definitive treatments were associated with significantly ($P = .03$) longer survival (median survival time [MST], 84 days; 95% CI, 45-190) than palliative treatment (MST, 26 days; 95% CI, 11-54) (Figure 5).

Univariate survival analysis is presented in Supplementary Table 3. The multivariable Cox proportional hazards model included seizures (hazards ratio [HR] 95% CI, 0.01-0.17) as a lower risk factor, and irregular (HR 95% CI, 4.2-237.3) or poorly defined (HR 95% CI, 2.0-22.2) margins, T2-weighted heterogeneous signal (HR 95% CI, 2.21-21.7), and drop metastases (HR 95% CI, 6.3-452.2) as risk factors for shorter survival (Table 6; Figure 6). No confounding risk factors or interactions were found and no evidence of violation of the proportional hazard assumption was found.

4 | DISCUSSION

Our study provides predictive information for the clinical diagnosis of glioma type and grade as well as their prognostic outcome for affected dogs. New MRI characteristics for differentiation of glioma type and grade are identified, and clinical and imaging findings are associated with survival. Additionally, we describe previously unreported features of these CNS tumors.

Glioma type and grade relative frequency in this study is consistent with data from prior literature, indicating that oligodendroglial and high-grade tumors are the most prevalent in dogs.^{3,8,36} We found no associations between glioma location and tumor type or grade; however, consistent with recent studies,^{8,13} our data suggest that gliomas in dogs, like their human counterparts,³⁰ arise mainly in the fronto-olfactory, temporal, and parietal regions of the cerebral hemispheres. The reported increased likelihood of histologic involvement of the diencephalon in astrocytomas in dogs was not observed in our cohort.^{5,13} All gliomas in dogs reported to be primarily intraventricular to date have been HOs.^{8,26,37}

Almost 80% of the gliomas included herein occurred in brachycephalic dog breeds belonging to the same phylogenetic clade,³⁴ supporting glioma pronounced predilection for these breeds.^{3,5,8-10,13} However, contrasting other reports,⁸ the Boxers and Bulldogs in our study did not show a higher prevalence of oligodendrogloma, although this might have been related to smaller case numbers in our sample. No associations were found between sex and tumor type or grade, but the recently reported male sex predilection⁸ was confirmed by our data and resembles the situation in humans.³⁰

The most common signs of neurologic dysfunction in this series included proprioceptive deficits, mentation changes, and seizures. Over 60% of the cases were diagnosed after an inaugural seizure, resembling previous studies in dogs^{4,5,38} and mirroring the situation in humans.^{17,39} While no presenting clinical sign was associated with glioma type or grade, seizures at onset was identified as a favorable prognostic factor for duration of survival in both low- and high-grade gliomas. Like in human gliomas, new-onset seizures might represent an early warning sign for the presence of a brain tumor as other more subtle signs of neurologic disease in dogs might go unnoticed by their

owners.³⁹ Definitive treatment modalities contribute to seizure control in human patients and this could have influenced the improved survival of these cases in our study; however, there were no associations between seizures at onset and treatment modality.

Although definitive diagnosis of glioma requires histopathologic analysis of tumor tissue, biopsy or resection of tumors is not always possible. Therefore, the ability to predict intracranial glioma type and grade based on MRI characteristics has recently been investigated in dogs.¹³⁻¹⁵ However, currently published MRI findings for predicting grade and tumor type have proven inaccurate.¹⁵ We further analyzed those MRI predictors in our larger sample and confirmed their low sensitivity and specificity. Additionally, the low agreement for predicted tumor type and grade using those features indicated high interobserver variability. These might have been related to the overlap of evaluated MRI features between tumor types and grades in our population and the high variability of described predictors within each tumor.

We assessed 74 brain MRI studies for additional indicators of glioma type and grade and found that oligodendrogliomas were associated with smooth margins and T1-weighted hypointensity compared to astrocytomas and undefined gliomas as well as more commonly in contact with the ventricles than astrocytomas. Tumor spread to neighboring brain structures was the only finding associated with high-grade diagnosis. These are in contrast with reported associations among peritumoral edema and astrocytomas, brain surface contact and oligodendrogliomas, and CE and cystic structures with tumor grade.^{13,14} Conversely to previous reports,^{13,14} ventricular contact alone, independent of distortion, was more common in oligodendrogliomas than astrocytomas. The only similarity between this and prior studies was the significantly low likelihood of T1-weighted hypointensity in astrocytomas,¹⁴ which was shared by undefined gliomas in this series. Although we used comparable methodology to a previous report,¹⁴ differing results might stem from inclusion of undefined gliomas in our series and the potentially magnified significance of individual outliers not representative of the general population in that study,¹⁴ where statistics were performed using 155 MRI observations from 5 investigators in 31 gliomas, instead of the consensus opinion used herein.

Interobserver agreement for individual MRI features associated with glioma type and grade in our study was good to excellent; however, despite reported 89% sensitivity for MRI diagnosis of neoplastic brain disease and 93.7% specificity and 84.4% sensitivity for diagnosis of glioma in dogs, other differential diagnoses with overlapping imaging characteristics still need to be considered.^{12,40}

Differently from our observations, CE on MRI and in particular, ring-enhancement, is usually associated with higher grade human gliomas.⁴¹⁻⁴³ However, human LAs and approximately 50% of LOs can show CE⁴⁴⁻⁴⁷ and its absence does not exclude high-grade glioma.^{44,48,49} On the other hand, human oligodendrogliomas are usually well demarcated and largely T1-hypointense,^{50,51} and glioblastomas might extend widely to adjacent brain structures,⁵² resembling our observations on canine oligodendrogliomas and high-grade gliomas, respectively.

Novel features of gliomas in dogs encountered in this study included histopathologically confirmed butterfly growth pattern in 3 HOs and pituitary gland infiltration in different glioma types. Reported human and canine butterfly gliomas to date are HAs; however, our findings indicate that, as in gliomatosis cerebri, this represents a pattern of spread rather than a distinct nosologic entity.^{19,24,53} Extension of glioma to the pituitary gland had not been described in dogs and has only been confirmed once in humans.⁵⁴ Other infrequent features reported here include penetration into the bone and multifocal distribution. Multifocality as a result of CSF drop metastases occurs in oligodendrogliomas in dogs²⁶⁻²⁸; however, truly multiple, independent gliomas have only been described in 1 dog and are a rare presentation in humans.^{55,56} Additionally, we confirmed CSF seeding in a HA in 1 dog, a dissemination pathway exhibited by less than 2% of human glioblastomas.⁵³ Finally, extra-axial appearance of astrocytoma had only been reported in a dog,¹⁵ and is an infrequent observation in humans.^{57,58}

Data regarding treatment and survival in dogs with histopathologically confirmed glioma is scarce and yet to be added to the new classification. The survival analysis presented here is the most complete to date; however, it has limitations inherent to the low case numbers and results should be interpreted accordingly. The multivariable analysis of available clinical and MRI findings identified prognostic factors affecting survival in intracranial gliomas in dogs for the first time. In addition to the favorable association between new-onset seizures and survival, a series of MRI features were identified as negative prognostic indicators. Poorly defined and irregular tumor margins associated death hazard was over 7 and 31 times as high as that associated with smooth margins, respectively. Tumor T2-weighted heterogeneous signal and observation of drop metastases were also associated with shorter survival. These prognostic factors differ from those reported for human gliomas; nevertheless, prognosis in humans is currently guided by isocitrate dehydrogenase mutation and 1p/19q status,¹⁹ for which parallelisms have not been found in canine gliomas.⁵⁹⁻⁶³ Case series with palliative treatment outcome information relating to glioma type or grade are lacking. Canine studies evaluating experimental therapies in >3 intracranial gliomas with detailed information on their type and grade have reported MSTs of 119 days (n = 7),⁶⁴ 224 days (n = 17),⁶⁵ 248 days (n = 8),⁶⁶ and 257 days (n = 8).⁶⁷ However, no comparisons were made between differing types or grades. Similarly, a recent study reported a MST of 66 days after surgical resection alone in 14 gliomas,⁶⁸ 8 of which were reclassified and included in this study. Thus, we decided to further evaluate therapeutic outcome in our larger sample of dogs surviving diagnosis. Despite marked variability in treatment modalities (surgery, radiotherapy, chemotherapy), MST for definitively treated cases (n = 23) was longer (84 days) than for palliative treatment cases (n = 22; 26 days), suggesting that definitive therapies provide a significant survival benefit to dogs with intracranial gliomas, although this benefit appears to be limited.

This series has some limitations intrinsic to its retrospective nature and reflects the challenges inherent to the study of gliomas in dogs, including variable MRI and treatment protocols, owner decisions

to euthanize rather than natural death, and erroneous or incomplete record-keeping. Thus, the authors invite researchers to contribute to the creation of a mutually accessible international multicenter database to better enable evidence-based research in this field.

Additional limitations of the current study include the fact that necropsy samples might not be representative of the original tumor phenotype, which could change with tumor progression or be influenced by treatments administered. Also, in cases where surgical biopsies were obtained, these might have failed to reflect the overall histologic features of the glioma sampled hampering accurate classification. Finally, tumor typing and grading was established by a single pathologist which could represent a potential source of bias in view of the moderate agreement for glioma type and grade observed between the multiple pathologists contributing to the CBTC classification.⁸

In conclusion, smooth margins, T1-weighted hypointensity and ventricular contact on MRI diagnosed intracranial gliomas, could allow differentiation between oligodendrogliomas and other glial tumor types in dogs. High-grade glioma should be suspected if spread over more than 1 brain region is observed. Definitive therapies appear to improve survival time. New onset seizures are associated with a more favorable prognosis, whereas MRI observed irregular or poorly defined tumor margins, T2-weighted heterogeneity and drop metastases are negative prognostic indicators. No associations were found between survival and tumor location or the CBTC morphologic classification.⁸

ACKNOWLEDGMENT

This work was supported by a grant from the University of Glasgow, Small Animal Hospital Fund.

CONFLICT OF INTEREST DECLARATION

Authors declare no conflict of interest.

OFF-LABEL ANTIMICROBIAL DECLARATION

Authors declare no off-label use of antimicrobials.

INSTITUTIONAL ANIMAL CARE AND USE COMMITTEE (IACUC) OR OTHER APPROVAL DECLARATION

Approved by the Research Ethics Committee of the School of Veterinary Medicine of the University of Glasgow (Ref33a/17).

HUMAN ETHICS APPROVAL DECLARATION

Authors declare human ethics approval was not needed for this study.

ORCID

Roberto José-López  <https://orcid.org/0000-0002-0661-5562>

Rodrigo Gutierrez-Quintana  <https://orcid.org/0000-0002-3570-2542>

Sonia Añor  <https://orcid.org/0000-0002-1099-7698>

REFERENCES

- McGrath JT. Intracranial pathology in the dog. *Acta Neuropathol.* 1962;1 (Suppl I):3-4.

2. Dorn CR, Taylor DO, Frye FL, et al. Survey of animal neoplasms in Alameda and Contra Costa counties, California. Methodology and description of cases. *J Natl Cancer Inst.* 1968;40:295-305.
3. Song RB, Vite CH, Bradle CW, et al. Postmortem evaluation of 435 cases of intracranial neoplasia in dogs and relationship of neoplasm with breed, age and body weight. *J Vet Intern Med.* 2013;27:1143-1152.
4. Bagley RS, Gavin PR, Moore MP, et al. Clinical signs associated with brain tumors in dogs: 97 cases (1992-1997). *J Am Vet Med Assoc.* 1999;215:818-819.
5. Snyder JM, Shofer FS, Van Winkle TJ, et al. Canine intracranial primary neoplasia: 173 cases (1986-2003). *J Vet Intern Med.* 2008;22:172-177.
6. Chen L, Zhang Y, Yang J, et al. Vertebrate animal models of glioma: understanding the mechanisms and developing new therapies. *Biochim Biophys Acta.* 1836;2013:158-165.
7. Bentley RT, Ahmed AU, Yanke AB, et al. Dogs are man's best friend: in sickness and in health. *Neuro Oncol.* 2017;19(3):312-322.
8. Koehler JW, Miller AD, Miller CR, et al. A revised diagnostic classification of canine glioma: towards validation of the canine glioma patient as a naturally occurring preclinical model for human glioma. *J Neuropathol Exp Neurol.* 2018;77(11):1039-1054.
9. Hayes HM, Priester WA Jr, Pendergrass TW. Occurrence of nervous-tissue tumors in cattle, horses, cats and dogs. *Int J Cancer.* 1975;15:39-47.
10. Truvé K, Dickinson P, Xiong A, et al. Utilizing the dog genome in the search for novel candidate genes involved in glioma development—genome wide association mapping followed by targeted massive parallel sequencing identifies a strongly associated locus. *PLoS Genet.* 2016;12(5):e1006000.
11. Kraft SL, Gavin PR, DeHaan C, et al. Retrospective review of 50 canine intracranial tumors evaluated by magnetic resonance imaging. *J Vet Intern Med.* 1997;11:218-225.
12. Ródenas S, Pumarola M, Gaitero L, et al. Magnetic resonance imaging findings in 40 dogs with histologically confirmed intracranial tumours. *Vet J.* 2011;187:85-91.
13. Young BD, Levine JM, Porter BF, et al. Magnetic resonance imaging features of intracranial astrocytomas and oligodendrogliomas in dogs. *Vet Radiol Ultrasound.* 2011;52:132-141.
14. Bentley RT, Ober CP, Anderson KL, et al. Canine intracranial gliomas: relationship between magnetic resonance imaging criteria and tumor type and grade. *Vet J.* 2013;198(2):463-471.
15. Stadler KL, Ruth JD, Pancotto TE, et al. Computed tomography and magnetic resonance imaging are equivalent in mensuration and similarly inaccurate in grade and type predictability of canine intracranial gliomas. *Front Vet Sci.* 2017;4:157.
16. Louis DN, Ohgaki H, Wiestler OD, et al. The 2007 WHO classification of tumours of the central nervous system. *Acta Neuropathol.* 2007;114:97-109.
17. Higgins RJ, Bollen AW, Dickinson PJ, et al. Tumors of the nervous system. In: Meuten DJ, ed. *Tumors in Domestic Animals*. 5th ed. Arnes, AL: Wiley-Blackwell; 2016:834-891.
18. Dickinson PJ. Advances in diagnostic and treatment modalities for intracranial tumors. *J Vet Intern Med.* 2014;28:1165-1185.
19. Louis DN, Ohgaki H, Wiestler OD, et al. The 2016 World Health Organization classification of tumors of the central nervous system: a summary. *Acta Neuropathol.* 2016;131:803-820.
20. Fernández F, Deviers A, Dally C, et al. Presence of neural progenitors in spontaneous canine gliomas: a histopathological and immunohistochemical study of 20 cases. *Vet J.* 2016;209:125-132.
21. Recio A, de la Fuente C, Pumarola M, et al. Magnetic resonance imaging and computed tomographic characteristics of a glioma causing calvarial erosion in a dog. *Vet Radiol Ultrasound.* 2019;60:E1-E5.
22. Lobacz MA, Serra F, Hammond G, et al. Imaging diagnosis – magnetic resonance imaging of diffuse leptomeningeal oligodendrogliomatosis in a dog with “dural tail sign”. *Vet Radiol Ultrasound.* 2018;59:E1-E6.
23. Zagzag D, Esencay M, Mendez O, et al. Hypoxia- and vascular endothelial growth factor-induced stromal cell-derived factor-1 α /CXCR4 expression in glioblastomas: one plausible explanation of Scherer's structures. *Am J Pathol.* 2008;173:545-560.
24. Rossmeisl JH, Clapp K, Pancotto TE, et al. Canine butterfly glioblastomas: a neuroradiological review. *Front Vet Sci.* 2016;3:40.
25. Schweizer-Gorgas D, Henke D, Oevermann A, et al. Magnetic resonance imaging features of canine gliomatosis cerebri. *Vet Radiol Ultrasound.* 2018;59:180-187.
26. Vigeral M, Bentley RT, Rancilio NJ, et al. Imaging diagnosis – ante-mortem detection of oligodendroglioma “cerebrospinal fluid drop metastases” in a dog by serial magnetic resonance imaging. *Vet Radiol Ultrasound.* 2018;59:E32-E37.
27. Koch MW, Sánchez MD, Long S. Multifocal oligodendroglioma in three dogs. *J Am Anim Hosp Assoc.* 2011;47:e77-e85.
28. Schkeeper AE, Moon R, Shrader S, et al. Imaging diagnosis – magnetic resonance imaging features of a multifocal oligodendroglioma in the spinal cord and brain of a dog. *Vet Radiol Ultrasound.* 2017;58:E49-E54.
29. Canal S, Bernardini M, Pavone S, et al. Primary diffuse leptomeningeal gliomatosis in 2 dogs. *Can Vet J.* 2013;54:1075-1079.
30. Ostrom QT, Cioffi G, Gittleman H, et al. CBTRUS statistical report: primary brain and other central nervous system tumors diagnosed in the United States in 2012-2016. *Neuro Oncol.* 2019;21(S5):v1-v100.
31. Sturges BK, Dickinson PJ, Bollen AW, et al. Magnetic resonance imaging and histological classification of intracranial meningiomas in 112 dogs. *J Vet Intern Med.* 2008;22:586-595.
32. Bittermann S, Lang J, Henke D, et al. Magnetic resonance imaging signs of presumed elevated intracranial pressure in dogs. *Vet J.* 2014;201:101-108.
33. Toyoda I, Vernau W, Sturges BK, et al. Clinicopathological characteristics of histiocytic sarcoma affecting the central nervous system in dogs. *J Vet Intern Med.* 2020;34:828-837.
34. Parker HG, Dreger DL, Rimbault M, et al. Genomic analyses reveal the influence of geographic origin, migration, and hybridization on modern dog breed development. *Cell Rep.* 2017;19:697-708.
35. Wood A, Garosi L, Platt S. Cerebrospinal fluid analysis. In: Platt S, Garosi L, eds. *Small Animal Neurological Emergencies*. London, UK: Manson Publishing; 2012:121-136.
36. Higgins RJ, Dickinson PJ, LeCouteur RA, et al. Spontaneous canine gliomas; overexpression of EGFR, PDGFR α , and IGFBP2 demonstrated by tissue microarray immunophenotyping. *J Neurooncol.* 2010;98:49-55.
37. Rissi DR, Levine JM, Eden KB, et al. Cerebral oligodendroglioma mimicking intraventricular neoplasia in three dogs. *J Vet Diagn Invest.* 2015;27:396-400.
38. Schwartz M, Lamb CR, Brodbelt DC, et al. Canine intracranial neoplasia: clinical risk factors for development of epileptic seizures. *J Small Anim Pract.* 2011;52:632-637.
39. Vecht CJ, Kerkhof M, Duran-Pena A. Seizure prognosis in brain tumors: new insights and evidence-based management. *Oncologist.* 2014;19:751-759.
40. Wolff CA, Holmes SP, Young BD, et al. Magnetic resonance imaging for the differentiation of neoplastic, inflammatory, and cerebrovascular brain disease in dogs. *J Vet Intern Med.* 2012;26:589-597.
41. Khalid L, Carone M, Dumrongpisutikul N, et al. Imaging characteristics of oligodendrogliomas that predict grade. *AJNR Am J Neuroradiol.* 2012;33:852-857.
42. Walker C, Baborie A, Crooks D, et al. Biology, genetics and imaging of glial cell tumors. *Br J Radiol.* 2011;84:S90-S106.
43. Watanabe M, Tanaka R, Takeda N. Magnetic resonance imaging and histopathology of cerebral gliomas. *Neuroradiology.* 1992;34:463-469.
44. Knopp EA, Cha S, Johnson G, et al. Glial neoplasms: dynamic contrast-enhanced T2*-weighted MR imaging. *Radiology.* 1999;211:791-798.

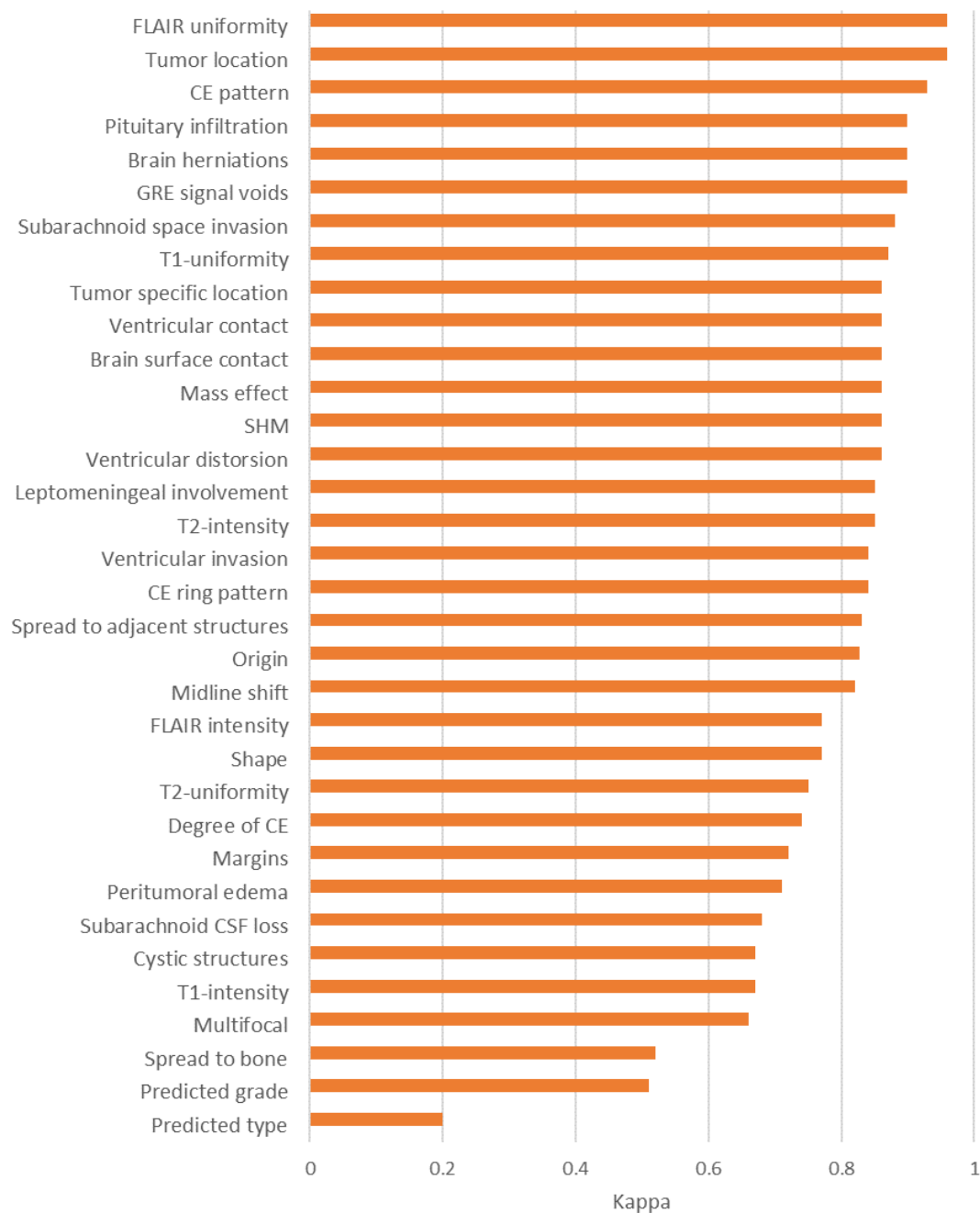
45. Reiche W, Grunwald I, Hermann K, et al. Oligodendrogliomas. *Acta Radiol.* 2002;43:474-482.
46. Walker C, du Plessis DG, Fildes D, et al. Correlation of molecular genetics with molecular and morphological imaging in gliomas with an oligodendroglial component. *Clin Cancer Res.* 2004;10:7182-7191.
47. Jenkinson MD, du Plessis DG, Smith TS, et al. Histological growth patterns and genotype in oligodendroglial tumors: correlation with MRI features. *Brain.* 2006;129:1884-1891.
48. Van den Bent MJ, Reni M, Gatta G, et al. Oligodendroglioma. *Crit Rev Oncol Hematol.* 2008;66:262-272.
49. Ginsberg LE, Fuller GN, Hashmi M, et al. The significance of lack of MR contrast enhancement of supratentorial brain tumors in adults: histopathological evaluation of a series. *Surg Neurol.* 1998;49:436-440.
50. Lee YY, Tassel PV. Intracranial oligodendrogliomas: imaging findings in 35 untreated cases. *AJR Am J Roentgenol.* 1989;152:361-369.
51. Engelhard HH, Stelea A, Mundt A. Oligodendroglioma and anaplastic oligodendroglioma: clinical features, treatment, and prognosis. *Surg Neurol.* 2003;60:443-456.
52. Matsukado Y, MacCarty CS, Kernohan JW. The growth of glioblastoma multiforme (astrocytomas, grades 3 and 4) in neurosurgical practice. *J Neurosurg.* 1961;18:636-644.
53. Rees JH, Smirniotopoulos JG, Jones RV, et al. Glioblastoma multiforme: radiologic-pathologic correlation. *Radiographics.* 1996;16:1413-1438.
54. Hardian RF, Goto T, Kuwabara H, et al. An autopsy case of wide-spread brain dissemination of glioblastoma unnoticed by magnetic resonance imaging after treatment with bevacizumab. *Surg Neurol Int.* 2019;10:137.
55. Walmsley GL, Chandler K, Davies ES, et al. Multi-focal cerebral oligoastrocytoma in a puppy. *J Small Anim Pract.* 2009;50:435-439.
56. Barnard RO, Geddes JF. The incidence of multifocal cerebral gliomas. A histologic study of large hemisphere sections. *Cancer.* 1987;60:1519-1531.
57. Ahn MS, Jackler RK. Exophytic brain tumors mimicking primary lesions of the cerebellopontine angle. *Laryngoscope.* 1997;107:466-471.
58. Wu B, Liu W, Zhu H, et al. Primary glioblastoma of the cerebellopontine angle in adults. *J Neurosurg.* 2011;114:1288-1293.
59. Kawakami S, Ochiai K, Azakami D, et al. R132 mutations in canine isocitrate dehydrogenase 1 (IDH1) lead to functional changes. *Vet Res Commun.* 2018;42:49-56.
60. Fraser AR, Bacci B, Chevoir MA, et al. Isocitrate dehydrogenase 1 expression in canine gliomas. *J Comp Pathol.* 2018;165:33-39.
61. Reitman ZJ, Olby NJ, Mariani CL, et al. IDH1 and IDH2 hotspot mutations are not found in canine glioma. *Int J Cancer.* 2010;127:245-246.
62. Amin SB, Anderson KJ, Boudreau CE, et al. Comparative molecular life history of spontaneous canine and human gliomas. *Cancer Cell.* 2020;37:243-257.e7.
63. Thomas R, Duke SE, Wang HJ, et al. 'Putting our heads together': insights into genomic conservation between human and canine intracranial tumors. *J Neurooncol.* 2009;94:333-349.
64. Rossmeisl JH Jr, Garcia PA, Pancotto TE, et al. Safety and feasibility of the NanoKnife system for irreversible electroporation ablative treatment of canine spontaneous intracranial gliomas. *J Neurosurg.* 2015;123:1008-1025.
65. Rossmeisl JH, Herpai D, Quigley M, et al. Phase I trial of convection-enhanced delivery of IL13RA2 and EPHA2 receptor targeted cytotoxins in dogs with spontaneous intracranial gliomas. *Neuro Oncol.* 2021;23(3):422-434. <https://doi.org/10.1093/neuonc/noaa196>.
66. Freeman AC, Platt SR, Holmes S, et al. Convection-enhanced delivery of cetuximab conjugated iron-oxide nanoparticles for treatment of spontaneous canine intracranial gliomas. *J Neurooncol.* 2018;137:653-663.
67. Bentley RT, Thomovsky SA, Miller MA, et al. Canine (pet dog) tumor microsurgery and intratumoral concentration and safety of metronomic chlorambucil for spontaneous glioma: a phase I clinical trial. *World Neurosurg.* 2018;116:e534-e542.
68. Suñol A, Mascort J, Font C, et al. Long-term follow-up of surgical resection alone for primary intracranial rostrotentorial tumors in dogs: 29 cases (2002-2013). *Open Vet J.* 2017;7:375-383.

SUPPORTING INFORMATION

Additional supporting information may be found online in the Supporting Information section at the end of this article.

How to cite this article: José-López R, Gutierrez-Quintana R, de la Fuente C, et al. Clinical features, diagnosis, and survival analysis of dogs with glioma. *J Vet Intern Med.* 2021;35(4): 1902-1917. <https://doi.org/10.1111/jvim.16199>

Supplementary Figure 1. Median inter-observer agreement for MRI criteria used by two board-certified neurologists interpreting the MRIs of 74 dogs with intracranial glioma.



Abbreviations: CE, contrast enhancement; CSF, cerebrospinal fluid; FLAIR, fluid-attenuation inversion recovery; GRE, gradient recall echo; MRI, magnetic resonance imaging; SHM, syringohydromyelia; T1, T1-weighted; T2, T2-weighted.

Supplementary Table 1. Treatment modalities and survival data.

Dog	Age (months)	Breed	Sex	CBTC schema diagnosis	Main anatomic location	Treatment	Survival (days)
1	96	German Shorthaired Pointer	FN	Oligodendroglioma (Low-grade)	Hemispheric	None	1
2	144	Boxer	M	Oligodendroglioma (Low-grade)	Hemispheric	Sx	89
3	108	Dogue de Bordeaux	M	Oligodendroglioma (Low-grade)	Hemispheric	Chemo (Lomustine)	101
4	18	Boxer	M	Oligodendroglioma (Low-grade)	Diencephalon	P	25
5	97	Boxer	M	Oligodendroglioma (Low-grade)	Hemispheric	P	194
6	90	Boxer	M	Oligodendroglioma (Low-grade)	Diencephalon	Chemo (Lomustine)	32
7	54	Boxer	M	Oligodendroglioma (Low-grade)	Diencephalon	None	1
8	65	Dogue de Bordeaux	FN	Oligodendroglioma (Low-grade)	Spinal cord	None	1
9	144	English Cocker Spaniel	M	Oligodendroglioma (Low-grade)	Hemispheric	None	1
10	48	French Bulldog	M	Oligodendroglioma (Low-grade)	Hemispheric	P	20
11	90	Staffordshire Bull Terrier	MN	Oligodendroglioma (High-grade)	Diencephalon	None	1
12	97	German Shepherd Dog	F	Oligodendroglioma (High-grade)	Hemispheric	P	54
13	88	French Bulldog	MN	Oligodendroglioma (High-grade)	Hemispheric	P	2
14	92	Boxer	F	Oligodendroglioma (High-grade)	Hemispheric	None	1
15	98	French Bulldog	F	Oligodendroglioma (High-grade)	Diencephalon	P	11
16	156	Boxer	F	Oligodendroglioma (High-grade)	Hemispheric	None	1
17	108	Boxer	F	Oligodendroglioma (High-grade)	Hemispheric	P	3
18	110	Boxer	M	Oligodendroglioma (High-grade)	Hemispheric	None	1
19	60	French Bulldog	F	Oligodendroglioma (High-grade)	Hemispheric	P	7
20	95	Boxer	F	Oligodendroglioma (High-grade)	Hemispheric	None	1
21	75	Boxer	F	Oligodendroglioma (High-grade)	Hemispheric	None	1
22	111	West Highland White Terrier	MN	Oligodendroglioma (High-grade)	Hemispheric	None	1
23	101	Boxer	FN	Oligodendroglioma (High-grade)	Hemispheric	None	1
24	38	French Bulldog	F	Oligodendroglioma (High-grade)	Hemispheric	P	47
25	44	Dogue de Bordeaux	M	Oligodendroglioma (High-grade)	Hemispheric	None	1
26	60	Border Terrier	MN	Oligodendroglioma (High-grade)	Diencephalon	None	1
27	108	German Shorthaired Pointer	F	Oligodendroglioma (High-grade)	Spinal cord	None	1
28	103	Boxer	FN	Oligodendroglioma (High-grade)	Hemispheric	None	1
29	90	German Shepherd Dog	FN	Oligodendroglioma (High-grade)	Hemispheric	P	492
30	54	Boxer	M	Oligodendroglioma (High-grade)	Hemispheric	Chemo (Clinical trial drug)	404
31	96	Boxer	FN	Oligodendroglioma (High-grade)	Hemispheric	Sx, Chemo (Temozolomide)	206
32	85	Boxer	F	Oligodendroglioma (High-grade)	Diencephalon	None	1
33	59	German Shepherd Dog	M	Oligodendroglioma (High-grade)	Infratentorial	None	1
34	108	Boxer	MN	Oligodendroglioma (High-grade)	Hemispheric	P	38
35	122	French Bulldog	F	Oligodendroglioma (High-grade)	Hemispheric	P	297
36	132	Boxer	M	Oligodendroglioma (High-grade)	Hemispheric	Sx	66
37	96	French Bulldog	M	Oligodendroglioma (High-grade)	Hemispheric	Sx	33
38	30	English Bulldog	M	Oligodendroglioma (High-grade)	Diencephalon	None	1
39	71	French Bulldog	F	Oligodendroglioma (High-grade)	Hemispheric	Sx	140
40	83	Golden Retriever	M	Oligodendroglioma (High-grade)	Hemispheric	Sx, Chemo (Lomustine)	720
41	84	Boxer	M	Oligodendroglioma (High-grade)	Hemispheric	Sx, Chemo (Lomustine)	76
42	95	Boxer	M	Oligodendroglioma (High-grade)	Hemispheric	None	1
43	141	Boxer	M	Oligodendroglioma (High-grade)	Hemispheric	P	5
44	77	French Bulldog	M	Oligodendroglioma (High-grade)	Hemispheric	None	1
45	89	Boxer	FN	Oligodendroglioma (High-grade)	Hemispheric	None	1
46	86	Boxer	MN	Oligodendroglioma (High-grade)	Hemispheric	None	1
47	55	Boxer	FN	Oligodendroglioma (High-grade)	Hemispheric	None	1
48	108	Boxer	M	Oligodendroglioma (High-grade)	Hemispheric	None	1
49	79	French Bulldog	MN	Oligodendroglioma (High-grade)	Spinal cord	None	1
50	156	Field Spaniel	FN	Oligodendroglioma (High-grade)	Hemispheric	Sx, Rad	94

51	78	French Bulldog	M	Oligodendroglioma (High-grade)	Hemispheric	None	1
52	102	French Bulldog	M	Oligodendroglioma (High-grade)	Diencephalon	None	1
53	117	Yorkshire Terrier	FN	Oligodendroglioma (High-grade)	Hemispheric	None	1
54	93	Boxer	M	Oligodendroglioma (High-grade)	Hemispheric	None	1
55	96	Boxer	M	Oligodendroglioma (High-grade)	Hemispheric	None	1
56	72	Boxer	M	Oligodendroglioma (High-grade)	Hemispheric	None	1
57	156	Yorkshire Terrier	F	Oligodendroglioma (High-grade)	Hemispheric	None	1
58	36	French Bulldog	FN	Oligodendroglioma (High-grade)	Hemispheric	Chemo (Cytarabine)	40
59	144	Crossbreed	M	Oligodendroglioma (High-grade)	Hemispheric	None	1
60	60	French Bulldog	FN	Oligodendroglioma (High-grade)	Hemispheric	None	1
61	120	Boxer	F	Oligodendroglioma (High-grade)	Hemispheric	Chemo (Temozolomide)	190
62	108	French Bulldog	F	Oligodendroglioma (High-grade)	Hemispheric	Chemo (Cytarabine)	2
63	88	Patterdale Terrier	FN	Astrocytoma (Low-grade)	Hemispheric	Chemo (Clinical trial drug)	1104
64	140	Staffordshire Bull Terrier	M	Astrocytoma (High-grade)	Hemispheric	None	1
65	79	Boxer	FN	Astrocytoma (High-grade)	Infratentorial	Chemo (Cytarabine)	3
66	84	Polish Tatra Sheepdog	FN	Astrocytoma (High-grade)	Hemispheric	P	1.5
67	101	Boxer	MN	Astrocytoma (High-grade)	Infratentorial	P	16
68	118	Boxer	M	Astrocytoma (High-grade)	Hemispheric	Chemo (Clinical trial drug)	67
69	114	French Bulldog	M	Astrocytoma (High-grade)	Hemispheric	P	90
70	40	Bulldog (unspecified)	M	Astrocytoma (High-grade)	Hemispheric	None	1
71	86	Border Terrier	MN	Astrocytoma (High-grade)	Hemispheric	P	50
72	57	Boxer	FN	Astrocytoma (High-grade)	Infratentorial	None	1
73	108	Boxer	M	Astrocytoma (High-grade)	Infratentorial	None	1
74	120	French Bulldog	FN	Astrocytoma (High-grade)	Hemispheric	None	1
75	96	French Bulldog	MN	Astrocytoma (High-grade)	Hemispheric	P	3
76	100	Boxer	M	Astrocytoma (High-grade)	Diencephalon	None	1
77	42	French Bulldog	F	Astrocytoma (High-grade)	Diencephalon	Chemo (Cytarabine)	84
78	52	French Bulldog	M	Astrocytoma (High-grade)	Hemispheric	None	1
79	100	Boxer	F	Astrocytoma (High-grade)	Hemispheric	P	33
80	125	French Bulldog	M	Undefined (High-grade)	Diencephalon	P	27
81	74	Boxer	FN	Undefined (High-grade)	Hemispheric	None	1
82	142	Crossbreed	F	Undefined (High-grade)	Hemispheric	Sx	162
83	84	Boxer	M	Undefined (High-grade)	Hemispheric	Sx	252
84	117	Bulldog (unspecified)	M	Undefined (High-grade)	Hemispheric	None	1
85	90	Boxer	FN	Undefined (High-grade)	Hemispheric	Rad	29
86	124	French Bulldog	MN	Undefined (High-grade)	Hemispheric	None	1
87	45	Boxer	F	Undefined (High-grade)	Diencephalon	Chemo (Lomustine)	18
88	96	French Bulldog	M	Undefined (High-grade)	Hemispheric	P	83
89	119	Beagle	F	Undefined (High-grade)	Hemispheric	None	1
90	78	Crossbreed	M	Undefined (High-grade)	Diencephalon	P	11
91	112	Border Terrier	M	Undefined (High-grade)	Hemispheric	Chemo (Clinical trial drug)	45

Chemo = Chemotherapy

F = Female

FN = Female neutered

M = Male

MN = Male neutered

P = Palliative

Rad = Radiation therapy

Survival = Survival from MRI diagnosis

Sx = Surgical resection

Supplementary Table 2. Summary of previously reported MRI features for predicting canine glioma type and grade.^{13,14}

Feature evaluated	Grade		Type	
	Low	High	Astrocytoma	Oligodendroglioma
Contrast enhancement	Mild to none	Moderate to severe	N/A	N/A
Cystic structures (single or multiple)	Usually absent	More common	N/A	N/A
Tumor location	Uncommon in thalamo-capsular region	Any	N/A	In contact with brain surface
Peritumoral edema	N/A	N/A	Moderate to extensive	Mild
Ventricular distortion	N/A	N/A	May be absent	Common

Abbreviations: MRI, magnetic resonance imaging; N/A, not applicable.

Supplementary Table 3. Univariate survival analysis of 36 dogs surviving >1 day after imaging diagnosis and available MRI study for evaluation.


		<i>N</i>	<i>P</i> value	Hazard	Low CI limit	High CI limit
<i>Location</i>						
	Diencephalon	5	.249	.36	.065	2.034
	Hemispheric	29	.022	.15	.030	.756
	Infratentorial	2				
<i>Type</i>						
	Astrocytoma	10	.224	.51	.175	1.503
	Oligodendroglioma	20	.103	.45	.169	1.178
	Undefined glioma	6				
<i>Grade</i>						
	Low	4	.268	1.97	.592	6.581
	High	32				
<i>Demographics</i>						
Age (>96 months)		15	.877	.94	.452	1.971
<i>Sex</i>						
	F	11	.092	.38	.125	1.168
	FN	8	.012	.19	.053	0.699
	M	12	.081	.38	.127	1.127
	MN	5				
Boxer breed		14	.747	.89	.450	1.774
Bulldog breed		14	.308	.70	.347	1.397
Boxer's phylogenetic clade ³⁴		28	.159	.52	.213	1.289
<i>Clinical features</i>						
Duration of signs (>3 days)		34	.512	.70	.244	2.020
Seizures		23	<.001	4.48	1.989	10.095
<i>Mentation</i>						
	Normal	13	.296	.67	.327	1.390
	Lethargy / disorientation	3	.979	.98	.289	3.346
	Depression					
Behavioral abnormalities		20	.640	.85	.431	1.678
Kyphosis / low-head carriage		2	.028	.16	.033	.821
Head tilt or turn		6	.092	.45	.181	1.137
<i>Gait abnormalities</i>						
Proprioceptive deficits		21	.044	.47	.230	.981
<i>Vision</i>						
	Normal	20	.612	1.33	.442	3.997
	Unilateral deficits	12	.216	2.08	.651	6.671
	Bilateral deficits	4				
Facial / nasal sensation deficits		3	.187	.43	.121	1.510
Facial asymmetry		--	--	--	--	--
Abnormal eye movements / position		3	.015	.20	.055	.728
Anisocoria / PLR deficits		1	.084	.151	.018	1.292
Hyperesthesia		8	.103	.51	.227	1.146
<i>MRI findings</i>						
		<i>N</i>	<i>P</i> value	Hazard	Low CI limit	High CI limit
<i>Margins</i>						
	Smooth	22				
	Irregular	2	.346	2.04	0.464	8.951
	Poorly defined	12	.018	2.47	1.165	5.217
<i>Shape</i>						
	Amorphous	11	.961	1.019	.479	2.167
	Lobulated	1	.989	---	---	---
	Spherical or ovoid/elongate	24				
<i>Signal</i>						
T2-hypointensity		-	-	-	-	-
T2-homogeneity		13	.249	.74	.365	1.481

T1-hypointensity	27	.629	.82	.368	1.830
T1-homogeneity	8	.889	.94	.423	2.107
FLAIR hypointensity	2	.602	.68	.156	2.938
FLAIR homogeneity	10	.911	1.04	.495	2.201
<i>Contrast enhancement</i>					
Moderate to severe	26	.340	.72	.366	1.416
CE pattern					
No CE	10	.863	.93	.418	2.076
Partial or complete ring	8	.489	.74	.314	1.739
Other patterns	18				
<i>Tumor characteristics</i>					
Cystic structures	14	.206	1.58	.777	3.221
Peritumoral edema					
None	3	.222	.42	.106	1.683
Peritumoral	23	.109	.53	.239	1.153
Extensive	10				
Mass effect	11	.297	.69	.337	1.393
Subarachnoid CSF signal loss	27	.044	.45	.202	.980
Midline shift	26	.891	.95	.452	1.993
Ventricular distortion	26	.333	.69	.324	1.465
<i>Brain herniations</i>					
None	22				
Transtentorial and/or subfalcine	9	.959	.98	.432	2.219
Foramen magnum	5	.010	4.12	1.413	11.994
SHM	9	.087	.50	.230	1.104
<i>Spread</i>					
Adjacent brain structures	22	.245	.66	.332	1.325
Brain surface contact	30	.003	4.36	1.632	11.649
Leptomeningeal	12	.713	.88	.434	1.771
Ventricular contact	28	.987	1.01	.454	2.231
CSF pathways					
Subarachnoid space	11	.713	.88	.434	1.771
Ventricular invasion	10	.869	1.07	.495	2.299
Drop metastases	1	.006	.09	.016	.491
Other structures					
Pituitary gland	3	.017	.19	.049	.752
Penetration of bone	4	.915	1.06	.367	3.057

Abbreviations: CE, contrast enhancement; CSF, cerebrospinal fluid; F, female; FN, female neutered; FLAIR, fluid-attenuation inversion recovery; M, male; MN, male neutered; MRI, magnetic resonance imaging; PLR, pupillary light reflex; SHM, syringohydromyelia; T1, T1-weighted; T2, T2-weighted.

ARTICLE 2

Expression of FOXP3 in Canine Gliomas: Immunohistochemical Study of Tumor-Infiltrating Regulatory Lymphocytes

Dolors Pi Castro , DVM, PhD student, Roberto José-López, DVM, DipECVN, PhD student, Francisco Fernández Flores, DVM, PhD, Rosa M. Rabanal Prados, BSc Biology, PhD, Maria Teresa Mandara, DVM, PhD, Carles Arús, BSc Biology, PhD, and Martí Pumarola Batlle, DVM, PhD, DipECVP

Abstract

Dogs develop gliomas with similar histopathological features to human gliomas and share with them the limited success of current therapeutic regimens such as surgery and radiation. The tumor microenvironment in gliomas is influenced by immune cell infiltrates. The present study aims to immunohistochemically characterize the tumor-infiltrating lymphocyte (TIL) population of naturally occurring canine gliomas, focusing on the expression of Forkhead box P3-positive (FOXP3⁺) regulatory T-cells (Tregs). Forty-three canine gliomas were evaluated immunohistochemically for the presence of CD3⁺, FOXP3⁺, and CD20⁺ TILs. In low-grade gliomas, CD3⁺ TILs were found exclusively within the tumor tissue. In high-grade gliomas, they were present in significantly higher numbers throughout

the tumor and in the brain-tumor junction. CD20⁺ TILs were rarely found in comparison to CD3⁺ TILs. FOXP3⁺ TILs shared a similar distribution with CD3⁺ TILs. The accumulation of FOXP3⁺ Tregs within the tumor was more pronounced in astrocytic gliomas than in tumors of oligodendroglial lineage and the difference in expression was significant when comparing low-grade oligodendrogliomas and high-grade astrocytomas. Only high-grade astrocytomas presented FOXP3⁺ cells with tumoral morphology. In spontaneous canine gliomas, TILs display similar characteristics (density and distribution) as described for human gliomas, supporting the use of the dog as an animal model for translational immunotherapeutic studies.

Key Words: Canine, Glioma, Immune response, Immunohistochemistry, Regulatory T-cells, Tumor-infiltrating lymphocytes.

From the Unit of Murine and Comparative Pathology (UPMiC), Department of Animal Medicine and Surgery, Veterinary Faculty, Universitat Autònoma de Barcelona, Barcelona, Spain (DPC, RJJ, RMRP, MPB); Networking Research Center on Bioengineering, Biomaterials and Nanomedicine (CIBER-BBN) (DPC, CA, MPB), Universitat Autònoma de Barcelona, Barcelona, Spain; School of Veterinary Medicine, College of Medical, Veterinary and Life Sciences, University of Glasgow, UK (RJJ); Department of Veterinary Pathology and Public Health, Institute of Veterinary Science, University of Liverpool, UK (FFF); Patologia Veterinaria (Università degli Studi di Perugia) (MTM); Departament de Bioquímica i Biologia Molecular, Universitat Autònoma de Barcelona, Barcelona, Spain (CA); and Institut de Biotecnologia i de Biomedicina (IBB), Universitat Autònoma de Barcelona (UAB), Barcelona, Spain (CA).

Send correspondence to: Dolors Pi Castro, DVM, PhD student, Department of Animal Medicine and Surgery, Veterinary Faculty, Universitat Autònoma de Barcelona, 08193 Bellaterra (Cerdanyola del Vallès), Barcelona, Spain; E-mail: dolorspicastro@gmail.com

Dolors Pi Castro and Roberto José-López contributed equally to this work.

Dolors Pi Castro holds a FI-DGR (2018FI_B_00472) grant from the Generalitat de Catalunya, Catalunya, Spain. The author(s) received financial support for the research, authorship, and/or publication of this article from the UPMiC, and partially from the Ministerio de Economía y Competitividad (MINECO) grant MOLIMAGLIO (SAF2014-52332-R). Also funded by Centro de Investigación Biomédica en Red-Bioingeniería, Biomateriales y Nanomedicina (CIBER-BBN [http://www.ciber-bbn.es/en]), an initiative of the Instituto de Salud Carlos III (Spain) cofunded by EU Fondo Europeo de Desarrollo Regional (FEDER).

The authors have no duality or conflicts of interest to declare.

INTRODUCTION

Canine brain tumors are becoming established as naturally occurring models for human disease to advance diagnostic and therapeutic understanding (1). The incidence of adult canine brain tumors is 2%–4.5%, compared with a human incidence of 1.4%–2.1% and, although individual studies vary, gliomas represent 40%–70% of primary brain tumors in dogs (2–10). Therefore, the dog presents a promising model for human gliomas because of the size and structure of its brain, the high incidence of spontaneous diffusely infiltrating gliomas representative of tumor true nature and behavior in humans, and the coexistence with an active immune system (1, 11).

As in the human counterpart, canine glioma occurs in middle- to old-age patients, with a median age at diagnosis of 8 years. It shows a male sex predilection (incidence ratio of 1.53 for males/females), and predominant lesion location includes the fronto-olfactory, temporal and parietal lobes within the brain (12). Interestingly, over 50% of all canine gliomas occur in certain brachycephalic breeds (e.g., Boxers, Bulldogs, Boston Terriers) belonging to the same phylogenetic clade (12–14). Furthermore, the Boston Terrier, Bulldog,

and Boxer breeds have been associated with a higher prevalence of oligodendroglioma (12).

To facilitate translational studies in recent years, standard veterinary practice has been to use the 2007 WHO human glioma classification to grade canine gliomas (13, 15). However, despite their similar histopathological features (12, 16), little is known about whether histological tumor type and grade correlates with biological behavior in canine gliomas as, to date, information on tumor progression and outcome following treatment is anecdotal (17). Additionally, numerous advances in molecular genetics and biology have enhanced the understanding and subclassification of human gliomas since 2007, and these have been included in the 2016 edition of the WHO classification (18). As a result, the NIH Comparative Brain Tumor Consortium has recently proposed a revised diagnostic classification of canine gliomas (12). The aim was to provide an updated canine-specific scheme for clinical and molecular data to be added into a morphologic diagnosis and, subsequently, improve comparison between human and canine glioma. Therefore, to fully integrate canine glioma models into neuro-oncological studies, canine grading has to match the advances made in the context of human gliomas. However, recent studies developed on canine gliomas have failed to demonstrate parallelisms with the isocitrate dehydrogenase and 1p/19q phenomena (19–22), some of the most common molecular abnormalities in human gliomas (18).

Nevertheless, the poor prognosis associated with human high-grade gliomas is closely related to their complex pathophysiology, including the evasion of the immune system that limits an effective antitumoral response (23). As in humans, high-grade gliomas are overall more frequent than low-grade gliomas in dogs (12) and, despite the apparent tumor molecular differences between species, antitumor immune response escape may also play a role in canine gliomas (24).

The tumor microenvironment in brain cancer is influenced by immune cell infiltrates and chronic mediators of inflammation that play an important role in promoting tumor development including initiation, progression and invasion (25). Although the role of the immune system in tumorigenesis is under discussion, some authors recognize its permissive role (26, 27).

Increased knowledge and understanding of associated mechanisms suggest a central role of the regulatory T-cells (Tregs) subset in immune evasion in human glioma (27–29). Tregs are a subtype of T lymphocytes with CD4⁺CD25⁺FOXP3⁺ immunophenotype. The activity of Tregs is associated with the nuclear expression of Forkhead box P3 (FOXP3), a member of the forkhead/winged-helix family of transcriptional regulators that is involved in Tregs development and function (30–32). The physiological function of Tregs is that of maintenance of homeostasis of the immune system and modulation of the immune response (33). Growing evidence suggests that cancer can induce Tregs activity contributing to suppression of the antitumor immune response (30, 31, 33, 34). This has been correlated with glioma development in both murine models and human patients (29). An increased number of Tregs has also been associated with increased malignancy and poor overall survival time in patients with other human solid tumors, such as breast

cancer or hepatocellular carcinoma (35, 36) and gliomas (37, 38).

As a result of the above, new treatment strategies such as immunotherapeutic targeting of Tregs are under study to improve the poor outcomes associated with the current standard of care in human gliomas (28, 39). However, despite several targeted immunotherapies showing promise in preclinical studies with murine models of glioma, none has produced meaningful clinical responses in human patients (39, 40). The discrepancy between success of preclinical studies and subsequent uniform failure of clinical trials most likely derives from the absence of an animal model that reproduces the human tumors with greater fidelity (11). Murine models represent a basic and widely used model, but they do not parallel human gliomas sufficiently (26). Rodent xenograft models are limited by the lack of spontaneously developing disease (11). Another important limiting factor is that these orthotopic xenograft glioma models generally grow in immunocompromised mice, and so fail to model the complexities of an active immune system (26). In contrast, dogs share all the above-mentioned similarities with their human counterparts. Moreover, an increased proportion of Tregs has been observed in peripheral blood, adjacent lymph nodes and intratumorally in a series of canine neoplastic diseases such as osteosarcoma, oral malignant melanoma, cutaneous melanoma, mammary carcinoma and, more recently, high-grade oligodendroglioma (24, 41–45). A positive correlation between Tregs accumulation and malignant tumor grade and behavior has also been found in mammary carcinomas (44, 45). These findings suggest a similar involvement of Tregs in tumorigenesis in dogs as that postulated in humans (32). Thus, spontaneous canine glioma could provide an effective model for immunotherapeutic studies for human patients (26).

The present study aims to immunohistochemically characterize the FOXP3⁺ lymphocytic infiltrates together with T and B lymphocytic subpopulations in naturally occurring canine gliomas of different types and grades, and to evaluate canine gliomas as a model for immune evasion in their human counterparts.

MATERIALS AND METHODS

Case Selection

Histopathologically confirmed canine gliomas diagnosed between 2008 and 2017 at the Unitat de Patologia Murina i Comparada (UPMiC) at the Universitat Autònoma de Barcelona (UAB, Spain) (n = 21), the School of Veterinary Medicine (University of Glasgow, UK) (n = 15), and Patologia Veterinaria (Università degli Studi di Perugia, Italy) (n = 7) were included in the study. Samples were obtained by means of surgical biopsy or at necropsy immediately after death. Written consent for necropsy and histopathological analysis was obtained from all animal owners.

Histology and Morphological Diagnosis

All samples were fixed in 10% neutral buffered formalin. Following fixation, transverse sections of the brain were made and samples including the tumor area were routinely

TABLE 1. Primary Antibodies Used for Immunohistochemistry

Antigen	Antibody Name	Supplier	Dilution	Pretreatment	Cell Labeling
CD3	Rabbit antihuman polyclonal	Dako A0452	1:100	Protease 0.1% in PBS 8 minutes 37°C	T cells
CD20	Rabbit antihuman polyclonal	Termo Fisher PA5-32313	1:300	Citrate buffer 10 mM pH 6.0, 20 minutes bain-marie at 96°C	B cells
FOXP3	Mouse antihuman monoclonal	eBioscience 14-7979	1:100	Tris-EDTA 11 mM pH 9.0, 20 minutes bain-marie at 96°C	Regulatory T cells
GFAP	Rabbit antibovine glial fibrillary acidic protein	Dako, Denmark Z0334	1:500	Citrate buffer 10 mM pH 6.0, 30 minutes at room temperature	Astrocytes
Olig2	Rabbit Olig2 polyclonal antibody	Merck Millipore AB 9610	1:100	Citrate buffer 10 mM pH 6.0, 30 minutes at room temperature	Oligodendrocytes

The antigen, antibody name, supplier, dilution, pretreatment, and cell labeling are shown for the immunohistochemical study.

processed. Morphological evaluation was performed on 5- μ m paraffin-embedded sections stained with hematoxylin and eosin. Glioma samples were evaluated and classified by a veterinary pathologist with expertise in canine neuropathology (M.P.B.). Where available, samples were further evaluated on the basis of immunohistochemistry for glial fibrillary acidic protein (GFAP) and rabbit polyclonal antibody to recombinant mouse Olig2 (Olig2), following the criteria defined in the 2007 WHO classification of tumors of the central nervous system (15). Finally, the diagnosis was adapted to the subsequently revised diagnostic schema for canine gliomas (12).

Immunohistochemistry

To characterize the tumor-infiltrating lymphocytes (TIL) population, primary antibodies specific for CD3 and CD20 (cell surface protein markers corresponding to T and B lymphocytes, respectively) and FOXP3 (nuclear transcription factor expressed on the nuclei of regulatory T cells) were used. Five micrometer-thick tumor sections were mounted on glass slides, deparaffinized, and rinsed with water. To block endogenous peroxidase activity, sections were treated with 3% peroxide hydrogen for 35 minutes. Nonspecific binding was blocked by 30% normal goat serum diluted with PBS for 1 hour at room temperature (RT). Samples were incubated overnight with primary antibodies at 4°C. The primary antibodies used, together with the supplier and dilutions, are summarized in Table 1. Sections were then rinsed with PBS and incubated for 40 minutes at RT with a labeled polymer according to the manufacturer's instructions (Labeled Polymer—Dako REAL Envision-HRP). Staining was completed by 10-minute incubation with 3, 3'-diaminobenzidine and counterstaining in hematoxylin for 3 seconds. The immunohistochemical study for GFAP and Olig2 was made according to the protocol previously described (16). The positive control used for antibodies to CD3, CD20, and FOXP3 was normal canine lymphoid tissue. In all experiments, for the negative control, an isotype-specific immunoglobulin was used as a

substitute for the primary antibody; no immunostaining was detected in these sections. Additionally, adult canine brain serial sections of a Boxer, a French Bulldog and a German Shepherd killed for reasons unrelated to brain pathology were used to determine the distribution of all antigens against CD3, FOXP3, and CD20 within the CNS. Normal astrocytes and oligodendrocytes in nonneoplastic canine cerebrum were used as positive controls for GFAP and Olig2, respectively.

Evaluation of Immunohistochemical Data and Statistical Analysis

Stained tumor slides were digitized for assessment using image analysis software (NanoZoomer Digital Pathology-view2; Hamamatsu, Japan). Depending on the size of the tumor, 1–6 slides per tumor were analyzed. For each tumor section, areas with the highest concentration of immunolabeled cells were identified and, within these, 5 round areas of 0.257 mm² each were selected for quantification under high-power magnification (400 \times). These areas were centered mostly over tumor-rich regions (not associated with necrosis or hemorrhage), but also over highly infiltrative regions at the brain-tumor junction (intersection zone between tumor and normal brain parenchyma). For each area, the number of TILs (CD3⁺, CD20⁺, and FOXP3⁺ cells) was manually determined twice by a trained observer (D.P.), blinded to tumor type and grade information, and supervised by an experienced veterinary pathologist (M.P.B.) to ultimately reach a consensus between both observers. Since cellularity was high in all selected fields, a mean value was obtained for the TIL counts of all areas assessed in each tumor and this was finally expressed as the number of positive cells per 0.257 mm² of tissue as previously described in human glioblastoma (38).

All data analysis models were made with GraphPad Prism 5.0 software. A Shapiro-Wilk test determined that the TIL counts did not follow a Gaussian distribution; therefore, nonparametric tests were performed to evaluate differences in

TIL counts. To compare TILs within gliomas, positively labeled cells for each CD3, CD20, and FOXP3 antibody were evaluated. Counts for CD3⁺, CD20⁺, and FOXP3⁺ TILs in different tumor subtypes (low-grade oligodendroglioma, high-grade oligodendroglioma, low-grade astrocytoma, high-grade astrocytoma, and high-grade undefined glioma) were compared with a Kruskal-Wallis one-way analysis of variance followed by Dunn multiple comparison test. In these tests, the results that were statistically significant were further studied. The Mann-Whitney *U* test (2-tailed) was performed for comparison between CD3-positive immunolabeling in low-grade oligodendrogliomas versus high-grade astrocytomas and high-grade oligodendrogliomas versus high-grade astrocytomas; and comparison of FOXP3-positive immunolabeling between low-grade oligodendrogliomas and high-grade astrocytomas. All other data are presented as a mean, mean \pm standard error of the mean (SEM). All reported *p* values were considered to be statistically significant at *p* < 0.05.

RESULTS

Clinicopathological Features

Forty-three gliomas were included in the present study, including 5 surgical biopsy samples and 38 samples obtained at postmortem examination. Sixty-five percent of the cases were brachycephalic breed dogs including 14 Boxers, 10 French Bulldogs, 2 Staffordshire Bull Terriers, 1 Dogue de Bordeaux, and 1 English Bulldog. Nonbrachycephalic dogs represented 35% of the cases: 3 crossbreeds, 2 German Short-haired Pointers, 2 German Shepherds, and 1 each of the following: Beagle, Basenji, Poodle, Labrador Retriever, Springer Spaniel, Border Terrier, West Highland White Terrier, and Yorkshire Terrier. Both sexes were similarly affected, as there were no significant differences between females and males (23/43, 53.5% females and 20/43, 46.5% males). Age ranged from 1.5 to 13 years with a median age of 7.6 years. Most tumors were located in the prosencephalon (35/43, 81.4%), followed by the spinal cord (4/43, 9.3%), mesencephalon (3/43, 7.0%), and rhombencephalon (1/43, 2.3%).

Following application of the revised diagnostic scheme for canine gliomas, tumors included 6 low-grade oligodendrogliomas, 18 high-grade oligodendrogliomas, 3 low-grade astrocytomas, 13 high-grade astrocytomas, and 3 high-grade undefined gliomas (12).

Astrocytomas and oligodendrogliomas were characterized by their typical histological features and further classified based on immunoreactivity against GFAP and Olig2 on >50% of neoplastic cells, respectively.

Immunohistochemical Features of TILs

We first analyzed the included canine gliomas for the presence of CD3⁺ T-lymphocytes, FOXP3⁺ Tregs, and CD20⁺ B-lymphocytes, describing the overall features and different patterns of distribution of these lymphocytic infiltrates.

CD3⁺ TILs were detected in all tumors. In low-grade gliomas, scattered CD3⁺ TILs were found exclusively within the tumor tissue, most frequently surrounding small vessels or

capillaries. In high-grade gliomas, CD3⁺ TILs were present at a higher density within the tumor and in the brain-tumor junction. The most common pattern was around glomeruloid vessels (Fig. 1A) forming perivascular cuffs (Fig. 1C), but scattered cells within the tumor (Fig. 1B, D) were also present. In high-grade astrocytomas, CD3⁺ TILs reached their highest density, both in the brain-tumor junction and throughout the tumor tissue, showing both perivascular (Fig. 1E) and diffuse patterns (Fig. 1F).

FOXP3 immunoreactivity resulted in positive staining of the nucleus of labeled lymphocytes. Their distribution was similar to CD3⁺ TILs (Fig. 2A). In low-grade gliomas, a few scattered FOXP3⁺ TILs were found confined to the neoplastic tissue. In high-grade gliomas, numerous FOXP3⁺ TILs were located mainly in perivascular areas within the tumor parenchyma and less frequently in the brain-tumor junction (Fig. 2B). High-grade astrocytomas contained high numbers of FOXP3⁺ TILs concentrated in perivascular areas (Fig. 2C) or scattered throughout the tumor tissue (Fig. 2D). At the brain-tumor junction, FOXP3⁺ TILs were predominantly located in perivascular areas. Interestingly, 2 high-grade astrocytomas also presented FOXP3⁺ expression in the nucleus of scattered tumoral cells (Fig. 2E).

CD20⁺ cells were not observed in all canine gliomas, and high-grade gliomas contained the most CD20⁺ TILs. Despite their low numbers, CD20⁺ TILs showed a clearly predominant perivascular pattern, especially in high-grade astrocytomas (Fig. 2F).

Quantification of TILs

Positive immunolabeling for the different lymphocytic markers evaluated in this study was quantified and results were statistically analyzed to assess the relationship between different TIL subsets and tumor type and grade.

The number of CD3⁺ TILs increased with tumor grade, as shown in Table 2. In low-grade oligodendrogliomas there was a mean of 6.07 ± 3.25 , which increased to 11.65 ± 7.46 for high-grade oligodendrogliomas. Additionally, the mean in low-grade astrocytomas was 5.73 ± 8.29 , which increased considerably in high-grade astrocytomas with a mean of 39.88 ± 34.39 . Furthermore, in high-grade undefined gliomas the mean was 5.21 ± 5.66 . Significant differences in the number of CD3⁺ TILs were observed between low-grade oligodendrogliomas and high-grade astrocytomas (*p* = 0.0097) and between high-grade oligodendrogliomas and high-grade astrocytomas (*p* = 0.0098), as shown in Figure 3.

We detected FOXP3⁺ TILs in the tumors analyzed with differences observed not only between grades but also between oligodendroglial and astrocytic types. In low-grade oligodendrogliomas rare FOXP3⁺ TILs were identified in only 50% (3/6) of the cases, and the mean number of FOXP3⁺ TILs was 0.42 ± 0.38 . FOXP3⁺ TILs were identified in 83.4% (15/18) high-grade oligodendrogliomas and the mean was 1.55 ± 0.90 (Table 3). Interestingly, 1 high-grade oligodendroglioma contained a proportionally very high number of immunolabeled cells for FOXP3 (mean; 8.00 ± 2.6).

We also identified a few FOXP3⁺ TILs in all low-grade astrocytomas with a mean of 1.27 ± 0.26 ; however, this was

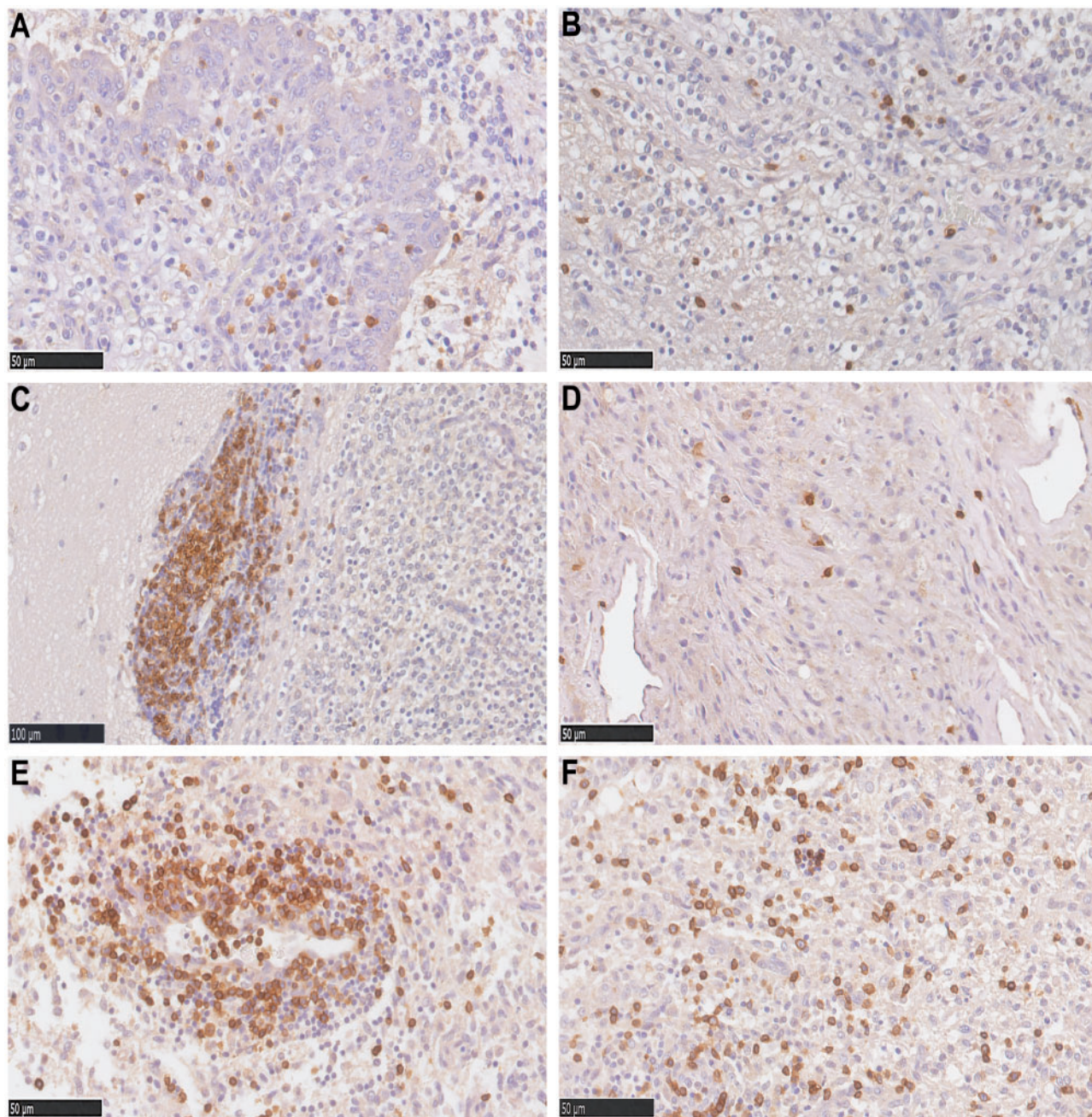


FIGURE 1. Images showing CD3 immunohistochemistry. **(A)** High-grade oligodendroglioma. CD3⁺ TILs within the tumor, surrounding glomeruloid vessels. **(B)** High-grade oligodendroglioma. CD3⁺ TILs scattered within the tumor. **(C)** High-grade oligodendroglioma. CD3⁺ TILs in perivascular cuffs at the brain-tumor junction. **(D)** High-grade astrocytoma. CD3⁺ TILs scattered within the tumor. **(E)** High-grade astrocytoma. CD3⁺ TILs in perivascular cuff within the tumor. **(F)** High-grade astrocytoma. CD3⁺ TILs diffusely within the tumor.

higher than in low-grade oligodendrogliomas. In high-grade astrocytomas, the number of FOXP3⁺ TILs was higher than oligodendroglial tumors with a mean of 4.80 ± 2.55 positive cells per tumor (Table 3). Additionally, FOXP3⁺ TILs were detected in the vast majority of high-grade astrocytomas, 92.3% (12/13). The number of FOXP3⁺ TILs was markedly higher in 3 of these tumors with a mean of 11.36 ± 4.00 . There was a significant difference in FOXP3⁺ expression between

low-grade oligodendrogliomas and high-grade astrocytomas ($p = 0.0136$) as shown in Figure 4. In 2 high-grade astrocytomas, there was a mean of 3.07 ± 0.47 cells with tumor morphology and positive immunostaining for FOXP3⁺ (Fig. 2E). FOXP3⁺ TILs were identified in all high-grade undifferentiated gliomas (3/3) and the mean was 1.23 ± 1.35 (Table 3).

Similar to the trend observed for CD3 immunoreactivity, the number of CD20⁺ TILs progressively increased with

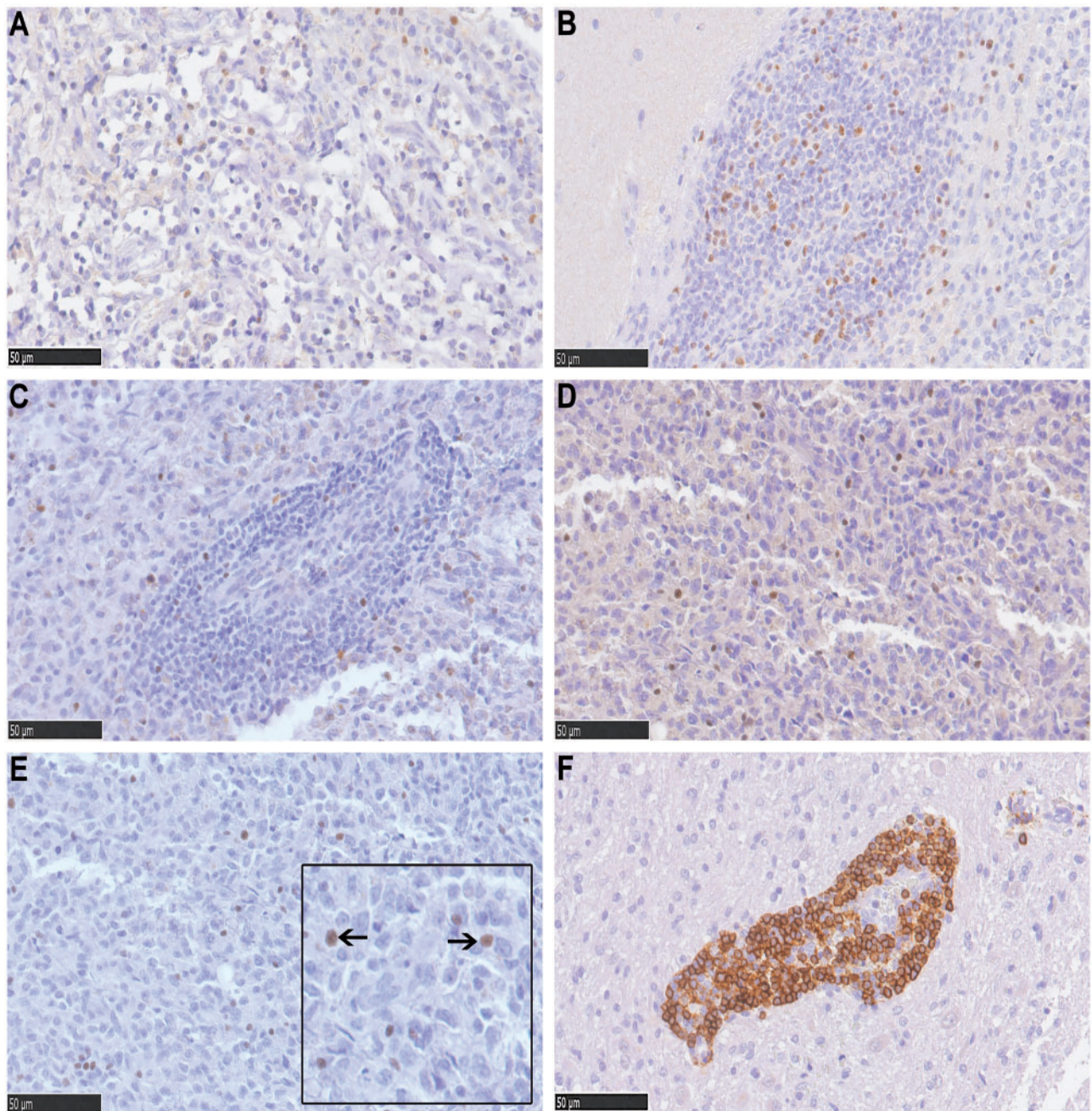


FIGURE 2. Images showing FOXP3 and CD20 immunohistochemistry. **(A)** High-grade oligodendroglioma. FOXP3⁺ TILs scattered within the tumor. **(B)** High-grade oligodendroglioma. FOXP3⁺ TILs in a perivascular cuff at the brain-tumor junction. **(C)** High-grade astrocytoma. Intratumoral FOXP3⁺ TILs in a perivascular cuff within the tumor. **(D)** High-grade astrocytoma. Scattered intratumoral FOXP3⁺ TILs. **(E)** High-grade astrocytoma. Intratumoral FOXP3⁺ TILs; inset, immunostained nuclei of tumor cells (black arrows). **(F)** High-grade astrocytoma. CD20 B⁺ TILs forming a perivascular cuff within the tumor.

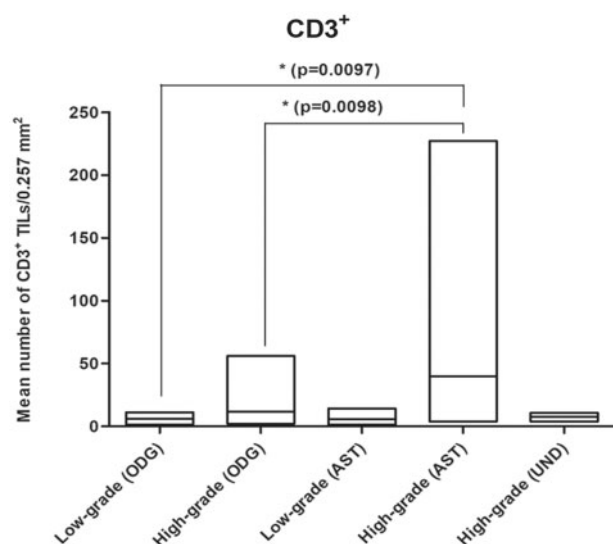
tumor grade (Table 2; Fig. 5). Specifically, in low-grade oligodendrogliomas there was a mean of 0.95 ± 1.07 , which increased for high-grade oligodendrogliomas (2.64 ± 2.43). Furthermore, the mean in low-grade astrocytomas was 2.67 ± 5.23 which augmented for high-grade astrocytomas 12.98 ± 10.17 . The mean was 2.01 ± 2.04 for high-grade undefined gliomas. No

statistically significant differences were observed between grades and types for CD20-positive immunolabeling. In addition, CD20⁺ TILs were not identified in 6 gliomas (2 low-grade oligodendrogliomas, 2 low-grade astrocytomas, and 2 high-grade oligodendrogliomas). We did not observe CD3⁺, CD20⁺, or FOXP3⁺ TILs in the brain tissue of control dogs (n = 3).

TABLE 2. Mean of CD3⁺ and CD20⁺ Tumor-Infiltrating Lymphocytes (TILs) in Gliomas

Tumor Type	Grade	Mean of CD3 ⁺ TILs (Number/0.257 mm ²)	Mean of CD20 ⁺ TILs (Number/0.257 mm ²)
Oligodendrogliomas	Low-grade	6.07	0.95
	High-grade	11.65	2.64
Astrocytomas	Low-grade	5.73	2.67
	High-grade	39.88	12.98
Undefined glioma	High-grade	5.21	2.01

Mean of CD3⁺ and CD20⁺ immunostained TILs in relation to tumor grade and type. Mean of CD3⁺ and CD20⁺ TILs expressed as cell numbers per 0.257 mm².

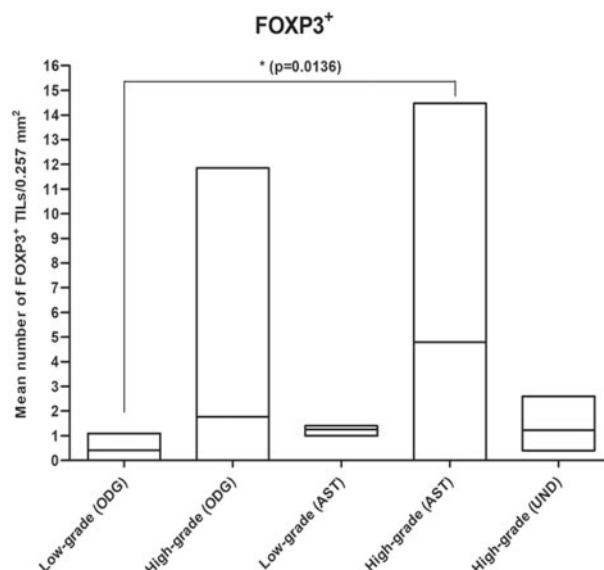
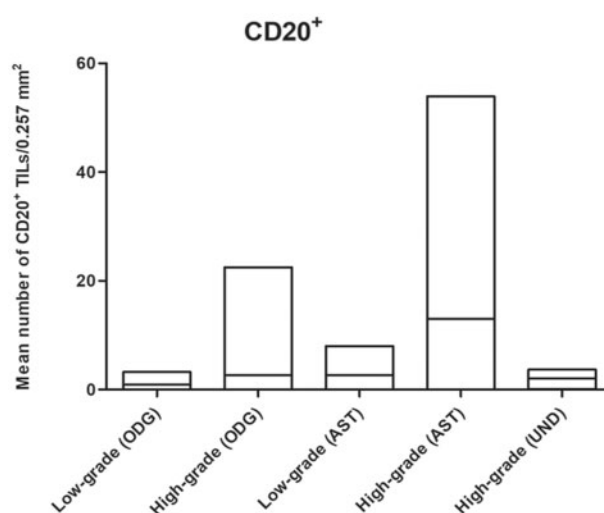
**FIGURE 3.** Mean number of CD3⁺ TILs in different grades and types of glioma. Mean of CD3⁺ TILs expressed as cell numbers per 0.257 mm². **p* < 0.05. ODG, oligodendroglioma; AST, astrocytoma; UND, undefined glioma.**TABLE 3.** Mean of FOXP3⁺ Tumor-Infiltrating Lymphocytes (TILs) in Gliomas

Tumor Type	Grade	Mean of FOXP3 ⁺ TILs (Number/0.257 mm ²)
Oligodendrogliomas	Low-grade	0.42
	High-grade	1.55
Astrocytomas	Low-grade	1.27
	High-grade	4.80
Undefined glioma	High-grade	1.23

Mean of FOXP3⁺ immunostained TILs in relation to tumor type and grade. Mean of FOXP3⁺ TILs expressed as cell numbers per 0.257 mm².

DISCUSSION

There is an emerging need to characterize the role of the immune system in glioma biology. Recent studies on human gliomas have investigated the correlation between TILs and

**FIGURE 4.** Mean number of FOXP3⁺ TILs in different grades and types of glioma. Mean of FOXP3⁺ TILs expressed as cell numbers per 0.257 mm². **p* < 0.05. ODG, oligodendroglioma; AST, astrocytoma; UND, undefined glioma.**FIGURE 5.** Mean number of CD20⁺ TILs in different grades and types of glioma. Mean of CD20⁺ TILs expressed as cell numbers per 0.257 mm². **p* < 0.05. ODG, oligodendroglioma; AST, astrocytoma; UND, undefined glioma.

clinical prognosis as well as the critical role that Tregs play in suppressing antitumor immunity and promoting tumor progression (46–48). Findings have prompted development of targeted immunotherapies with promising efficacy in preclinical studies (49). However, murine models of glioma have failed to reliably predict which of the therapies that are efficacious in preclinical studies will be effective in the clinic (11, 39, 40). Thus, validation of spontaneous canine glioma as a model for immune evasion is intended to contribute to the identification of therapeutic targets in human gliomas.

Only 2 studies have investigated the presence of infiltrating lymphocytes in canine oligodendrogliomas (24, 50). In this study, we characterize the TIL population of a large cohort of different type canine gliomas by describing the immunohistochemical expression of CD3, CD20, and FOXP3 markers corresponding to T-, B- and Treg lymphocytes, respectively. We incorporate for the first-time canine glioma immunophenotype information into the newly proposed canine morphological classification (12). We also assess the relationship between different TIL subsets and tumor type and grade. Our results resemble findings reported in human gliomas, supporting the use of canine glioma to model translation to human studies.

In the gliomas included in this study, CD20⁺ TILs were rarely found compared with CD3⁺ TILs. They were present in small numbers in some low-grade tumors, while their numbers increased moderately in high-grade tumors, especially in high-grade astrocytomas. Their distribution was similar to that observed for CD3⁺ TILs, most predominantly in perivascular areas. There are few studies identifying B-cell infiltration in human gliomas and only a few reports in human glioblastomas have described a very low percentage of B lymphocytes among the inflammatory infiltrate, which was associated to perivascular areas in 1 study (51–53). The specific role of B lymphocytes in the development of gliomas remains unclear (51). Our results are in agreement with recently published studies on canine low- and high-grade oligodendrogliomas and feline gliomas, respectively, in which the infiltration of tumors by B lymphocytes was much smaller than CD3⁺ lymphocyte infiltration (50, 54). Similar to our findings, the study conducted on canine oligodendrogliomas showed that B-lymphocyte distribution was restricted to perivascular cuffs within the tumor (50). In feline gliomas, B-lymphocytes have also been observed predominantly within perivascular spaces at the brain-tumor junction (54).

Low-grade gliomas in our study contained CD3⁺ TILs within the tumor, most commonly surrounding vascular elements, and few cells were present scattered throughout the tumor tissue. In high-grade gliomas, CD3⁺ TILs were present within the tumor, mainly surrounding glomeruloid vessels and forming perivascular cuffs, but also scattered throughout the tumor tissue. Moreover, they were present in the brain-tumor junction where the most common distribution pattern was perivascular. Our results are in agreement with those observed in human low- and high-grade astrocytomas in which infiltrating CD3⁺ lymphocytes have been described diffusely and perivascularly within the tumor (55). There are no previous descriptions of infiltrating CD3⁺ lymphocytes in the brain-tumor junction in human gliomas. In veterinary medicine, a recent study evaluating inflammatory changes in low- and high-grade canine oligodendrogliomas showed that CD3⁺ lymphocytes were common as perivascular aggregates or scattered throughout the tumor (50). A similar study including feline low- and high-grade gliomas showed a similar pattern of CD3⁺ lymphocyte distribution (54). Thus, our findings on the presence of CD3⁺ TILs and their distribution in this varied group of canine gliomas reinforce previous descriptions in veterinary medicine (50, 54).

FOXP3⁺ TILs, consistent with Tregs, shared a similar distribution to CD3⁺ lymphocytes in our study. In low-grade gliomas these cells were scattered exclusively within the tumor. In high-grade gliomas, FOXP3⁺ TILs were found scattered and perivascularly within the tumor and less frequently, in the brain-tumor junction (mostly around perivascular areas). Similar histological features have been observed in FOXP3⁺ Tregs in low- and high-grade human gliomas where intratumoral FOXP3⁺ Tregs were mainly localized in perivascular areas (37, 56) but also scattered throughout the tumor (37). As with infiltrating CD3⁺ lymphocytes, there are no previous descriptions in human gliomas of the presence of FOXP3⁺ Tregs in the brain-tumor junction. This may be related to human studies being mostly based on tumor biopsy samples that might not include brain-tumor junction tissue. To the best of authors' knowledge, this is the first description of FOXP3⁺ TILs distribution in canine gliomas.

Interestingly, in 2 high-grade astrocytomas, FOXP3⁺ expression was also observed in cells with clear tumoral morphology. These cells were scattered within the tumor tissue. In human tumors, FOXP3⁺ has also been identified in tumoral cells of different types (57). In human gliomas, a high percentage of tumor cells with FOXP3⁺ expression has been observed in high-grade astrocytomas, particularly in glioblastomas (37). Consequently, it has been postulated that expression of FOXP3⁺ in glioma cells contributes to the development of high-grade gliomas (37).

In our study, we observed that the number of CD3⁺ TILs in high-grade gliomas was significantly greater than in low-grade gliomas, and this number markedly increased in high-grade astrocytomas. A study including only canine oligodendrogliomas failed to demonstrate a significant difference in CD3⁺ lymphocyte density between low- and high-grade tumors (50). In feline gliomas, it has been observed that the number of CD3⁺ lymphocytes in glioblastomas, classified according to the 2007 WHO classification, is higher than that observed in low- and high-grade oligodendrogliomas, but without significant differences (54). Our results are, therefore, very similar to those published for feline and human gliomas, where the density of CD3⁺ TILs increased with tumor grade, and mean CD3⁺ TIL population in high-grade astrocytomas was significantly higher compared with low-grade gliomas (58). Moreover, in human glioblastomas an increased number of CD3⁺ lymphocytes correlates with increased survival time (51, 58).

Our immunohistochemical analysis indicated that the amount of FOXP3⁺ TILs within the tumoral lymphocytic infiltrate increased as the tumor grade increased. Similar results have been reported in human literature, where an increased proportion of Tregs within the T-cell infiltrate correlates positively with a higher tumor grade (37, 47). Also, the accumulation of FOXP3⁺ Tregs within the tumor was more pronounced in astrocytic gliomas than in tumors of oligodendroglial lineage. Similar observations have been reported in human gliomas, where expression of FOXP3⁺ Tregs seems higher in astrocytic than oligodendroglial tumors (47). Therefore, human high-grade astrocytomas, in particular glioblastomas, contain the highest proportion of intratumoral Tregs (46, 48, 59).

Although individual studies vary, growing evidence suggests that increased intratumoral proportion of FOXP3⁺ Treg infiltrates has a negative correlation with survival in human gliomas (37, 38, 60). Actually, accumulation of FOXP3⁺ Tregs is one of the hallmark features of glioblastoma (28, 39).

The observation of increasing FOXP3⁺ TILs density with tumor grade, greater presence of FOXP3⁺ TILs in astrocytic tumors, and the expression of FOXP3 by tumor cells in the present study is in line with findings associated with increased malignancy in human gliomas (37).

Currently, there is scarce information on the role of Tregs in canine cancer. Only one previous study including canine high-grade oligodendrogliomas demonstrated greater accumulation of Tregs in these tumors (24). In canine meningiomas, variable numbers of Tregs have been documented in the transitional and meningothelial subtypes (61). Outside of the nervous tissue, other reports in dogs with osteosarcomas and oral malignant melanomas showed a significantly increased percentage of Tregs within tumor tissue compared with healthy dogs (41, 42). In a recent study of canine melanocytic neoplasms, authors observed that a high level of FOXP3⁺ cells was positively associated with a more malignant histological diagnosis (43). Similarly, studies in mammary carcinomas demonstrated that Treg infiltration was positively correlated with high-grade tumors and a more aggressive phenotype, such as lymphatic invasion and tumoral necrosis (44, 45). Another report in dogs with intestinal B-cell lymphoma supported these findings (62). All this evidence indicates that the increased Treg proportion in canine tumors plays a role in maintaining an immunosuppressive microenvironment, contributing to reduction of the antitumor immune response and promoting tumor progression.

In conclusion, our morphological and immunohistochemical study of TILs in spontaneous canine gliomas shows many of the characteristics found in human gliomas, and these findings support the use of the dog as a realistic animal model in the evaluation and development of new immunotherapies.

ACKNOWLEDGMENTS

We gratefully acknowledge Ester Blasco, Lola Pérez, and Tamara Rivero for technical assistance, and Tom Yohannan for editorial assistance. We are also grateful to all veterinary neurologists for providing cases. Preliminary results were presented as an oral communication at the 29th Symposium of the Spanish Society of Veterinary Pathology (SEAPV), Cáceres, Spain, June 14–16, 2017.

REFERENCES

- Hicks J, Platt S, Kent M, et al. Canine brain tumours: A model for the human disease? *Vet Comp Oncol* 2015;15:252–72
- Klotz M. Incidence of brain tumors in patients hospitalized for chronic mental disorders. *Psych Quar* 1957;31:669–80
- McGrath JT. Intracranial pathology of the dog. In: Frauchiger E, Seitelberger F, eds. *Symposium Über Vergleichende Neuropathologie*. Berlin, Heidelberg: Springer Berlin Heidelberg 1962:3–4
- Dorn CR, Taylor DON, Frye FL, et al. Survey of animal neoplasms in Alameda and Contra Costa Counties, California I methodology and description of cases. *J Natl Cancer Inst* 1968;40:295–305
- Bagley RS, Gavin PR, Moore MP, et al. Clinical signs associated with brain tumours in dogs: 97 cases (1992–1997). *J Am Vet Med Assoc* 1999;215:818–9
- Snyder JM, Shofer FS, Winkle TJ, et al. Canine intracranial primary neoplasia: 173 cases (1986–2003). *J Vet Intern Med* 2006;20:669–75
- Dolecek TA, Propp JM, Stroup NE, et al. CBTRUS statistical report: Primary brain and central nervous system tumors diagnosed in the united states in 2005–2009. *Neuro Oncol* 2012;14:v1–49
- Song RB, Vite CH, Bradley CW, et al. Postmortem evaluation of 435 cases of intracranial neoplasia in dogs and relationship of neoplasm with breed, age, and body weight. *J Vet Intern Med* 2013;27:1143–52
- Ostrom QT, Bauchet L, Davis FG, et al. The epidemiology of glioma in adults: A state of the science review. *Neuro Oncol* 2014;16:896–913
- Siegel RL, Miller KD, Jemal A. *Cancer statistics, 2017*. *CA Cancer J Clin* 2017;67:7–30
- Bentley RT, Ahmed AU, Yanke AB, et al. Dogs are man's best friend: In sickness and in health. *Neuro Oncol* 2017;19:312–22
- Koehler JW, Miller AD, Miller CR, et al. A revised diagnostic classification of canine glioma: Towards validation of the canine glioma patient as a naturally occurring preclinical model for human glioma. *J Neuropathol Exp Neurol* 2018;77:1039–54
- Higgins RJ, Bollen AW, Dickinson PJ, et al. Tumors of the nervous system. In: Meuten DJ, ed. *Tumors in Domestic Animals*. Hoboken, NJ: John Wiley & Sons, Inc. 2016:834–91
- Parker HG, Dreger DL, Rimbault M, et al. Genomic analyses reveal the influence of geographic origin, migration, and hybridization on modern dog breed development. *Cell Rep* 2017;19:697–708
- Louis DN, Ohgaki H, Wiestler OD, et al. The 2007 WHO classification of tumours of the central nervous system. *Acta Neuropathol* 2007;114:97–109
- Herranz C, Fernández F, Martín-Ibáñez R, et al. Spontaneously arising canine glioma as a potential model for human glioma. *J Comp Pathol* 2016;154:169–79
- Dickinson PJ. Advances in diagnostic and treatment modalities for intracranial tumors. *J Vet Intern Med* 2014;28:1165–85
- Louis DN, Perry A, Reifenberger G, et al. The 2016 World Health Organization classification of tumors of the central nervous system: A summary. *Acta Neuropathol* 2016;131:803–20
- Kawakami S, Ochiai K, Azakami D, et al. R132 mutations in canine isocitrate dehydrogenase 1 (IDH1) lead to functional changes. *Vet Res Commun* 2018;42:49–56
- Fraser AR, Bacci B, Chevoir MA, et al. Isocitrate dehydrogenase 1 expression in canine gliomas. *J Comp Pathol* 2018;165:33–9
- Amin S, Boudreau B, Martinez-Ledesma JE, et al. Comparative molecular life history of spontaneous canine and human gliomas. (Abstract) *Neuro Oncol* 2018;20:vi64–5
- Reitman ZJ, Olby NJ, Mariani CL, et al. IDH1 and IDH2 hotspot mutations are not found in canine glioma. *Int J Cancer* 2010;127:245–6
- Domingues P, González-Tablas M, Otero A, et al. Tumor infiltrating immune cells in gliomas and meningiomas. *Brain Behav Immun* 2016;53:1–15
- Filley A, Henriquez M, Bhowmik T, et al. Immunologic and gene expression profiles of spontaneous canine oligodendrogliomas. *J Neurooncol* 2018;137:469–79
- Mostofa AGM, Punganuru SR, Madala HR, et al. The process and regulatory components of inflammation in brain oncogenesis. *Biomolecules* 2017;7:1–33
- Chen L, Zhang Y, Yang J, et al. Vertebrate animal models of glioma: Understanding the mechanisms and developing new therapies. *Biochim Biophys Acta* 2013;1836:158–65
- Nduom EK, Weller M, Heimberger AB. Immunosuppressive mechanisms in glioblastoma. *Neuro Oncol* 2015;17:vii9–14
- Humphries W, Wei J, Sampson JH, et al. The role of Tregs in glioma-mediated immunosuppression: Potential target for intervention. *Neurosurg Clin N Am* 2010;21:125–37
- Ooi YC, Tran P, Ung N, et al. The role of regulatory T-cells in glioma immunology. *Clin Neurol Neurosurg* 2014;119:125–32
- Zou W. Regulatory T cells, tumour immunity and immunotherapy. *Nat Rev Immunol* 2006;6:295–307
- Mougiakakos D, Choudhury A, Lladser A, et al. Regulatory T cells in cancer. *Adv Cancer Res* 2010;107:57–117
- Garden OA, Pinheiro D, Cunningham F. All creatures great and small: Regulatory T cells in mice, humans, dogs and other domestic animal species. *Int Immunopharmacol* 2011;11:576–88

33. Campbell DJ, Koch MA. Phenotypical and functional specialization of FOXP3⁺ regulatory T cells. *Nat Rev Immunol* 2011;11:119–30
34. Veiga-Parga T. Regulatory T cells and their role in animal disease. *Vet Pathol* 2016;53:737–45
35. Huang Y, Wang F, Wang Y, et al. Intrahepatic interleukin-17⁺ T cells and FoxP3⁺ regulatory T cells cooperate to promote development and affect the prognosis of hepatocellular carcinoma. *J Gastroenterol Hepatol* 2014;29:851–9
36. Zhu S, Lin J, Qiao G, et al. Differential regulation and function of tumor-infiltrating T cells in different stages of breast cancer patients. *Tumor Biol* 2015;36:7907–13
37. Wang L, Zhang B, Xu X, et al. Clinical significance of FOXP3 expression in human gliomas. *Clin Transl Oncol* 2014;16:36–43
38. Yue Q, Zhang X, Ye H, et al. The prognostic value of Foxp3⁺ tumor-infiltrating lymphocytes in patients with glioblastoma. *J Neurooncol* 2014;116:251–9
39. Wainwright DA, Dey M, Chang A, et al. Targeting tregs in malignant brain cancer: Overcoming IDO. *Front Immunol* 2013;4:1–17
40. Kurz SC, Wen PY. Quo vadis—do immunotherapies have a role in glioblastoma? *Curr Treat Options Neurol* 2018;20:1–23
41. Biller BJ, Guth A, Burton JH, et al. Decreased ratio of CD8⁺ T cells to regulatory T cells associated with decreased survival in dogs with osteosarcoma. *J Vet Intern Med* 2010;24:1118–23
42. Tominaga M, Horiuchi Y, Ichikawa M, et al. Flow cytometric analysis of peripheral blood and tumor-infiltrating regulatory T cells in dogs with oral malignant melanoma. *J Vet Diagn Invest* 2010;22:438–41
43. Porcellato I, Brachelente C, De Paolis L, et al. FoxP3 and IDO in canine melanocytic tumors. *Vet Pathol* 2019;56:189–99
44. Kim JH, Hur JH, Lee SM, et al. Correlation of Foxp3 positive regulatory T cells with prognostic factors in canine mammary carcinomas. *Vet J* 2012;193:222–7
45. Carvalho MI, Pires I, Prada J, et al. Intratumoral FoxP3 expression is associated with angiogenesis and prognosis in malignant canine mammary tumors. *Vet Immunol Immunopathol* 2016;178:1–9
46. Sayour EJ, McLendon P, McLendon R, et al. Increased proportion of FoxP3⁺ regulatory T cells in tumor infiltrating lymphocytes is associated with tumor recurrence and reduced survival in patients with glioblastoma. *Cancer Immunol Immunother* 2015;64:419–27
47. Heimberger AB, Abou-Ghazal M, Reina-Ortiz C, et al. Incidence and prognostic impact of FoxP3⁺ regulatory T cells in human gliomas. *Clin Cancer Res* 2008;14:5166–72
48. Han S, Zhang C, Li Q, et al. Tumour-infiltrating CD4⁺ and CD8⁺ lymphocytes as predictors of clinical outcome in glioma. *Br J Cancer* 2014;110:2560–8
49. See AP, Parker JJ, Waziri A. The role of regulatory T cells and microglia in glioblastoma-associated immunosuppression. *J Neurooncol* 2015;123:405–12
50. Sloma EA, Creneti CT, Erb HN, et al. Characterization of inflammatory changes associated with canine oligodendroglioma. *J Comp Pathol* 2015;153:92–100
51. Kmiecik J, Poli A, Brons NHC, et al. Elevated CD3⁺ and CD8⁺ tumor-infiltrating immune cells correlate with prolonged survival in glioblastoma patients despite integrated immunosuppressive mechanisms in the tumor microenvironment and at the systemic level. *J Neuroimmunol* 2013;264:71–83
52. Hussain SF, Yang D, Suki D, et al. The role of human glioma-infiltrating microglia/macrophages in mediating antitumor immune responses. *Neuro Oncol* 2006;8:261–79
53. Orrego E, Castaneda CA, Castillo M, et al. Distribution of tumor-infiltrating immune cells in glioblastoma. *CNS Oncol* 2018;7:CNS21
54. Rissi DR, Porter BF, Boudreau CE, et al. Immunohistochemical characterization of immune cell infiltration in feline glioma. *J Comp Pathol* 2018;160:15–22
55. Yang I, Han SJ, Sughrue ME, et al. Immune cell infiltrate differences in pilocytic astrocytoma and glioblastoma: Evidence of distinct immunological microenvironments that reflect tumor biology. *JNS* 2011;115:505–11
56. Jacobs JFM, Idema AJ, Bol KF, et al. Regulatory T cells and the PD-L1/PD-1 pathway mediate immune suppression in malignant human brain tumors. *Neuro Oncol* 2009;11:394–402
57. Ebert LM, Tan BS, Browning J, et al. The regulatory T cell-associated transcription factor FoxP3 is expressed by tumor cells. *Cancer Res* 2008;68:3001–9
58. Lohr J, Ratliff T, Huppertz A, et al. Effector T-cell infiltration positively impacts survival of glioblastoma patients and is impaired by tumor-derived TGF- β . *Clin Cancer Res* 2011;17:4296–308
59. Kim YH, Jung TY, Jung S, et al. Tumour-infiltrating T-cell subpopulations in glioblastomas. *Br J Neurosurg* 2012;26:21–7
60. Jacobs JFM, Idema AJ, Bol KF, et al. Prognostic significance and mechanism of Treg infiltration in human brain tumors. *J Neuroimmunol* 2010;225:195–9
61. Boozer LB, Davis TW, Borst LB, et al. Characterization of immune cell infiltration into canine intracranial meningiomas. *Vet Pathol* 2012;49:784–95
62. Pinheiro D, Chang Y-M, Bryant H, et al. Dissecting the regulatory microenvironment of a large animal model of Non-Hodgkin lymphoma: Evidence of a negative prognostic impact of FOXP3⁺ T cells in canine B cell lymphoma. *PLoS One* 2014;9:e105027–15

ARTICLE 3

Immunohistochemical study of programmed death ligand 1 expression and tumor-infiltrating lymphocytes in canine gliomas

Roberto José-López, Dolors Pi Castro, Edgar G. Manzanilla, Rodrigo Gutierrez-Quintana, Stefania Magnano, Luca Aresu, Richard Mellanby, Pavlina Zatloukalova, Borek Vojtesek, Ted Hupp, Paul M. Brennan, Martí Pumarola

Mouse and Comparative Pathology Unit, Department of Animal Medicine and Surgery, Veterinary Faculty, Universitat Autònoma de Barcelona, Bellaterra, Barcelona, Spain (R.J.L., D.P.C., M.P.); School of Veterinary Medicine, College of Medical, Veterinary and Life Sciences, University of Glasgow, Glasgow, UK (R.J.L., R.G.Q.); School of Veterinary Medicine, University College Dublin, Dublin, Ireland (E.G.M.); TEAGASC, The Irish Food and Agriculture Authority, Fermoy, Cork, Ireland (E.G.M.); Department of Veterinary Sciences, Università degli Studi di Torino, Grugliasco, Italy (L.A.); The Hospital for Small Animals, The Royal (Dick) School of Veterinary Studies, The University of Edinburgh, Midlothian (R.M); Research Centre for Applied Molecular Oncology, Masaryk Memorial Cancer Institute, Brno, Czech Republic (P.Z., B.V.); Institute of Genetics & Molecular Medicine, Edinburgh Cancer Research Centre, Edinburgh, UK (T.H.); Translational Neurosurgery, Centre for Clinical Brain Sciences, University of Edinburgh, Edinburgh, UK (P.M.B.); Networking Research Center on Bioengineering, Biomaterials and Nanomedicine (CIBER-BBN), Universitat Autònoma de Barcelona, Bellaterra, Barcelona, Spain (D.P.C., M.P.).

Running title: PD-L1 expression in canine gliomas

Corresponding author: Roberto José-López, DVM, Department of Animal Medicine and Surgery, Veterinary Faculty, Universitat Autònoma de Barcelona, Edifici V, Travessera dels Turons, 08193 Bellaterra, Barcelona, Spain (roberto.joselopez.bcn@gmail.com).

Keywords: astrocytoma, dog, immune checkpoint, oligodendroglioma, PD-1-PD-L1 axis.

Abstract

Background: Immune checkpoint inhibitors targeting programmed cell death protein 1 (PD-1) or its ligand (PD-L1) in human gliomas are intensely studied; however, preclinical promise in murine models of glioma has not translated into meaningful clinical responses in human patients. We assessed whether canine gliomas model the PD-1-PD-L1 immunomodulating pathway in human disease.

Methods: We analyzed immunohistochemical expression of PD-L1, PD-1, CD3 and CD20 in 21 spontaneous canine gliomas.

Results: PD-L1 expression of variable extent was observed in all glioma specimens and 19/21 (90.5%) were considered positive ($\geq 1\%$ PD-L1+ tumor cells [TCs]). Astrocytomas were associated with higher levels of intratumoral ($P = .014$) and infiltration zone ($P = .023$) expression than oligodendrogliomas. PD-L1+ TCs were less frequently found in the tumor core ($P < .001$) than in the tumor periphery and infiltration zone. Tumor-infiltrating lymphocytes (TILs) were found in all gliomas (CD3+ 21/21, 100%; PD-1+ 19/21, 90.5%; CD20+ 17/21, 81%). Intratumoral and infiltration zone PD-1+ TIL density correlated positively with intratumoral and infiltration zone CD3+ TIL density ($P = .002$; $P = .009$, respectively). A positive correlation ($P = .030$) between PD-1+ TIL density in the tumor infiltration zone and previously reported FOXP3+ TIL accumulation in this same cohort was found.

Conclusions: PD-1 and PD-L1 are immunohistochemically detectable in canine gliomas of different types and grades, demonstrating that spontaneous canine glioma is closer than mice modelling this mechanism of immune evasion in the human counterpart. This supports the use of canine gliomas in translational human studies.

Introduction

The incidence of adult canine brain tumors is 2.8-4.5% of all tumors diagnosed at necropsy, compared with a human incidence of 1.3-2% of all cancers.¹⁻⁵ Although individual studies vary, gliomas represent 36-70% of primary brain tumors in dogs.^{4,6} Consequently, canine glioma is increasingly recognized as a naturally occurring model for human glioma. Benefits include the size and structure of the canine brain, phylogenetically closer to the human brain than the mouse counterpart, the incidence of spontaneously developing gliomas, and the coexistence with an active immune system, as opposed to the most often used immunodeficient murine xenotransplant model.⁷

As in the human counterpart, canine glioma occurs in middle- to old-age patients (median age at diagnosis is 8 years), it shows a male sex predilection (1.28-1.53 males to females ratio), and predominant lesion location includes the fronto-olfactory, temporal and parietal lobes of the brain.^{3,4,8,9} Over 50% of all gliomas in dogs occur in certain brachycephalic breeds belonging to the same phylogenetic clade.^{3,4,8-10} Among these, the Boston Terrier, Bulldog and Boxer breeds have a higher prevalence of oligodendroglioma.⁸ In general, high-grade gliomas are considerably more frequent than low-grade gliomas in humans and in dogs.^{8,9,11} Advances in molecular genetics and biology in recent years have enhanced the understanding and subclassification of human gliomas, leading to an updated edition of the WHO brain tumor classification in 2016.¹² The NCI's Comparative Brain Tumor Consortium (CBTC) subsequently revised the diagnostic classification of canine gliomas in 2018.⁸ The aim was to provide an updated canine-specific schema for clinical and molecular data to be added into a morphologic diagnosis, to assist with prediction of tumor behavior and to facilitate translational research.

However, despite their histopathologic similarities, parallelisms with some of the most common molecular abnormalities found in human gliomas, the isocitrate dehydrogenase and

1p/19q phenomena,¹² have not been found in dogs.¹³⁻¹⁷ Furthermore, no associations were found between canine glioma type or grade and outcome after treatment, in a recent study,⁹ unlike in humans.

The poor prognosis associated with human high-grade gliomas has been linked to evasion of the immune system that limits an effective antitumoral response.¹⁸ Despite the apparent tumor molecular differences between species, antitumor immune response escape might also play a role in canine gliomas.¹⁹⁻²¹

Programmed cell death protein 1 (PD-1), a cell surface co-inhibitory receptor expressed on CD3+/CD8+ T-cells, and its ligand, programmed death ligand 1 (PD-L1), play a pivotal role in the ability of tumor cells (TCs) to evade the host's immune system.²² Under physiological conditions, the PD-1-PD-L1 axis acts as an immune checkpoint to control autoimmunity.^{22,23} Binding of PD-1 to PD-L1 inhibits activated effector T-cell proliferation and cytokine production, leading to functional exhaustion and apoptosis.^{22,24} Human gliomas exploit this immune inhibitory mechanism to maintain an immunosuppressive microenvironment and evade immune eradication.²⁵⁻³⁴ TCs evade host's immune attack by expressing PD-L1 and stimulating PD-1 expression on tumor-infiltrating lymphocytes (TILs).²³ Additionally, glioma-related PD-L1 expression induces regulatory T-cells (Tregs), further suppressing immune reactivity.³⁵

Human high-grade and astrocytic gliomas express higher levels of PD-L1,²⁶⁻²⁸ and increased levels of expression are associated with poorer prognosis.³²⁻³⁴ A phase III human clinical trial recently failed to reproduce the success shown by immunotherapeutic targeting of the PD-1-PD-L1 axis in preclinical studies with murine models of glioma,^{36,37} possibly because of the limited ability of murine models of glioma to accurately recapitulate spontaneous human disease, not least the complexities within the immunosuppressive tumor microenvironment.⁷

By contrast, dogs spontaneously develop glioma and TILs, increasing levels of Tregs in high-grade and astrocytic tumors, as well as tumoral PD-L1 expression and presence of PD-1+ T-cells in oligodendrogliomas, have been described.¹⁹⁻²¹ Thus, spontaneous canine glioma may provide a useful model for immunotherapeutic studies to treat human patients.

Systematic studies on the expression of PD-L1 in canine gliomas are lacking. We aimed to characterize immunohistochemical expression of PD-L1 and its association with PD-1 expression in TILs and other tissue-based parameters in a case series of canine gliomas of different types and grades. We investigated associations between PD-L1 expression and tumor type and grade. We define a standardized protocol for immunohistochemical analysis in these tumors.

Materials and methods

Patients and materials

We retrospectively identified formalin-fixed paraffin-embedded (FFPE) tumor tissue specimens of 21 canine gliomas diagnosed between 2008 and 2017 at the Department of Animal Medicine and Surgery, Veterinary Faculty, Universitat Autònoma de Barcelona, Spain (n = 9), the School of Veterinary Medicine, University of Glasgow, UK (n = 8), and Patologia Veterinaria, Università degli Studi di Perugia, Italy (n = 4). Samples were obtained at necropsy within 24 hours from death and fixed in 10% neutral buffered formalin. Fixation times varied because of the multicentric and retrospective nature of the study; however, this was always <5 days. Following fixation, transverse sections of the brain or spinal cord were made and samples including the tumor area were processed. Morphologic evaluation was performed on 5µm paraffin-embedded sections stained with hematoxylin and eosin.

Histological diagnosis of glioma type and grade was performed according to the CBTC diagnostic schema by a board-certified veterinary pathologist with expertise in canine

neuropathology (M.P.).⁸ When available, samples were further evaluated by immunohistochemistry for glial fibrillary acidic protein (GFAP) and Olig2 protein. Clinical data was extracted by patient medical records review. The Research Ethics Committee of the School of Veterinary Medicine of the University of Glasgow approved the study (Ref EA16/20).

Immunohistochemical staining

Immunohistochemistry for PD-L1, PD-1, CD3 and CD20 was performed. For immunostaining, serial 5µm sections of the FFPE blocks were deparaffinized in xylene and rehydrated through graded alcohols (100%, 96-50%). Endogenous peroxidase activity was blocked by immersion in 3% peroxide hydrogen for 40 minutes at room temperature (RT). Nonspecific binding was blocked by 30% normal goat serum diluted with PBS for 1 hour at RT. Samples were incubated overnight with the respective primary antibody at 4°C. Antibodies and immunostaining protocols are listed in Supplementary Table 1. For PD-1 staining we used a canine-specific anti-PD-1 antibody (PD-1-1.1). Binding specificity was validated as specified in Fig. 1. Sections were then rinsed with PBS and incubated for 40 minutes at RT with a labeled polymer according to the manufacturer's instructions (Labeled Polymer – Dako REAL Envision-HRP, Dako). Staining was completed by 10-minute incubation with 3, 3'-diaminobenzidine (DAB, Dako) and counterstaining with hematoxylin for 3 seconds. Immunostaining was performed on adjacent sections to facilitate comparison of regional distributions of PD-L1 expression and TIL infiltration.²⁹ FFPE tissue sections of normal canine peripheral lymph nodes and tonsil (TILs) and a young dog's thymus (PD-L1) were used as positive controls. For the negative control, the same specimens were used omitting the primary antibody.

The immunohistochemical study for GFAP and Olig2 was performed according to a previously described protocol.³⁸ Normal astrocytes and oligodendrocytes in non-neoplastic canine cerebrum were used as controls for GFAP and Olig2, respectively.

Evaluation of immunohistochemical data

Stained tumor slides were digitized for assessment using image analysis software (NanoZoomer Digital Pathology.view2; Hamamatsu). Evaluation was performed by a trained observer (R.J.L.), blinded to tumor type and grade information, and supervised by a board-certified veterinary pathologist (M.P.) to ultimately reach a consensus between both observers. All available tumor tissue was evaluated to descriptively record expression of PD-L1 by TCs and PD-1 by TILs according to the cellular and topographical localization of the immunohistochemical signal.²⁹ Distribution of CD3+ and CD20+ TIL subsets, corresponding to T- and B-lymphocytes, respectively, was also assessed to further characterize the TIL population in the same areas.²⁹

Subsequently, areas of maximal PD-L1 labeling were sought for quantification.²⁷ Three areas of 3.14mm² including tumor-rich tissue,³¹ infiltration zone and adjacent CNS were then selected and within each of these locations, 4 areas of 0.025mm² were quantified under high-power magnification (400X). For each area, the number of PD-L1+ TCs and PD-1+, CD3+, and CD20+ TILs was manually determined in adjacent tissue sections. A mean value was obtained for PD-L1 expression and TIL counts of all areas assessed in each tumor and this was finally expressed as the percentage of positive cells over all nucleated cells in the same areas^{27,31} for each glioma region (intratumoral, infiltration zone and surrounding CNS). The infiltration zone was determined manually as the region between tumor-rich tissue and normal CNS parenchyma, where abundant tumor cells were still interspersed with neurons and/or neuropil.

Tumors were considered positive for PD-L1 expression if there was staining of cytoplasm or membranes in $\geq 1\%$ TCs within the studied area.³⁰ The percentage of PD-L1+ TCs in tumor-rich and infiltration areas was scored semiquantitatively as follows³⁹: 0, $<1\%$ PD-L1+ TCs (negative sample); 1, $\geq 1\%$ but $< 5\%$ PD-L1+ TCs (weak positive); 2, $\geq 5\%$ but $< 50\%$ PD-L1+ TCs (moderate); 3, $\geq 50\%$ PD-L1+ TCs (strong positive). PD-1 expression was regarded as positive if staining was observed in the cytoplasm or membranes of $\geq 1\%$ TILs, and this was further scored as³⁹: 0, $<1\%$ PD-1+ TILs (negative sample); 1, $\geq 1\%$ but $< 5\%$ PD-1+ TILs (weak positive); 2, $\geq 5\%$ but $< 10\%$ PD-1+ TILs (moderate); 3, $\geq 10\%$ PD-1+ TILs (strong positive).

Statistical analyses

All statistical analyses were carried out with SAS 9.4 (SAS Institute, Cary, NC). Alpha for determination of significance was 0.05 and trends are reported for alpha 0.10. Differences between grade and type in the different variables were analyzed using non-parametric tests (Wilcoxon-Mann-Whitney and Kruskal Wallis). Differences in PD-L1 immunopositivity within different locations was analyzed using Fisher's exact test. The correlation between the different variables was analyzed using Spearman's correlation.

Results

Clinicopathologic features

Data including dog demographics and tumor location are listed in Table 1. Of the twenty-one gliomas included in this study, 8 (38.1%) were classified as high-grade astrocytoma (HA), 8 (38.1%) as high-grade oligodendroglioma (HO), 2 (9.5%) as high-grade undefined glioma (HU), 2 (9.5%) as low-grade astrocytoma (LA), and 1 (4.8%) as low-grade oligodendroglioma (LO). Tumors were graded based on their morphologic features as per the

CBTC schema and further classified based on immunoreactivity against GFAP and Olig2 on >50% of TCs, respectively.

PD-L1 Expression

All included gliomas contained PD-L1+ TCs. However, 2 HOs contained <1% PD-L1+ TCs and were regarded as negative on semiquantitative assessment. Table 2 details the results of evaluation of PD-L1 expression by tumor type and grade. Astrocytomas were associated with higher levels of expression intratumorally ($P = .014$) and in the infiltration zone ($P = .023$) than oligodendrogliomas (Fig. 2A and B). No associations were found with tumor grade. TCs displayed a predominantly granular or diffuse PD-L1 cytoplasmic staining in all gliomas, and incomplete membranous immunolabelling was seen in 12/21 (57.1%). PD-L1 expression was typically found in a patchy distribution throughout the tumor tissue although was significantly ($P < .001$) less frequent in the tumor core (11/21, 52.4%; Fig. 2C) than in the tumor periphery (Fig. 2D) and infiltration zone (all cases, respectively), or perivascular (19/21, 90.5%). Scattered PD-L1+ TCs were occasionally seen in the CNS parenchyma adjacent to the infiltration zone in 14/21 (66.7%) gliomas.

We found diffuse or granular PD-L1 cytoplasmic staining in TILs in 17/21 (81%) gliomas (Fig. 2E and F). Occasional PD-L1+ microglia/macrophages were noted in 8/21 (38.1%) specimens.

Evaluation of the surrounding CNS parenchyma showed mostly faint granular cytoplasmic anti-PD-L1 staining of neurons and astrocytes in 20/21 (95.2%) and 17/21 (81%) cases, respectively.

PD-1 Expression and Tumor-infiltrating Lymphocytes

TIL infiltration of variable density was observed in all gliomas (Fig. 3A-C). CD3+ TILs were the most abundant and were detected in all tumors, whereas CD20+ TILs were only present

in 17/21 (81%) specimens. PD-1+ TILs were found in 19/21 (90.5%) gliomas; however, only 4/21 (19%) were regarded as positive for PD-1 expression ($\geq 1\%$ PD-1+ TILs).

TIL infiltration was generally of sparse-to-moderate density, and TILs were mainly located in perivascular areas of the tumor periphery and infiltration zone. TILs were only found infrequently within the tumor core, either scattered or perivascular. High-grade gliomas were associated with accumulation of CD3+ TILs in their infiltration zone ($P = .034$). Table 3 shows the results of evaluation of PD-1 expression and the density and distribution of the different TIL subsets by tumor type and grade.

Granular cytoplasmic and/or incomplete membranous PD-1 staining of TCs (Fig. 3E) was observed in 17/21 (81%) gliomas, all high-grade; and PD-1+ macrophages/microglia (Fig. 3F) were seen in 6/21 (28.6%) tumors.

Comparison of the Spatial Distribution of Tissue-based Parameters

Comparative evaluation of the spatial distribution of the various TIL subsets on adjacent sections showed regional overlap of TIL infiltration as CD3+ and PD-1+ TILs were evident in the same areas in consecutive sections (19/21 [90.5%]; Fig. 3A and B). Regional overlap of TIL infiltration and PD-L1 expression was frequent (14/21 [66.7%]; Fig. 3A-D). In the cases containing PD-1+ TILs, these were often observed in the immediate proximity to PD-L1+ TCs (9/19 [47.4%]; Fig. 3B and D).

Correlation of Tissue-based Parameters

Intratumoral PD-1+ TIL density correlated positively with intratumoral CD3+ ($P = .002$) and CD20+ ($P = .046$) TIL density. PD-1+ TIL density in the zone of tumor infiltration into the CNS parenchyma was positively correlated with intratumoral ($P < .001$) and infiltration zone ($P = .009$) CD3+ TIL density as well as intratumoral CD20+ TIL density ($P = .004$). We also found a positive correlation ($P = .030$) between PD-1+ TIL density in the tumor infiltration

zone and previously reported FOXP3⁺ Tregs accumulation in the intratumoral and infiltration zones of this cohort of canine gliomas.²⁰

PD-L1 expression intratumorally and in the infiltration zone was not correlated with PD1⁺, CD3⁺, and CD20⁺ TIL density in the same corresponding regions. Only PD-L1 expression in TCs scattered into the CNS parenchyma surrounding the tumor correlated positively with PD-1⁺ TIL density in that same area ($P = .018$). There was also a trend to correlation between intratumoral ($P = .073$) and infiltration zone ($P = .094$) PD-L1 expression and previously reported FOXP3⁺ TILs.²⁰

Discussion

The PD-1-PD-L1 axis is considered central to human glioma immune evasion and its immunotherapeutic targeting is intensely studied. However, murine models of glioma have failed to predict clinical responses in human patients.^{36,37} By contrast, spontaneous canine glioma which shares the poor prognosis associated with the current standard of care in the human counterpart,^{9,40} may model immune escape in human glioma with greater fidelity.¹⁹⁻²¹ Here we show expression of PD-L1 by TCs in different types and grades of spontaneous canine glioma. Additionally, we developed and validated a canine-specific anti-PD-1 antibody, critical for the immunohistochemical study of canine glioma as a model for the PD-1-PD-L1 immunomodulating pathway in human gliomas. This allowed us to characterize PD-1⁺ TIL infiltration in this series of canine gliomas along with the CD3⁺ and CD20⁺ TIL subsets and their correlations. Correlations with previously reported FOXP3⁺ Tregs in this same cohort are also described.

We observed PD-L1 expression in all glioma specimens included here in agreement with results of RNA in situ hybridization in a previous series of canine oligodendrogliomas.¹⁹ The main PD-L1 expression pattern in canine glioma TCs consisted of granular and/or diffuse

cytoplasmic staining, observed in all cases, with interspersed incomplete membranous immunostaining in 57.1% tumors. Concomitant cytoplasmic and membranous PD-L1 expression of varying predominance has been reported in human gliomas.^{25-27,29,31,32,34} This variability in cellular localization of expression is suspected to relate to the heterogeneous microarchitecture of these tumors as well as potentially internalized surface PD-L1 molecules for storage and degradation in lysosomes.²⁹

In human glioma studies, various methods with numerous antibodies have been used to immunohistochemically detect PD-L1 expression, leading to a lack of consensus for interpretation of positivity.²⁵⁻³⁴ Cutpoints for positivity in previous studies ranged from >1% to >5% TCs showing immunoreactivity to PD-L1 in their membranes, cytoplasm or both.^{28,30,32,34} Several semiquantitative methods stratifying results into groups of percent positivity of TCs or tumor area rather than using a single cutoff have also been reported.^{25,26,29} These same issues apply to interpretation of positivity for PD-1 expression in TILs.^{28,30,31} Thus, we decided to adopt an immunoreactivity scoring system used for non-small cell lung carcinoma, another malignancy with well characterized PD-L1 and PD-1 expression and a more harmonized semiquantitative classification method.³⁹

Most tumors included here contained $\geq 1\%$ PD-L1+ TCs within the studied areas, with the majority showing moderate intratumoral expression ($\geq 5\%$ but $< 50\%$ PD-L1+ TCs). PD-L1 expression in human glioma patients is frequent and is confined to a minority subpopulation of TCs. It is possible that in dogs as in humans, a small amount of PD-L1 expression could be sufficient to restrain the immune system.³³

As in human high-grade and astrocytic gliomas, in particular glioblastomas,²⁶⁻²⁸ canine HAs expressed higher levels of PD-L1 than any other tumor type and grade; however, expression in this series of canine gliomas was associated with tumor astrocytic lineage rather than grade.

Notably, PD-L1+ TILs and microglia/macrophages were also found in this study, resembling these observations in humans.^{26,27,29,30,33,34} PD-L1 expression in naïve T-cells has been shown to play a role in dendritic cell maturation, while its expression by Tregs further suppresses effector T-cell function.^{18,33,41} Furthermore, human gliomas also promote immunosuppression by inducing PD-L1 expression in tumor-associated macrophages.⁴² Finally, granular cytoplasmic PD-L1 staining of neurons and astrocytes in the adjacent CNS parenchyma, as described in human glioblastomas, was noted in most cases.²⁹ Glial cells (astrocytes, microglia, oligodendrocytes) and neurons have been shown to express low or undetectable PD-L1 under basal conditions but are able to upregulate PD-L1 in response to cytokine release in neuroinflammatory processes.⁴³

As previously reported in canine and human gliomas, TILs could be seen scattered throughout the tumor tissue, though they tended to cluster around normal and glomeruloid vasculature in the tumor margins and infiltration zone, and CD3+ TILs were present in higher numbers than CD20+ TILs.^{20,21,29,44,45} Despite different methodologies, our previous study on TILs in canine gliomas as well as the present one, suggest an association between increased CD3+ TIL counts and canine high-grade glioma similar to that described in humans; however, this was not found in a larger canine study.^{20,21,45} CD3+/CD8+ T-cells are the primary effectors of host antitumor immune responses and human studies have shown a predominance of CD8+ TILs within the T-cell subset, suggesting an attempt at a cytotoxic response that is ultimately unsuccessful.^{45,46} Absence of antibodies suitable for use in FFPE tissue sections prevented further subset analysis in our samples, although a study of canine gliomas using in situ hybridization showed a greater presence of CD8+ than CD4+ TILs.¹⁹ In this study, PD-1+ TIL numbers correlated positively with increasing CD3+ and CD20+ TIL infiltrates. In particular, strong positive correlations were found between PD-1+ TIL counts and CD3+ TIL density intratumorally and in the infiltration zone, indicating T-cell

exhaustion. This resembles observations in humans and demonstrates this pathophysiological mechanism of cytotoxic attack evasion in canine gliomas.²⁹ Additionally, intratumoral PD-1+ TIL density was positively correlated with greater presence of FOXP3+ Tregs in this cohort, further suggesting Treg infiltration may also contribute to effector T-cell inhibition in canine gliomas. Conversely, the reported association between PD-L1 expression and FOXP3+ TIL accumulation in human gliomas could not be demonstrated here though we found a trend to correlation.³⁵

Gliomas included herein were evaluated post-mortem, thus, we were able to assess whole size FFPE tumor sections to characterize the topographical distribution of PD-L1 expression and TILs. PD-L1+ TCs were significantly less frequently encountered in the tumor core than in the tumor margins and infiltration zone where they seemed to accumulate, mirroring the situation in humans.^{27,30} Regional overlap between TILs and PD-L1+ TCs was frequent. Also, when present, PD-1+ TILs were often near areas of PD-L1 expression, suggesting canine gliomas express PD-L1 in TCs at the forefront of inflammation to escape the host's antitumoral response.

The above findings also indicate that surgical biopsy planning of canine gliomas included in translational clinical trials targeting the PD-1-PD-L1 immune checkpoint, should comprise the tumor periphery. Likewise, whole slide sections may be preferable for immunohistochemical analysis of PD-L1 expression in canine gliomas as ability to detect it in tissue microarrays may be limited by its focal and patchy distribution.

Occasional PD-1+ microglia/macrophages have been reported in human glioblastomas.³⁴ Similarly, these were only present in canine high-grade gliomas in this study, predominantly HAs. Finally, PD-1+ cells with clear tumoral morphology were found in most of our canine high-grade gliomas. Interestingly, PD-1+ TC subpopulations have been described in murine and human melanomas and reported to promote tumorigenesis.⁴⁷

This study is limited by its retrospective nature and the sample size. Thus, larger and prospectively collected cohorts are necessary to confirm our findings and to clarify whether canine glioma-related PD-L1 expression could be associated with tumor grade, PD-1+ TIL density, Tregs intratumoral accumulation, outcome, or any other clinical parameter. In conclusion, this analysis shows that PD-1 and/or PD-L1 are immunohistochemically detectable in canine gliomas of different types and grades, demonstrating that spontaneous canine glioma models this mechanism of immune evasion in the human counterpart. This supports the use of canine gliomas in translational immunotherapeutic studies to improve the success of subsequent human clinical trials.

Funding: This work was partially supported by a grant from the University of Glasgow, Small Animal Hospital Fund (145973-02). P.Z. and B.V. were supported by the European Regional Development Fund - Project ENOCH (No.CZ.02.1.01/0.0/0.0/16_019/0000868) and by the Ministry of Health Development of Research Organization, MH CZ - DRO (MMCI, 00209805) to produce the canine-specific anti-PD-1 antibodies.

Acknowledgements: We thank Ester Blasco and Tamara Rivero for technical assistance.

Conflict of interest statement: B.V. is a consultant for Moravian-biotechnology, who originally produced the PD-1-1.1 and PD-1-2.1 monoclonal antibodies used in this study. The company did not provide financial support or have any influence over the design, execution, or interpretation of the data.

References

1. Klotz, M. Incidence of brain tumors in patients hospitalized for chronic mental disorders. *Psych Quar.* 1957;31:669-680.
2. Siegel RL, Miller KD, Fuchs HE, Jemal A. Cancer statistics, 2021. *Ca Cancer J Clin.* 2021;71:7-33.
3. Dorn CR, Taylor DO, Frye FL, et al. Survey of animal neoplasms in Alameda and Contra Costa counties, California. Methodology and description of cases. *J Natl Cancer Inst.* 1968;40:295-305.
4. McGrath JT. Intracranial pathology in the dog. *Acta Neuropathol.* 1962;1(suppl.I):3-4.
5. Song RB, Vite CH, Bradle CW, Cross JR. Postmortem evaluation of 435 cases of intracranial neoplasia in dogs and relationship of neoplasm with breed, age and body weight. *J Vet Intern Med.* 2013;27:1143-1152.
6. Snyder JM, Shofer FS, Van Winkle TJ, Massicotte C. Canine intracranial primary neoplasia: 173 cases (1986-2003). *J Vet Intern Med.* 2008;22:172-177.
7. Chen L, Zhang Y, Yang J, Hagan JP, Li M. Vertebrate animal models of glioma: understanding the mechanisms and developing new therapies. *Biochim Biophys Acta.* 2013;1836:158-165.
8. Koehler JW, Miller AD, Miller CR, et al. A revised diagnostic classification of canine glioma: towards validation of the canine glioma patient as a naturally occurring preclinical model for human glioma. *J Neuropathol Exp Neurol.* 2018;77(11):1039-1054.
9. José-López R, Gutierrez-Quintana R, De la Fuente C, et al. Canine gliomas: clinical features, diagnosis and survival analysis. *J Vet Intern Med.* 2021;35(4):1902-1917.
10. Parker HG, Dreger DL, Rimbault M, et al. Genomic analyses reveal the influence of geographic origin, migration, and hybridization on modern dog breed development. *Cell Rep.* 2017;19:697–708.

11. Ostrom QT, Cioffi G, Gittleman H, et al. CBTRUS statistical report: primary brain and other central nervous system tumors diagnosed in the United States in 2012-2016. *Neuro Oncol.* 2019;21(suppl.5):v1-v100.
12. Louis DN, Ohgaki H, Wiestler, OD, et al. The 2016 world health organization classification of tumors of the central nervous system: a summary. *Acta Neuropathol.* 2016;131(6):803-820.
13. Kawakami S, Ochiai K, Azakami D, et al. R132 mutations in canine isocitrate dehydrogenase 1 (IDH1) lead to functional changes. *Vet Res Commun.* 2018;42:49-56.
14. Fraser AR, Bacci B, Chevoir MA, et al. Isocitrate dehydrogenase 1 expression in canine gliomas. *J Comp Pathol.* 2018;165:33-39.
15. Reitman ZJ, Olby NJ, Mariani CL, et al. IDH1 and IDH2 hotspot mutations are not found in canine glioma. *Int J Cancer.* 2010;127:245-246.
16. Amin SB, Anderson KJ, Boudreau CE, et al. Comparative molecular life history of spontaneous canine and human gliomas. *Cancer Cell.* 2020;37:243-257.e7.
17. Thomas R, Duke SE, Wang HJ, et al. ‘Putting our heads together’: insights into genomic conservation between human and canine intracranial tumors. *J Neurooncol.* 2009;94:333-349.
18. Nduom EK, Weller M, Heimberger AB. Immunosuppressive mechanisms in glioblastoma. *Neuro Oncol.* 2015;17(suppl.7):vii9-vii14.
19. Filley A, Henriquez M, Bhowmik T, et al. Immunologic and gene expression profiles of spontaneous canine oligodendrogliomas. *J Neurooncol.* 2018;137(3):469-479.
20. Pi Castro D, José-López R, Fernández Flores F, et al. Expression of FOXP3 in canine gliomas: immunohistochemical study of tumor-infiltrating regulatory lymphocytes. *J Neuropathol Exp Neurol.* 2020;79(2):184-193.

21. Krane GA, O'Dea CA, Malarkey DE, et al. Immunohistochemical evaluation of immune cell infiltration in canine gliomas. *Vet Pathol.* 2021; doi:10.1177/03009858211023946.
22. McDermott DF, Atkins MB. PD-1 as a potential target in cancer therapy. *Cancer Med.* 2013;2(5):662-673.
23. Chikuma S. Basics of PD-1 in self-tolerance, infection, and cancer immunity. *Int J Clin Oncol.* 2016;21:448-455.
24. Dong H, Strome SE, Salomao DR, et al. Tumor-associated B7-H1 promotes T-cell apoptosis: a potential mechanism of immune evasion. *Nat Med.* 2002;8(8):793–800.
25. Wintterle S, Schreiner B, Mitsdoerffer M, et al. Expression of the B7-related molecule B7-H1 by glioma cells: a potential mechanism of immune paralysis. *Cancer Res.* 2003;63:7462-7467.
26. Wilmotte R, Burkhardt K, Kindler V, et al. B7-homolog 1 expression by human glioma: a new mechanism of immune evasion. *Neuroreport.* 2005;16:1081-1085.
27. Yao Y, Tao R, Wang Y, et al. B7-H1 is correlated with malignancy-grade gliomas but is not expressed exclusively on tumor stem-like cells. *Neuro Oncol.* 2009;11:757-766.
28. Garber ST, Hashimoto Y, Weathers SP, et al. Immune checkpoint blockade as a potential therapeutic target: surveying CNS malignancies. *Neuro Oncol.* 2016;18(10):1357-1366.
29. Berghoff AS, Kiesel B, Widhalm G, et al. Programmed death ligand 1 expression and tumor-infiltrating lymphocytes in glioblastoma. *Neuro Oncol.* 2015;17(8):1064-1075.
30. Majzner RG, Simon JS, Grosso JF, et al. Assessment of programmed death-ligand 1 expression and tumor-associated immune cells in pediatric cancer tissues. *Cancer.* 2017;123:3807-3815.
31. Rahman M, Kresak J, Yang C, et al. Analysis of immunologic markers in primary and recurrent glioblastoma. *J Neurooncol.* 2018;137(2):249-257.
32. Zeng J, Zhang XK, Chen HD, et al. Expression of programmed cell death-ligand 1 and its correlation with clinical outcomes in gliomas. *Oncotarget.* 2016;7(8):8944:8955.

33. Nduom EK, Wei J, Yaghi NK, et al. PD-L1 expression and prognostic impact in glioblastoma. *Neuro Oncol.* 2016;18(2):195-205.
34. Han J, Hong Y, Lee YS. PD-L1 expression and combined status of PD-L1/PD-1-positive tumor infiltrating mononuclear cell density predict prognosis in glioblastoma patients. *J Pathol Transl Med.* 2017;51(1):40-48.
35. DiDomenico J, Lamano JB, Oyon D, et al. The immune checkpoint protein PD-L1 induces and maintains regulatory T cells in glioblastoma. *Oncoimmunology.* 2018;7(7):e1448329.
36. Reardon DA, Gokhale PC, Klein SR, et al. Glioblastoma eradication following immune checkpoint blockade in an orthotopic, immunocompetent model. *Cancer Immunol Res.* 2016;4(2):124-135.
37. Reardon DA, Brandes AA, Omuro A, et al. Effect of nivolumab vs bevacizumab in patients with recurrent glioblastoma: the CheckMate 143 phase 3 randomized clinical trial. *JAMA Oncol.* 2020;6(7):1003-1010.
38. Fernández F, Deviers A, Dally C, et al. Presence of neural progenitors in spontaneous canine gliomas: a histopathological and immunohistochemical study of 20 cases. *Vet J.* 2016;209:125-132.
39. Monroig-Bosque P, Driver B, Morales-Rosado JA, et al. Correlation between programmed death receptor-1 expression in tumor-infiltrating lymphocytes and programmed death ligand-1 expression in non-small cell lung carcinoma. *Arch Pathol Lab Med.* 2018;142(11):1388-1393.
40. Ostrom QT, Bauchet L, Davis FG, et al. The epidemiology of glioma in adults: a “state of the science” review. *Neuro Oncol.* 2014;16(7):896-913.

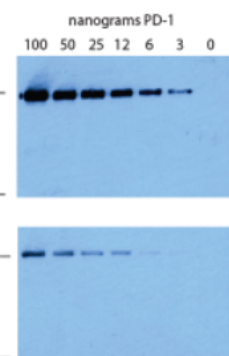
41. Talay O, Shen CH, Chen L, Chen J. B7-H1 (PD-L1) on T cells is required for T-cell-mediated conditioning of dendritic cell maturation. *Proc Natl Acad Sci USA*. 2009;106(8):2741-2746.
42. Bloch O, Crane CA, Kaur R, et al. Gliomas promote immunosuppression through induction of B7-H1 expression in tumor-associated macrophages. *Clin Cancer Res*. 2013;19(12):3165-3175.
43. Pitter CL, Newcombe J, Antel JP, Arbour N. The majority of infiltrating CD8T lymphocytes in multiple sclerosis lesions is insensitive to enhanced PD-L1 levels on CNS cells. *Glia*. 2011;59(5):841-856.
44. Sloma EA, Creneti CT, Erb HN, Miller AD. Characterization of inflammatory changes associated with canine oligodendroglioma. *J Comp Pathol*. 2015;153(2-3):92-100.
45. Yang I, Han SJ, Sughrue ME, Tihan T, Parsa AT. Immune cell infiltrate differences in pilocytic astrocytoma and glioblastoma: evidence of distinct immunological microenvironments that reflect tumor biology. *J Neurosurg*. 2011;115(3):505-511.
46. Kim YH, Jung TY, Jung S, et al. Tumor-infiltrating T-cell subpopulations in glioblastomas. *Br J Neurosurg*. 2012;26(1):21-27.
47. Keffel S, Posch C, Barthel SR, et al. Melanoma cell-intrinsic PD-1 receptor functions promote tumor growth. *Cell*. 2015;162:1242-1256.

Figure captions

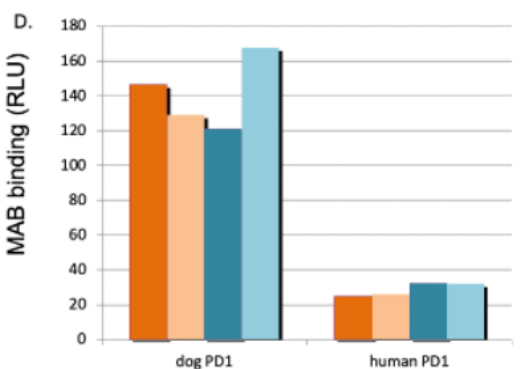
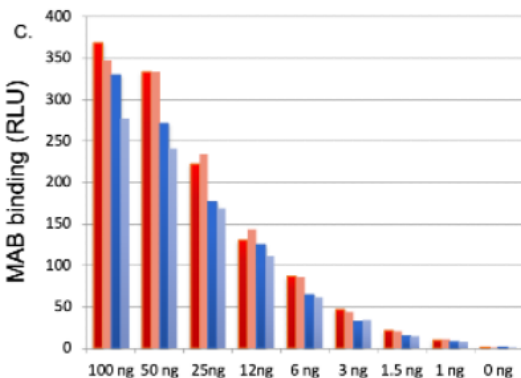
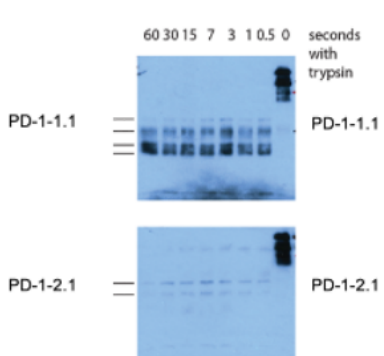
Figure 1. Canine-specific anti-PD-1 antibody binding specificity validation. Two hybridomas were obtained from the fusion, named PD-1-1.1 and PD-1-2.1. A and B, Western blot. A, Increasing amounts of recombinant PD-1 were immunoblotted against each purified monoclonal antibody (at 1µg/mL). The data demonstrate a higher affinity of PD-1-1.1 for PD-1 based on the increased sensitivity in detection of lower levels of recombinant PD-1 protein (3ng). B, The PD-1 was left un-trypsinized (right lanes) or incubated in PBS buffer with 1ng of trypsin for the indicated time points. Samples were quenched with SDS sample buffer and were immunoblotted against each purified monoclonal antibody (at 1µg/mL). Blots were processed using peroxidase conjugated secondary antibodies with ECL (NA935, Cytiva). The data demonstrate that PD-1-1.1 can detect fragmented polypeptides of a mass of approximately 27kDa, whilst the epitope of PD-1-2.1 is essentially destroyed by the tryptic cleavage. The data indicate that the two antibodies can detect relatively different epitopes in PD-1. C, Two clones of PD-1-1.1 and PD-1-2.1 were tested for binding to different amounts of canine PD-1 coated onto ELISA wells with a sensitivity down to 1ng of protein. D, Canine or human PD-1 were coated onto ELISA wells and two clones of PD-1-1.1 and PD-1-2.1 were tested for binding to both species. The IgG is relatively specific for canine PD-1. E-H, Canine peripheral blood mononuclear cells were isolated and left unstimulated or stimulated with increasing levels of Concanavalin A. Cells were incubated with either human anti-PD-1 IgG (E), PD-1-1.1 (F), or PD-1-2.1 (G), and then secondary fluorescent antibodies to mouse IgG (including isotype controls). The data quantify IgG binding to unstimulated and stimulated CD4⁺ and CD8⁺ canine cell populations. H, A summary of the relative binding of the indicated IgG to stimulated canine T-cells. The data demonstrate that PD-1-1.1 binds to more cell numbers than PD-1-2.1, which is consistent with its marginally higher affinity by ELISA. I-L, The produced monoclonal antibodies were evaluated by immunohistochemistry

in normal canine tonsil (scale bars, 500µm, I and J) and lymph node (scale bars, 100µm, K and L) FFPE, demonstrating that the canine-specific anti-PD-1 antibodies can detect a subset of immune cells in normal tissue with superior immunostaining for PD-1-1.1.

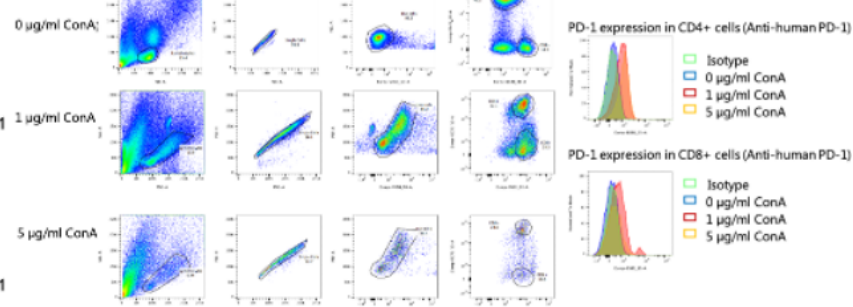
A. Antigen titration



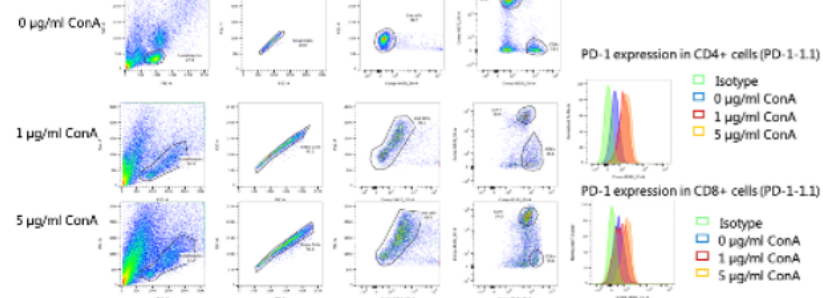
B. Effects of trypsin on epitope fragments



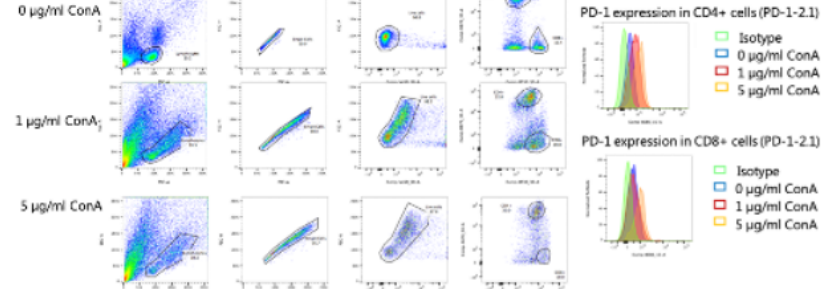
E.



F.



G.



H.

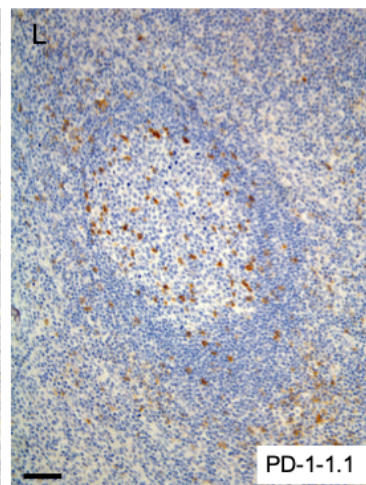
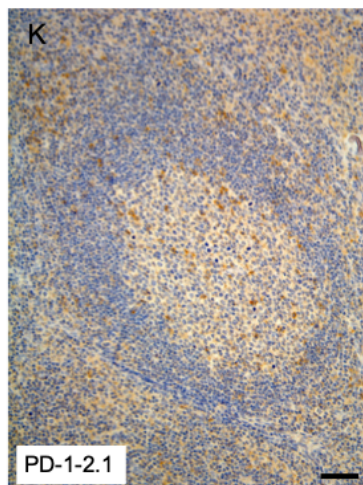
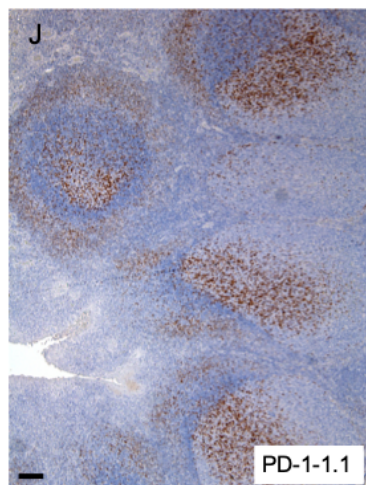
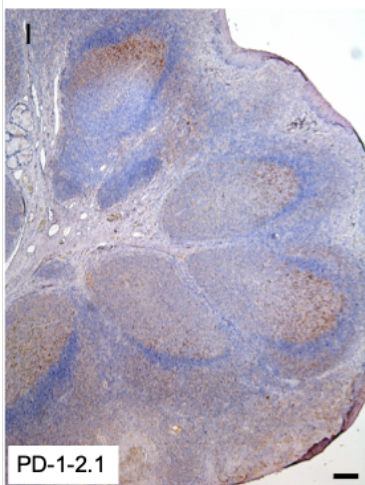
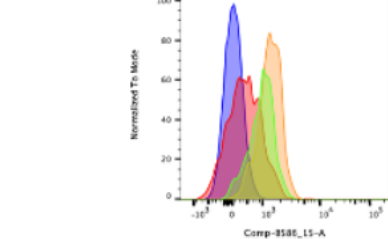


Figure 2. PD-L1 expression in canine gliomas. A and B, Intratumoral diffuse/granular cytoplasmic PD-L1 expression in a HA (A) and a HO (B). Anti-PD-L1 immunostaining, hematoxylin counterstaining. Scale bars, 100µm (A) and 50µm (B). C and D, absent PD-L1 expression in TCs at the core of a HA (C) versus diffuse cytoplasmic immunostaining of TCs in the periphery of the same tumor (D). Anti-PD-L1 immunostaining, hematoxylin counterstaining. Scale bars, 100µm (C) and 50µm (D). E and F, PD-L1+ TILs in a perivascular cuff in the infiltration zone of a HO (E) and CD3 immunostaining at the same level in an adjacent tissue section of the same specimen (F). Anti-PD-L1 immunostaining, hematoxylin counterstaining (E). Scale bars, 100µm.

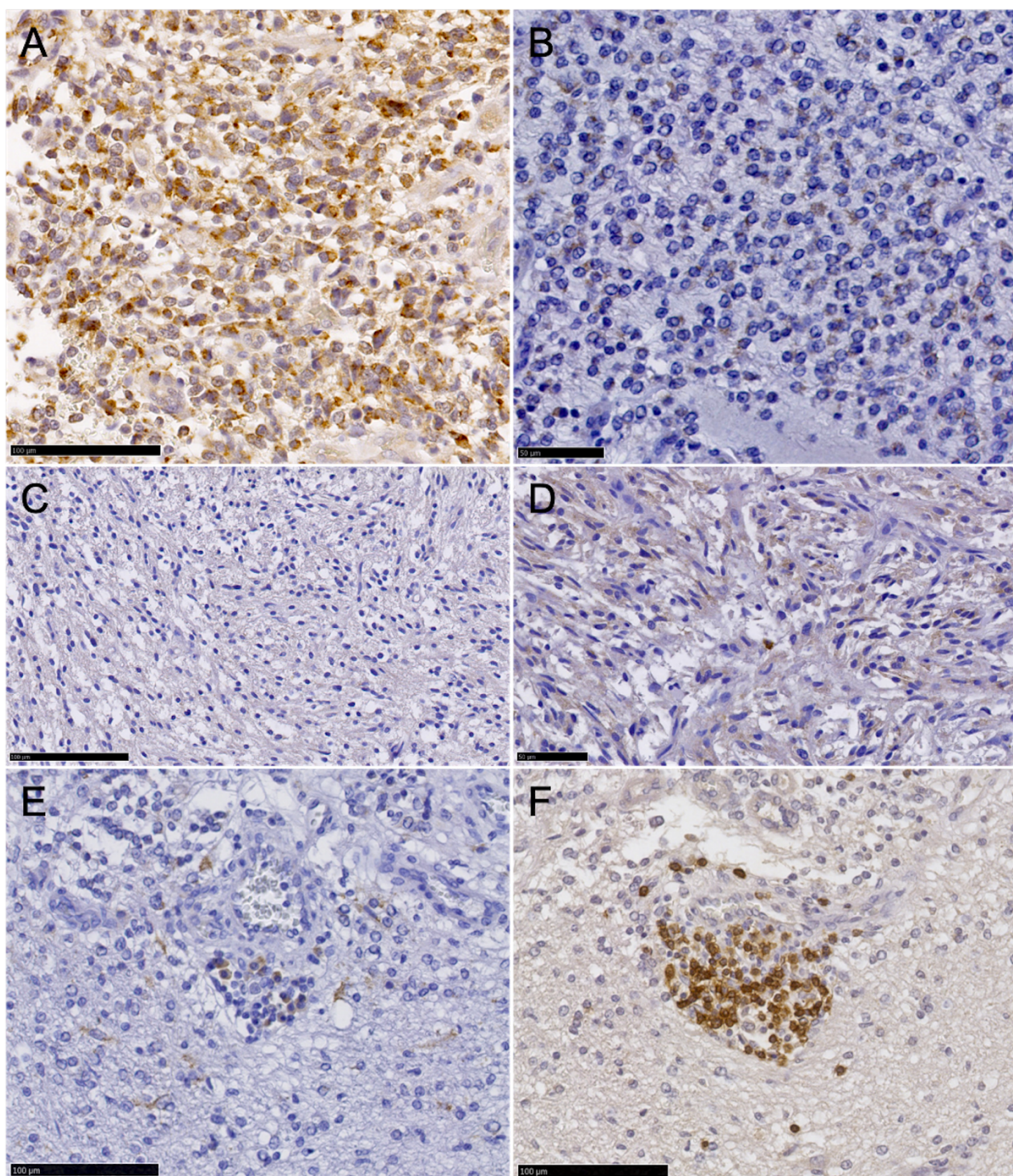


Figure 3. A-D, Consecutive sections of the same HA tissue specimen. A, Dense perivascular CD3⁺ TIL infiltration in the periphery of the tumor. B, Membranous and granular cytoplasmic PD-1 immunolabelling of TILs in the same perivascular infiltrate. C, CD20⁺ TIL infiltration in the same area as in A and B. D, PD-L1⁺ TCs near the perivascular TIL infiltrates in A-C. E, Incomplete membranous (arrows) and granular cytoplasmic (arrowheads) anti-PD-1 immunostaining of TCs in a HA. F, PD-1 immunostaining of morphologically apparent macrophages (arrows) in a HA. Hematoxylin counterstaining (A-F). Scale bars, 50µm.

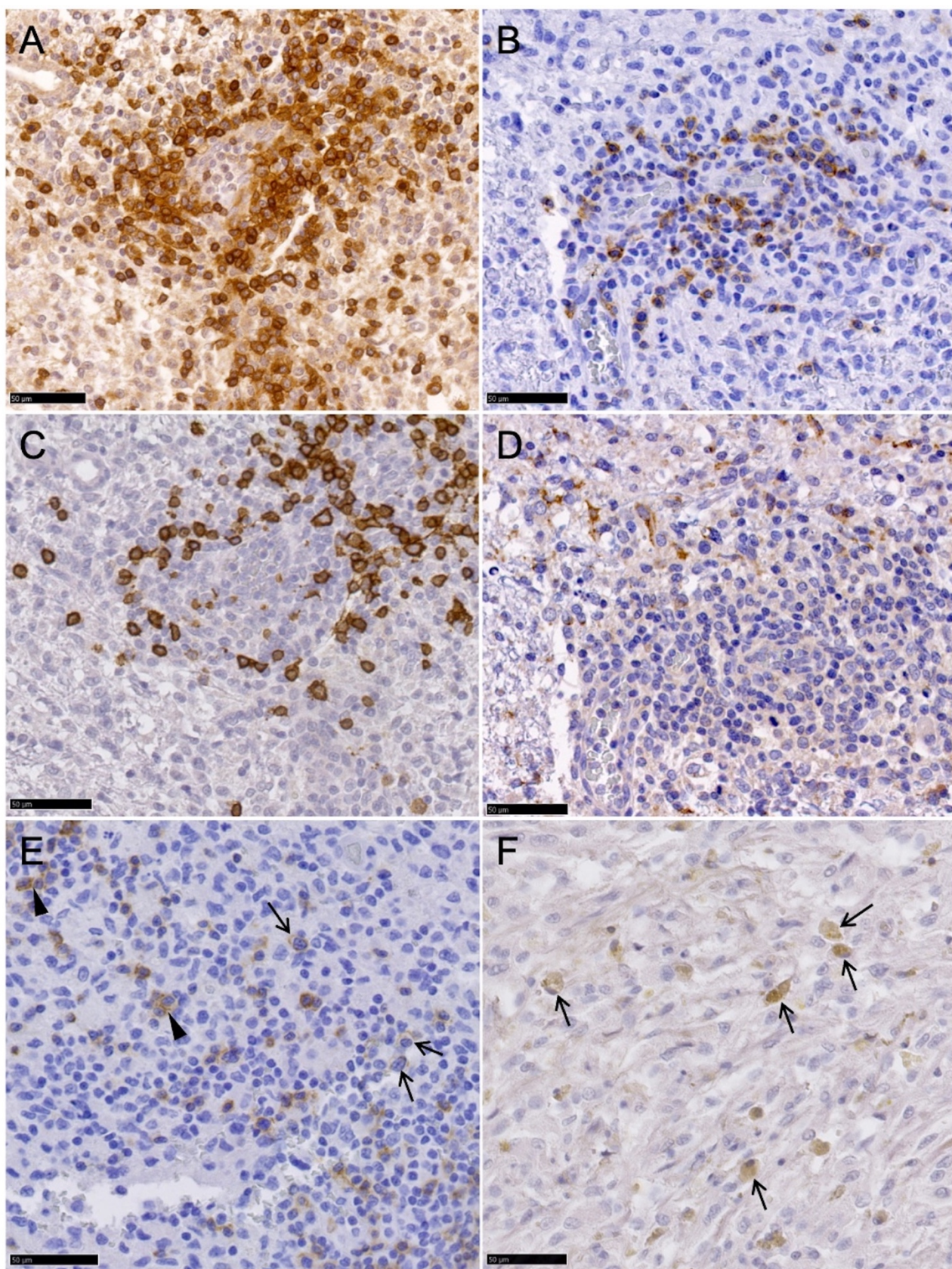


Table 1. Dog demographics and tumor location.

	Entire population (n = 21)	
	n	%
Median age, years (range)	8 (1.5 – 11.7)	
Sex		
Male	13	61.9
Female	8	38.1
Breed		
Boxer's phylogenetic clade ^{10,a}	15	71.4
Other breeds ^b	6	28.6
Tumor location		
Hemispheric	12	57.1
Diencephalon	5	23.8
Infratentorial	3	14.3
Spinal cord	1	4.8

^a Breeds in the Boxer's phylogenetic clade group included 7 Boxers, 6 Bulldogs (French, 5; English, 1), 1 Dogue de Bordeaux and 1 Staffordshire Bull Terrier.

^b Other dog breeds group included 1 each of the following: German Shorthaired Pointer, Yorkshire Terrier, West Highland White Terrier, Border Terrier, Springer Spaniel and crossbreed.

Table 2. Programmed death ligand 1 expression by glioma type and grade.

	HA (n = 8)		HO (n = 8)		HU (n = 2)		LA (n = 2)		LO (n = 1)	
	n	%	n	%	n	%	n	%	n	%
PD-L1+ TCs										
Intratumoral										
Median % ^a (range)	17.8 (10.5-52.9)		6.4 (0.8-50.2)		10.9 (5.6-16.3)		11.3 (9.1-13.4)		8.2	
Score										
0 (<1% PD-L1+ TCs)	0/8	0	2/8	25	0/2	0	0/2	0	0/1	0
1 (≥ 1%, < 5% PD-L1+ TCs)	0/8	0	1/8	12.5	0/2	0	0/2	0	0/1	0
2 (≥ 5%, < 50% PD-L1+ TCs)	7/8	87.5	3/8	37.5	2/2	100	2/2	100	1/1	100
3 (≥ 50% PD-L1+ TCs)	1/8	12.5	1/8	12.5	0/2	0	0/2	0	0/1	0
Infiltration zone										
Median % ^a (range)	9.8 (2.1-19.3)		3.2 (0.9-13.5)		5.2 (3.3-7.2)		8.2 (7.9-8.6)		3.0	
Score										
0 (<1% PD-L1+ TCs)	0/8	0	2/8	25	0/2	0	0/2	0	0/1	0
1 (≥ 1%, < 5% PD-L1+ TCs)	1/8	12.5	4/8	50	1/2	50	0/2	0	1/1	100
2 (≥ 5%, < 50% PD-L1+ TCs)	7/8	87.5	2/8	25	2/2	50	2/2	100	0/1	0
3 (≥ 50% PD-L1+ TCs)	0/8	0	0/8	0	0/2	0	0/2	0	0/1	0
Surrounding CNS										
Median % ^a (range)	2.3 (0-8.0)		1.0 (0-2.2)		0.5 (0-1.1)		0.7 (0-1.4)		0.7	
Score										
0 (<1% PD-L1+ TCs)	3/8	37.5	4/8	50	1/2	50	1/2	50	1/1	100
1 (≥ 1%, < 5% PD-L1+ TCs)	3/8	37.5	4/8	50	1/2	50	1/2	50	0/1	0
2 (≥ 5%, < 50% PD-L1+ TCs)	2/8	25	0/8	0	0/2	0	0/2	0	0/1	0
3 (≥ 50% PD-L1+ TCs)	0/8	0	0/8	0	0/2	0	0/2	0	0/1	0
PD-L1+ TILs	7/8	87.5	7/8	87.5	2/2	100	1/2	50	0/1	0
PD-L1+ microglia/macrophages	5/8	62.5	3/8	37.5	0/2	0	0/2	0	0/1	0

Abbreviations: HA, high-grade astrocytoma; HO, high-grade oligodendroglioma; HU, high-grade undefined glioma; LA, low-grade astrocytoma; LO, low-grade oligodendroglioma; PD-L1, programmed death ligand 1; TC, tumor cell; TIL, tumor-infiltrating lymphocyte.

^a Percentage of PD-L1+ TCs over all nucleated cells.

Table 3. Programmed cell death protein 1 expression and density of tumor-infiltrating lymphocytes by glioma type and grade.

	HA (n = 8)		HO (n = 8)		HU (n = 2)		LA (n = 2)		LO (n = 1)	
	n	%	n	%	n	%	n	%	n	%
PD-1+ TILs										
Intratumoral										
Median % ^a (range)	0.3 (0-8.3)		0 (0-8.2)		0.3 (0.2-0.3)		1.2 (0.8-1.7)		0	
Score										
0 (<1% PD-1+ TILs)	6/8	75	7/8	87.5	2/2	100	1/2	50	1/1	100
1 (≥ 1%, < 5% PD-1+ TILs)	1/8	12.5	0/8	0	0/2	0	1/2	50	0/1	0
2 (≥ 5%, < 10% PD-1+ TILs)	1/8	12.5	1/8	12.5	0/2	0	0/2	0	0/1	0
3 (≥ 10% PD-1+ TILs)	0/8	0	0/8	0	0/2	0	0/2	0	0/1	0
Infiltration zone										
Median % ^a (range)	0.4 (0-5.7)		0 (0-4.9)		0.3 (0.2-0.5)		0.2 (0-0.5)		0	
Score										
0 (<1% PD-1+ TILs)	6/8	75	7/8	87.5	2/2	100	2/2	100	1/1	100
1 (≥ 1%, < 5% PD-1+ TILs)	1/8	12.5	1/8	12.5	0/2	0	0/2	0	0/1	0
2 (≥ 5%, < 10% PD-1+ TILs)	1/8	12.5	0/8	0	0/2	0	0/2	0	0/1	0
3 (≥ 10% PD-1+ TILs)	0/8	0	0/8	0	0/2	0	0/2	0	0/1	0
Surrounding CNS										
Median % ^a (range)	0.1 (0-1.1)		0 (0-0.5)		0.1 (0-0.2)		0.1 (0-0.2)		0	
Score										
0 (<1% PD-1+ TILs)	7/8	87.5	8/8	100	2/2	100	2/2	100	1/1	100
1 (≥ 1%, < 5% PD-1+ TILs)	1/8	12.5	0/8	0	0/2	0	0/2	0	0/1	0
2 (≥ 5%, < 10% PD-1+ TILs)	0/8	0	0/8	0	0/2	0	0/2	0	0/1	0
3 (≥ 10% PD-1+ TILs)	0/8	0	0/8	0	0/2	0	0/2	0	0/1	0
CD3+ TILs										
Intratumoral										
Median % ^a (range)	3.9 (0.7-23.5)		1.9 (0.8-27.4)		2.6 (2-3.2)		8.1 (0.7-15.4)		0.1	
Infiltration zone										
Median % ^a (range)	3.0 (0-25.8)		2.7 (1.4-21.3)		2.1 (1.7-2.5)		0.6 (0.5-0.8)		0.2	
Surrounding CNS										

Median % ^a (range)	2.1 (0-13.5)		3.2 (0.6-4.6)		1.7 (0.8-2.7)		0.3 (0-0.5)		0	
CD20+ TILs										
<i>Intratumoral</i>										
Median % ^a (range)	0.5 (0-11.5)		0.1 (0-24.2)		0.3 (0.1-0.5)		1.0 (0-2.0)		0	
<i>Infiltration zone</i>										
Median % ^a (range)	0.3 (0-24.7)		0.3 (0-14.0)		0.2 (0-0.3)		0.1 (0-0.2)		0	
<i>Surrounding CNS</i>										
Median % ^a (range)	0.1 (0-7.0)		0.5 (0-0.7)		0.1 (0.1-0.1)		0.1 (0-0.2)		0	
PD-1+ microglia/macrophages	5/8	62.5	1/8	12.5	0/2	0	0/2	0	0/1	0
PD-1+ TCs	8/8	100	7/8	87.5	2/2	100	0/2	0	0/1	0

Abbreviations: HA, high-grade astrocytoma; HO, high-grade oligodendroglioma; HU, high-grade undefined glioma; LA, low-grade astrocytoma; LO, low-grade oligodendroglioma; PD-1, programmed cell death protein 1; TC, tumor cell; TIL, tumor-infiltrating lymphocyte.

^a Percentage of immunopositive TILs over all nucleated cells.

Supplementary Table 1: Antibodies and immunostaining protocols.

Maker	Cell types	Antibody Clone	Company	Dilution	Pretreatment	Detection and amplification system
PD-L1	Antigen presenting cells; tumor cells; microglia / macrophages; astrocytes; neurons	Monoclonal rabbit antibody, Anti-mB7-H1/PD1 Clone 2096C (MAB 90781)	R&D Systems, Oxon, UK	1:25	Citrate buffer 10 mM pH 6.0 20' 98°C + 30 min at RT	EnVision+ System-HRP (K4011), Dako, Glostrup, Denmark
PD-1	Exhausted T-cells; tumor cells; macrophages	Monoclonal mouse antibody, Anti-PD1 antibody (Dr. Vojtěšek, PD-1-1.1 and PD-1-2.1)	Moravian Biotechnology, Brno, Czech Republic	1:2000	Tris-EDTA 10mM pH 9.0, 20' 98°C + 30 min at RT	EnVision+ System-HRP (K4007), Dako, Glostrup, Denmark
CD3	General T-cell population; effector T-cells	Rabbit antihuman polyclonal, A0452	DakoCytomation Glostrup, Denmark	1:100	Protease 0.1% in PBS, 8 minutes at 37°C	EnVision+ System-HRP (K4011), Dako, Glostrup, Denmark
CD20	B-cells	Rabbit antihuman polyclonal, PA5-32313	Thermo Fisher Scientific, Cheshire, UK	1:300	Citrate buffer 10 mM pH 6.0 20' 98°C + 30 min at RT	EnVision+ System-HRP (K4011), Dako, Glostrup, Denmark
GFAP	Astrocytes; astrocytoma tumor cells	Rabbit antibovine anti-glial fibrillary acidic protein, Z0334	DakoCytomation Glostrup, Denmark	1:5000	Citrate buffer 10 mM pH 6.0 20' 98°C + 30 min at RT	EnVision+ System-HRP (K4011), Dako, Glostrup, Denmark
Olig2	Oligodendrocytes; oligodendroglioma tumor cells	Rabbit anti-Olig2 polyclonal antibody, AB9610	Chemicon, Merck KGaA, Darmstadt, Germany	1:500	Citrate buffer 10 mM pH 6.0 20' 98°C + 30 min at RT	EnVision+ System-HRP (K4011), Dako, Glostrup, Denmark

DISCUSSION

7. DISCUSSION

This doctoral thesis has produced a large body of information contributing towards validation of canine glioma as a naturally occurring model for human glioma.

We obtained valuable information on canine gliomas epidemiologic, clinicopathologic and diagnostic imaging features, furthering the current knowledge. Most importantly, we provide predictive information for the clinical diagnosis of glioma type and grade as well as their prognostic outcome for affected dogs. New MRI characteristics for differentiation of glioma type and grade are identified, and clinical and imaging findings are associated with survival. Additionally, we report a survival benefit of definitive treatments (surgery, radiotherapy and/or chemotherapy) compared to palliative treatment.

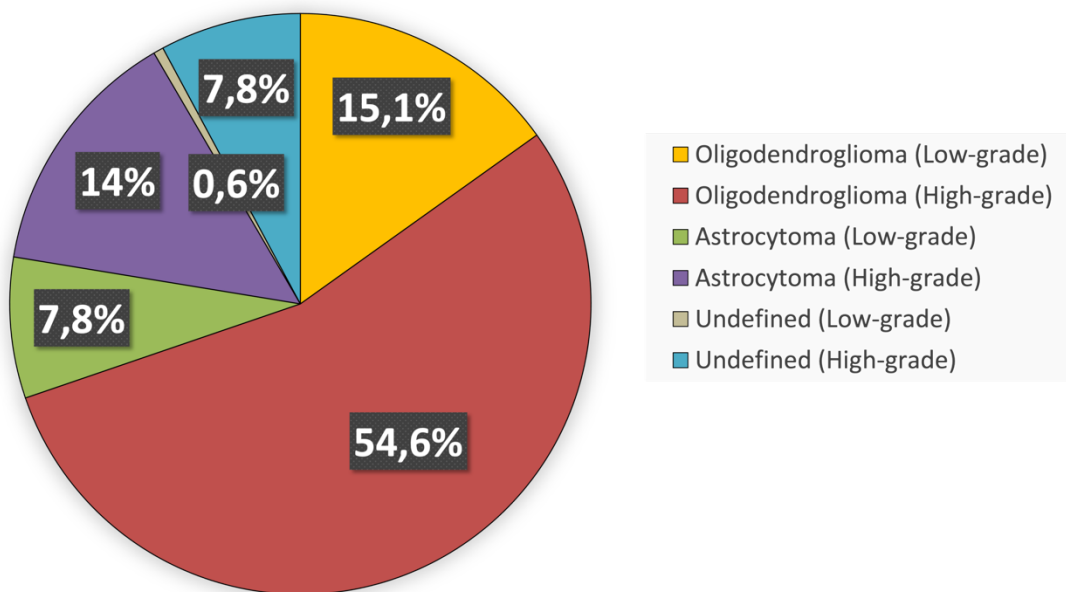
We also demonstrate a similar immunophenotype of canine gliomas to that expressed in the human counterpart in terms of accumulation of FOXP3⁺ Tregs within the tumor and the expression of the PD-1-PD-L1 immune checkpoint. As in human gliomas, FOXP3⁺ Tregs accumulation and PD-L1 expression is more pronounced in astrocytic gliomas than in tumors of oligodendroglial lineage, and TILs display similar characteristics in terms of density and distribution. This suggests that spontaneous canine glioma is closer than mice modelling these mechanisms of immune evasion in the human counterpart and supports its use in translational immunotherapeutic studies.

Our observed glioma type and grade relative frequency is consistent with data from prior literature and, together with a more recent study also applying the CBTC diagnostic scheme to a sample of 73 canine gliomas, provides fairly strong evidence oligodendroglial and high-grade tumors are the most prevalent in dogs (Figure 1).^{22,178,180} While high-grade gliomas are also considerably most frequent than low-grade gliomas in humans, the much higher

incidence of oligodendrogliomas in dogs represents a key difference with humans in which astrocytomas are most prevalent.³

Figure 1. Distribution^a of brain and other CNS gliomas in dogs according to their CBTC scheme's histologic subtype.^{22,178,180}

CBTC schema classified canine gliomas
(n = 357)



^a Percentages may not add up to 100% due to rounding.

Abbreviations: CBTC, Comparative Brain Tumor Consortium; CNS, central nervous system.

We found no associations between glioma location and tumor type or grade; however, our data supports previous studies suggesting that gliomas in dogs, like their human counterparts, arise mainly in the fronto-olfactory, temporal, and parietal regions of the cerebral hemispheres with decreasing frequency caudally within the CNS.^{3,22,26} We did not observe the previously reported increased likelihood of histologic involvement of the diencephalon in astrocytomas^{14,26} and, as in the CBTC study,²² oligodendrogliomas involved this region most commonly. Interestingly, all gliomas in dogs reported to be primarily intraventricular to date have been HOs.^{22,114,123,178}

Differently from the CBTC study, we could not confirm a higher prevalence of oligodendrogliomas in our Boxers and Bulldogs, probably due to smaller case numbers in our cohort; however, our data supports the reported predilection of gliomas for breeds in that phylogenetic clade.^{13,14,22,24,26,107} We also provide further evidence indicating a male sex predilection in canine gliomas which resembles the situation in humans.^{3,22}

The most common signs of neurologic dysfunction in our cohort included proprioceptive deficits, mentation changes, and seizures. Over 60% of the cases were diagnosed after an inaugural seizure, resembling previous studies in dogs,^{14,105,124} and mirroring the situation in humans.¹²⁵ Furthermore, we identified seizures at onset as a favorable prognostic factor for duration of survival in canine gliomas. Like in human gliomas, new onset seizures might represent an early warning sign for the presence of a brain tumor.¹²⁵

For this thesis, we analyzed previously published MRI predictors of intracranial canine glioma type and grade in a sample of 74 brain MRI studies of dogs with glioma, the largest reported to date, and confirmed their low sensitivity and specificity.^{26,30,31} Additionally, low agreement for predicted tumor type and grade using those features indicates high interobserver variability.

Thus, we looked for additional MRI indicators of intracranial glioma type and grade and found that oligodendrogliomas were associated with smooth margins and T1-weighted hypointensity compared to astrocytomas and undefined gliomas as well as more commonly in contact with the ventricles than astrocytomas. Tumor spread to neighboring brain structures was the only finding associated with high-grade diagnosis. These are in contrast with reported associations between peritumoral edema and astrocytomas, brain surface contact and oligodendrogliomas, and CE and cystic structures with tumor grade.^{26,30} Conversely to previous reports,^{26,30} ventricular contact alone, independent of distortion, was more common in oligodendrogliomas than astrocytomas. The only similarity between ours and prior studies

was the significantly low likelihood of T1-weighted hypointensity in astrocytomas,³⁰ which was shared by undefined gliomas our cohort.

Interobserver agreement for individual MRI features associated with glioma type and grade in this thesis is good to excellent; however, further studies are necessary now to establish their overall sensitivity and specificity in predicting canine glioma histologic subtype as well as the intra- and interobserver agreement for such diagnosis.

Differently from our observations, CE on MRI and in particular, ring-enhancement, is usually associated with higher grade human gliomas.^{34,127,128} However, human LAs and approximately 50% of LOs can show CE¹²⁹⁻¹³¹ and its absence does not exclude high-grade glioma.^{129,132,133} On the other hand, human oligodendrogliomas are usually well demarcated and largely T1-hypointense,^{35,36} and glioblastomas might extend widely to adjacent brain structures,¹³⁴ resembling our observations on canine oligodendrogliomas and high-grade gliomas, respectively.

Another similarity with human gliomas in our cohort of canine tumors was the rarity of spread to non-CNS structures and the lack of observation of extraneural metastases, both uncommon findings in humans.

The survival analysis presented here is the most complete to date in dogs with histopathologically confirmed glioma and is the first to incorporate such data to the new diagnostic classification. However, it has limitations inherent to the low case numbers and results need to be interpreted accordingly. The multivariable analysis of available clinical and MRI findings identified prognostic factors affecting survival in canine intracranial gliomas for the first time. In addition to the favorable association between new onset seizures and survival, a series of MRI features were identified as negative prognostic indicators. Poorly defined and irregular tumor margins, tumor T2-weighted heterogeneous signal, and

observation of drop metastases were associated with shorter survival. These prognostic factors differ from those reported for human gliomas; nevertheless, prognosis in humans is currently guided by isocitrate dehydrogenase mutation and 1p/19q status,²¹ for which parallelisms have not been found in canine gliomas.¹⁴¹⁻¹⁴⁵

Despite marked variability in treatment modalities, we demonstrated definitive therapies provide a significant survival benefit to dogs with intracranial gliomas when compared to palliative treatment. Also, we provide information on the MST of the largest series to date of histopathologically confirmed canine gliomas receiving palliative treatments, critical for assessment of therapies. However, we failed to find associations between survival and canine glioma type or grade in any treatment category. Although the latter might have been related to the small case numbers in our sample, it supports the need for further studies evaluating tumor immunologic and molecular profiles in combination with clinical outcome and survival data before the canine glioma classification and grading system can be used for prognostication of tumor biological behavior and therapeutic decisions as in the human counterpart.

Toward that aim, and because validation of spontaneous canine glioma as a model for immune evasion is intended to contribute to the identification of therapeutic targets in humans, we investigated the immunohistochemical expression of Tregs and the PD-1-PD-L1 immune checkpoint in a large cohort of dogs with glioma.

Concomitant to our research, a study using RNA in situ hybridization demonstrated intratumoral FOXP3+ Treg infiltration, greater proportion of FOXP3+ Tregs in peripheral blood, tumoral PD-L1 expression and presence of PD-1+ TILs in a series of 10 canine oligodendrogliomas.¹⁵⁴ In this thesis, we immunohistochemically detected FOXP3+ Tregs in a cohort of 43 canine gliomas including all types and grades. FOXP3+ TIL intratumoral accumulation coincided with areas of CD3+ TIL infiltration and was more pronounced in

astrocytic than oligodendroglial tumors. Mean FoxP3 expression was greater in high-grade gliomas, with significant differences between low-grade oligodendrogliomas and high-grade astrocytomas. A more recent study describing tumoral recruitment of Tregs and polarization of tumor-associated macrophages toward an M2 phenotype in a series of 73 canine gliomas also found FOXP3+ TILs in all cases and differences in FOXP3+ TIL counts between different tumor grades, with significantly increased counts in high-grade tumors.¹⁸⁰ However, they failed to find differences in FOXP3+ TIL counts between oligodendrogliomas and astrocytomas. The latter might have been related to the limited number of astrocytomas in their cohort and/or the use of different cell counting methodologies between studies. Whilst we manually counted regions with the highest concentrations of immunolabeled cells, they analyzed entire tumor sections via computerized image analysis.

In human gliomas, an increased proportion of Tregs within the TIL infiltrate correlates positively with a higher tumor grade.^{158,164} Also, the accumulation of FOXP3+ Tregs seems higher in astrocytic than oligodendroglial tumors.¹⁶⁴ Actually, human HAs, in particular glioblastomas, contain the highest proportion of intratumoral Tregs.^{53,164,175}

We also show expression of PD-L1 by TCs in a series of 21 spontaneous canine gliomas of different types and grades. Importantly, we developed and validated a canine-specific anti-PD-1 antibody, critical for the immunohistochemical study of canine glioma as a model for the PD-1-PD-L1 immunomodulating pathway in human gliomas. This allowed us to characterize PD-1+ TIL infiltration in this series of canine gliomas along with the CD3+ and CD20+ TIL subsets and their correlations. Correlations with observed FOXP3+ Tregs in this same cohort included in our previous study are also described.

We observed PD-L1 expression in all glioma specimens included in our last study. Most tumors contained $\geq 1\%$ PD-L1+ TCs within the studied areas, with the majority showing moderate intratumoral expression ($\geq 5\%$ but $< 50\%$ PD-L1+ TCs). PD-L1 expression in

human glioma patients is frequent and is confined to a minority subpopulation of TCs. It is possible that in dogs as in humans, a small amount of PD-L1 expression could be sufficient to restrain the immune system.⁹⁸

As in human high-grade and astrocytic gliomas, in particular glioblastomas,⁹¹⁻⁹³ canine HAs expressed higher levels of PD-L1 than any other tumor type and grade; however, expression in this series of canine gliomas was associated with tumor astrocytic lineage rather than grade.

Notably, PD-L1+ TILs and microglia/macrophages were also found in this study, resembling these observations in humans.^{91,92,94,95,98,99} PD-L1 expression in naïve T-cells has been shown to play a role in dendritic cell maturation, while its expression by Tregs further suppresses effector T-cell function.^{16,98,184} Furthermore, human gliomas also promote immunosuppression by inducing PD-L1 expression in tumor-associated macrophages.¹⁸⁵

As previously reported in canine and human gliomas, in the tumors studied for this thesis TILs could be seen scattered throughout the tumor tissue, though they tended to cluster around vasculature in the tumor margins and infiltration zone, and CD3+ TILs were present in higher numbers than CD20+ TILs.^{94,166,171} Despite different cell counting methodologies between our study on FOXP3+ Tregs and the subsequent one on PD-1 and PD-L1 expression in canine gliomas, results from both studies suggest an association between increased CD3+ TIL counts and canine high-grade glioma similar to that described in humans.¹⁷¹ However, this was not found in the aforementioned larger canine study on FOXP3 expression.¹⁸⁰ CD3+/CD8+ T-cells are the primary effectors of host antitumor immune responses and human studies have shown a predominance of CD8+ TILs within the T-cell subset, suggesting an attempt at a cytotoxic response that is ultimately unsuccessful.^{171,175} Absence of antibodies suitable for use in FFPE tissue sections prevented further subset analysis in our

samples, although the abovementioned study of canine oligodendrogliomas using in situ hybridization showed a greater presence of CD8+ than CD4+ TILs.¹⁵⁴

We found strong positive correlations between PD-1+ TIL counts and CD3+ TIL density, indicating T-cell exhaustion. This resembles observations in humans and demonstrates this pathophysiological mechanism of cytotoxic attack evasion in canine gliomas.⁹⁴ Additionally, intratumoral PD-1+ TIL density was positively correlated with greater presence of FOXP3+ Tregs, further suggesting Treg infiltration may also contribute to effector T-cell inhibition in canine gliomas. Although we found a trend to correlation, we could not demonstrate an association between PD-L1 expression and FOXP3+ TIL accumulation in our cohort of canine gliomas differently from that observed in humans where glioma-related PD-L1 expression induces and maintains Tregs.¹⁸¹

PD-L1+ TCs were significantly less frequently encountered in the tumor core than in the tumor margins and infiltration zone where they seemed to accumulate, mirroring the situation in humans.^{92,95} Regional overlap between TILs and PD-L1+ TCs was frequent. When present, PD-1+ TILs were often near areas of PD-L1 expression, suggesting canine gliomas also express PD-L1 in TCs at the forefront of inflammation to escape the host's antitumoral response.

Accumulation of Tregs and the PD-1-PD-L1 axis are considered central to human glioma immune evasion and their immunotherapeutic targeting is intensely studied. However, preclinical promise in murine models of glioma has not translated into improved patient outcomes in people.^{17,18,47,182}

The results of this doctoral thesis research further support the use of naturally occurring canine glioma as a model for spontaneous human disease. Demonstration of these mechanisms of antitumor immune response escape in the dog indicates canine gliomas

recapitulate the complexities within the tumor immunosuppressive microenvironment in human gliomas more accurately than mice. Therefore, canine glioma may provide a useful model for immunotherapeutic studies to treat human patients.

CONCLUSIONS

8. CONCLUSIONS

Based on the results of the three studies comprising this doctoral thesis, we can conclude the following:

1. Although canine gliomas are most commonly oligodendrogliomas and human gliomas most often consist of astrocytomas, gliomas in dogs hold key epidemiologic and clinicopathologic similarities with their human counterparts. These include tumor location, a male sex predilection, and seizures as a common presenting sign prompting diagnosis.
2. On MRI diagnosed intracranial gliomas, smooth margins, T1-weighted hypointensity and ventricular contact could allow differentiation between oligodendrogliomas and other glial tumor types in dogs. High-grade glioma should be suspected if spread over more than one brain region is observed.
3. Definitive therapies appear to improve survival time of dogs with glioma.
4. New onset seizures are associated with a more favorable prognosis, whereas MRI observed irregular or indistinct tumor margins, T2-weighted heterogeneity and drop metastases are negative prognostic indicators.
5. The lack of associations between survival and the CBTC morphologic classification indicates further studies evaluating tumor immunologic and molecular profiles in combination with clinical outcome and survival data are necessary before the canine glioma classification and grading system can be used for prognostication of tumor biological behavior and therapeutic decisions as in the human counterpart.
6. Despite the apparent tumor molecular differences between human and canine glioma, they seem to share a similar immunophenotype.

7. FOXP3⁺ Treg infiltration can be detected immunohistochemically in all canine glioma subtypes and, as in the human counterpart, accumulation of FOXP3⁺ Tregs is more pronounced in high-grade and astrocytic gliomas.
8. PD-1 and PD-L1 are immunohistochemically detectable in canine gliomas of different types and grades and similarly to human gliomas, astrocytic tumors express higher levels of PD-L1.
9. Development and validation of our canine-specific anti-PD-1 antibody will enable further immunohistochemical studies of the PD-1-PD-L1 pathway in dogs.
10. TILs display similar density and distribution characteristics in dogs as described for human gliomas. They can be scattered throughout the tumor tissue but are most commonly perivascular in the tumor periphery. CD3⁺ TILs are higher in numbers than CD20⁺ TILs, that might not always be present. Increased CD3⁺ TIL counts seem associated with canine high-grade glioma, and FOXP3⁺ and PD-1⁺ TIL subsets coincide with regions of CD3⁺ TIL infiltration.
11. Gliomas in dogs present a realistic animal model for the evaluation and development of new immunotherapies for human gliomas.

9. BIBLIOGRAPHY

1. Louis DN, Ohgaki H, Wiestler OD, et al. The 2007 WHO classification of tumours of the central nervous system. *Acta Neuropathol* 2007; 114:97-109.
2. Ostrom QT, Bauchet L, Davis FG, et al. The epidemiology of glioma in adults: a “state of the science” review. *Neuro Oncol* 2014; 16(7):896-913.
3. Ostrom QT, Cioffi G, Gittleman H, et al. CBTRUS statistical report: primary brain and other central nervous system tumors diagnosed in the United States in 2012-2016. *Neuro Oncol* 2019; 21(suppl.5): v1-v100.
4. Furnari FB, Fenton T, Bachoo RM, et al. Malignant astrocytic glioma: genetics, biology, and paths to treatment. *Genes Dev* 2007; 21:2683-2710.
5. Stupp R, Mason WP, van den Bent MJ, et al. Radiotherapy plus concomitant and adjuvant temozolomide for glioblastoma. *N Engl J Med* 2005; 352:987-996.
6. Lim JH, Koh S, Olby NJ, et al. Isolation and characterization of neural progenitor cells from adult canine brains. *Am J Vet Res* 2012; 73:1963-1968.
7. Chen L, Zhang Y, Yang J, Hagan JP, Li M. Vertebrate animal models of glioma: understanding the mechanisms and developing new therapies. *Biochim Biophys Acta* 2013; 1836:158-165.
8. Hicks J, Platt SR, Kent M, et al. Canine brain tumours: a model for the human disease? *Vet Comp Oncol* 2017; 15(1):252-272.
9. Klotz, M. Incidence of brain tumors in patients hospitalized for chronic mental disorders. *Psych Quar* 1957; 31:669-680.
10. Siegel RL, Miller KD, Fuchs HE, Jemal A. Cancer statistics, 2021. *Ca Cancer J Clin* 2021; 71:7-33.

11. Dorn CR, Taylor DO, Frye FL, et al. Survey of animal neoplasms in Alameda and Contra Costa counties, California. Methodology and description of cases. *J Natl Cancer Inst* 1968; 40:295-305.
12. McGrath JT. Intracranial pathology in the dog. *Acta Neuropathol* 1962; 1(suppl.I):3-4.
13. Song RB, Vite CH, Bradle CW, Cross JR. Postmortem evaluation of 435 cases of intracranial neoplasia in dogs and relationship of neoplasm with breed, age and body weight. *J Vet Intern Med* 2013; 27:1143-1152.
14. Snyder JM, Shofer FS, Van Winkle TJ, Massicotte C. Canine intracranial primary neoplasia: 173 cases (1986-2003). *J Vet Intern Med* 2008; 22:172-177.
15. Baumeister SH, Freeman GJ, Dranoff G, et al. Coinhibitory pathways in immunotherapy for cancer. *Annu Rev Immunol* 2016; 34:539-573.
16. Nduom EK, Weller M, Heimberger AB. Immunosuppressive mechanisms in glioblastoma. *Neuro Oncol* 2015;17(suppl.7): vii9-vii14.
17. Reardon DA, Gokhale PC, Klein SR, et al. Glioblastoma eradication following immune checkpoint blockade in an orthotopic, immunocompetent model. *Cancer Immunol Res* 2016; 4(2):124-135.
18. Kurz SC, Wen PY. Quo Vadis – Do immunotherapies have a role in glioblastoma? *Curr Treat Options Neurol* 2018; 20:14.
19. Koestner A, Bilzer T, Fatzer R, et al. Histological classification of Tumors of the Nervous System of Domestic Animals. Washington, DC: Armed Forces Institute of Pathology 1999.
20. Dickinson PJ. Advances in diagnostic and treatment modalities for intracranial tumors. *J Vet Intern Med* 2014; 28:1165-1185.

21. Louis DN, Ohgaki H, Wiestler, OD, et al. The 2016 world health organization classification of tumors of the central nervous system: a summary. *Acta Neuropathol* 2016; 131:803-820.
22. Koehler JW, Miller AD, Miller CR, et al. A revised diagnostic classification of canine glioma: towards validation of the canine glioma patient as a naturally occurring preclinical model for human glioma. *J Neuropathol Exp Neurol* 2018; 77(11):1039-1054.
23. Higgins RJ, Bollen AW, Dickinson PJ, Sisó-Llonch S. Tumors of the Nervous System. In: Meuten DJ, ed. *Tumors in Domestic Animals*. 5th ed. Arnes, AI: Willey-Blackwell, 2016; 834-891.
24. Hayes HM, Priester WA, Jr., Pendergrass TW. Occurrence of nervous-tissue tumors in cattle, horses, cats and dogs. *Int J Cancer* 1975; 15:39-47.
25. Higgins RJ, Dickinson PJ, LeCouteur RA, et al. Spontaneous canine gliomas: overexpression of EGFR, PDGFR α and IGFBP2 demonstrated by tissue microarray immunophenotyping. *J Neurooncol* 2010; 98:49-55.
26. Young BD, Levine JM, Porter BF, et al. Magnetic resonance imaging features of intracranial astrocytomas and oligodendrogliomas in dogs. *Vet Radiol Ultrasound* 2011; 52:132-141.
27. Stoica G, Levine J, Wolff, J, et al. Canine astrocytic tumors: a comparative review. *Vet Pathol* 2011; 48:266-275.
28. Kraft SL, Gavin PR, DeHaan C, et al. Retrospective review of 50 canine intracranial tumors evaluated by magnetic resonance imaging. *J Vet Intern Med* 1997; 11:218-225.
29. Ródenas S, Pumarola M, Gaitero L, et al. Magnetic resonance imaging findings in 40 dogs with histologically confirmed intracranial tumours. *Vet J* 2011; 187:85-91.

30. Bentley RT, Ober CP, Anderson KL, et al. Canine intracranial gliomas: relationship between magnetic resonance imaging criteria and tumor type and grade. *Vet J* 2013; 198(2):463-471.
31. Stadler KL, Ruth JD, Pancotto TE, et al. Computed tomography and magnetic resonance imaging are equivalent in mensuration and similarly inaccurate in grade and type predictability of canine intracranial gliomas. *Front Vet Scie* 2017; 4:157.
32. Jenkinson MD, Du Plessis DG, Walker C, Smith TS. Advanced MRI in the management of adult gliomas. *Br J Neurosurg* 2007; 21(6):550-561.
33. Dean BL, Drayer BP, Bird CR, et al. Gliomas: classification with MR imaging. *Radiology* 1990; 174:411-415.
34. Watanabe M, Tanaka R, Takeda N. Magnetic resonance imaging and histopathology of cerebral gliomas. *Neuroradiology* 1992; 34:463-469.
35. Engelhard HH, Stelea A, Mundt A. Oligodendroglioma and anaplastic oligodendroglioma: clinical features, treatment, and prognosis. *Surg Neurol* 2003; 60:443-456.
36. Lee YY, Tassel PV. Intracranial oligodendrogliomas: imaging findings in 35 untreated cases. *AJR Am J Roentgenol* 1989; 152:361-369.
37. Heidner GL, Kornegay JN, Page RL, et al. Analysis of survival in a retrospective study of 86 dogs with brain tumors. *J Vet Intern Med* 1991; 5:219–226.
38. Niebauer GW, Dayrell-Hart BL, Speciale J. Evaluation of craniotomy in dogs and cats. *J Am Vet Med Assoc* 1991; 198:89–95.
39. Brearley MJ, Jeffery ND, Phillips SM, et al. Hypofractionated radiation therapy of brain masses in dogs: A retrospective analysis of survival of 83 cases (1991–1996). *J Vet Intern Med* 1999; 13:408–412.

40. Chen DS, Mellman I. Oncology meets immunology: the cancer-immunity cycle. *Immunity* 2013; 39:1-10.
41. Alterman RL, Stanley ER. Colony stimulating factor-1 expression in human glioma. *Mol Chem Neuropathol* 1994; 21(2-3):177-188.
42. Pyonteck SM, Akkari L, Schuhmacher AJ, et al. CSF-1R inhibition alters macrophage polarization and blocks glioma progression. *Nat Med* 2013; 19(10):1264-1272.
43. Zou W. Regulatory T cells, tumour immunity and immunotherapy. *Nat Rev Immunol* 2006; 6:295-307.
44. Mougiakakos D, Choudhury A, Lladser A, et al. Regulatory T cells in cancer. *Adv Cancer Res* 2010; 107:57-117.
45. Garden OA, Pinheiro D, Cunningham F. All creatures great and small: Regulatory T cells in mice, humans, dogs and other domestic animal species. *Int Immunopharmacol* 2011; 11:576-588.
46. Veiga-Parga T. Regulatory T cells and their role in animal disease. *Vet Pathol* 2016; 53(4):737-745.
47. Wainwright DA, Dey M, Chang A, et al. Targeting Tregs in malignant brain cancer: overcoming IDO. *Front Immunol* 2013; 4:1-17.
48. Campbell DJ, Koch MA. Phenotypical and functional specialization of FOXP3+ regulatory T cells. *Nat Rev Immunol* 2011; 11:119-130.
49. Ooi YC, Tran P, Ung N, et al. The role of regulatory T-cells in glioma immunology. *Clin Neurol Neurosurg* 2014; 119:125-132.
50. See AP, Parker JJ, Waziri A. The role of regulatory T cells and microglia in glioblastoma-associated immunosuppression. *J Neurooncol* 2015; 123: 405-412.

51. Humphries W, Wei J, Sampson JH, et al. The role of Tregs in glioma-mediated immunosuppression: Potential target for intervention. *Neurosurg Clin N Am* 2010; 21:125–137.
52. Jacobs JFM, Idema AJ, Bol KF, et al. Prognostic significance and mechanism of Treg infiltration in human brain tumors. *J Neuroimmunol* 2010; 225:195–199.
53. Sayour EJ, McLendon P, McLendon R, et al. Increased proportion of FoxP3⁺ regulatory T cells in tumor infiltrating lymphocytes is associated with tumor recurrence and reduced survival in patients with glioblastoma. *Cancer Immunol Immunother* 2015; 64:419–427.
54. Biller BJ, Elmslie RE, Burnett RC, Avery AC, Dow SW. Use of FOXP3 expression to identify regulatory T cells in healthy dogs and dogs with cancer. *Vet Immunol Immunopathol* 2007; 116:69-78.
55. Horiuchi Y, Tominaga M, Ichikawa M, et al. Relationship between regulatory and type 1 T cells in dogs with oral malignant melanoma. *Microbiol Immunol* 2010; 54(3):152-159.
56. Kim JH, Hur JH, Lee SM, et al. Correlation of Foxp3 positive regulatory T cells with prognostic factors in canine mammary carcinomas. *Vet J* 2012; 193:222–227.
57. Mahmoud SMA, Paish EC, Powe DG, et al. An evaluation of the clinical significance of FOXP3⁺ infiltrating cells in human breast cancer. *Breast Cancer Res Treat* 2011; 127(1):99-108.
58. McDermott DF, Atkins MB. PD-1 as a potential target in cancer therapy. *Cancer Med* 2013; 2(5):662-673.
59. Dong H, Strome SE, Salomao DR, et al. Tumor-associated B7-H1 promotes T-cell apoptosis: a potential mechanism of immune evasion. *Nat Med* 2002; 8(8):793–800.
60. Okazaki T, Honjo T. The PD-1-PD-L pathway in immunological tolerance. *Trends Immunol* 2006; 27:195-201.

61. Chen L. Co-inhibitory molecules of the B7-CD28 family in the control of T-cell immunity. *Nat Rev Immunol* 2004; 4:336-347.
62. Greenwald RJ, Freeman GJ and Sharpe AH. The B7 family revisited. *Annu Rev Immunol* 2005; 23:515-548.
63. Sharpe AH, Wherry EJ, Ahmed R, et al. The function of programmed cell death 1 and its ligands in regulating autoimmunity and infection. *Nat immunol* 2007; 8:239-245.
64. Chimuka S. Basics of PD-1 in self-tolerance, infection, and cancer immunity. *Int J Clin Oncol* 2016; 21:448-455.
65. Leach DR, Krummel MF, Allison JP. Enhancement of antitumor immunity by CTLA-4 blockade. *Science* 271:1734-1736.
66. Ghebeh H, Mohammed S, Al-Omair A, et al. The B7-H1 (PD-L1) T lymphocyte-inhibitory molecule is expressed in breast cancer patients with infiltrating ductal carcinoma: correlation with important high-risk factors. *Neoplasia* 2006; 8(3):190-198.
67. Ghebeh H, Tulbah A, Mohammed S, et al. Expression of B7-H1 in breast cancer patients strongly associated with high proliferative Ki-67-expressing tumor cells. *Int J Cancer* 2007; 121(4):751-758.
68. Hamanishi J, et al. Programmed cell death 1 ligand 1 and tumor-infiltrating CD8+ T lymphocytes are prognostic factors of human ovarian cancer. *Proc Natl Acad Sci USA* 2007; 104:3360-3365.
69. Karim R, Jordanova ES, Piersma SJ, et al. Tumor-expressed B7-H1 and B7-DC in relation to PD-1+ T-cell infiltration and survival of patients with cervical carcinoma. *Clin Cancer Res* 2009; 15:6341-6347.
70. Tsushima F, Tanaka K, Otsuki N, et al. Predominant expression of B7-H1 and its immunoregulatory roles in oral squamous cell carcinoma. *Oral Oncol* 2006; 42:268-274.

71. Lyford-Pike S, Peng S, Young GD, et al. Evidence for a role of the PD-1:PD-L1 pathway in immune resistance of HPV-associated head and neck squamous cell carcinoma. *Cancer Res* 2013; 73:1733-1741.
72. Mu CY, Huang JA, Chen Y, et al. High expression of PD-L1 in lung cancer may contribute to poor prognosis and tumor cells immune escape through suppressing tumor infiltrating dendritic cells maturation. *Med Oncol* 2011; 28:682-688.
73. D’Incecco A, Andreozzi M, Ludovini V, et al. PD-1 and PDL-1 expression in molecularly selected non-small-cell lung cancer patients. *Br J Cancer* 2015; 112(1):95-102.
74. Hsu MC, Hsiao JR, Chang KC, et al. Increase of programmed death-1-expressing intratumoral CD8+ T cells predicts a poor prognosis for nasopharyngeal carcinoma. *Mod Pathol* 2010; 23:1393-1403.
75. Ohigashi Y, Sho M, Yamada Y, et al. Clinical significance of programmed death-1 ligand-1 and programmed death-1 ligand-2 expression in human esophageal cancer. *Clin Cancer Res* 2005; 11:2947-2953.
76. Wu C, Zhu Y, Jiang J, et al. Immunohistochemical localization of programmed death-1 ligand-1 (PD-L1) in gastric carcinoma and its clinical significance. *Acta Histochem* 2006; 108:19-24.
77. Gao Q, Wang XY, Qiu SJ, et al. Overexpression of PD-L1 significantly associates with tumor aggressiveness and postoperative recurrence in human hepatocellular carcinoma. *Clin Cancer Res* 2009; 15:971-979.
78. Hua D, Sun J, Mao Y, et al. B7-H1 expression is associated with expansion of regulatory T cells in colorectal carcinoma. *World J Gastroenterol* 2012; 18:971-978.

79. Geng L, Huang D, Liu J, et al. B7-H1 up-regulated expression in human pancreatic carcinoma tissue associates with tumor progression. *J Cancer Res Clin Oncol* 2008; 134:1021-1027.
80. Thompson RH, et al. Costimulatory B7-H1 in renal cell carcinoma patients: indicator of tumor aggressiveness and potential therapeutic target. *Proc Natl Acad Sci USA* 2004; 101:17174-17179.
81. Nakanishi J, Wada Y, Matsumoto K, et al. Overexpression of B7-H1 (PD-L1) significantly associates with tumor grade and postoperative prognosis in human urothelial cancers. *Cancer Immunol Immunother* 2007; 56:1173-1182.
82. Hino R, et al. Tumor cell expression of programmed cell death 1 ligand 1 is a prognostic factor for malignant melanoma. *Cancer* 2010; 116:1757-1766.
83. Wilcox RA, Feldman AL, Wada DA, et al. B7-H1 (PD-L1, CD274) suppresses host immunity in T-cell lymphoproliferative disorders. *Blood* 2009; 114:2149-2158.
84. Chen X, Liu S, Wang L, et al. Clinical significance of B7-H1 (PD-L1) expression in human acute leukemia. *Cancer Biol Ther* 2008; 7:622-627.
85. Iway Y, Ishida M, Tanaka Y, et al. Involvement of PD-L1 on tumor cells in the escape from host immune system and tumor immunotherapy by PD-L1 blockade. *Proc Natl Acad Sci USA* 2002; 99:12293-12297.
86. Curiel TJ, et al. Blockade of B7-H1 improves myeloid dendritic cell-mediated antitumor immunity. *Nat Med* 2003; 9:562-567.
87. Topalian SL, et al. Safety, activity and immune correlates of anti-PD-1 antibody in cancer. *N Eng J Med* 2012; 366:2443-2454.
88. Brahmer JR, et al. Safety and activity of anti-PD-L1 antibody in patients with advanced cancer. *N Eng J Med* 2012; 366:2455-2465.

89. Kleffel S, Posch C, Barthel SR, et al. Melanoma cell-intrinsic PD-1 receptor functions promote tumor growth. *Cell* 2015; 162:1242-1256.
90. Wintterle S, Schreiner B, Mitsdoerffer M, et al. Expression of the B7-related molecule B7-H1 by glioma cells: a potential mechanism of immune paralysis. *Cancer Res* 2003; 63:7462-7467.
91. Wilmotte R, Burkhardt K, Kindler V, et al. B7-homolog 1 expression by human glioma: a new mechanism of immune evasion. *Neuroreport* 2005; 16:1081-1085.
92. Yao Y, Tao R, Wang Y, et al. B7-H1 is correlated with malignancy-grade gliomas but is not expressed exclusively on tumor stem-like cells. *Neuro Oncol* 2009; 11:757-766.
93. Garber ST, Hashimoto Y, Weathers SP, et al. Immune checkpoint blockade as a potential therapeutic target: surveying CNS malignancies. *Neuro Oncol* 2016; 18(10):1357-1366.
94. Berghoff AS, Kiesel B, Widhalm G, et al. Programmed death ligand 1 expression and tumor-infiltrating lymphocytes in glioblastoma. *Neuro Oncol* 2015; 17(8):1064-1075.
95. Majzner RG, Simon JS, Grosso JF, et al. Assessment of programmed death-ligand 1 expression and tumor-associated immune cells in pediatric cancer tissues. *Cancer* 2017; 123:3807-3815.
96. Rahman M, Kresak J, Yang C, et al. Analysis of immunologic markers in primary and recurrent glioblastoma. *J Neurooncol* 2018; 137(2):249-257.
97. Zeng J, Zhang XK, Chen HD, et al. Expression of programmed cell death-ligand 1 and its correlation with clinical outcomes in gliomas. *Oncotarget* 2016; 7(8):8944:8955.
98. Nduom EK, Wei J, Yaghi NK, et al. PD-L1 expression and prognostic impact in glioblastoma. *Neuro Oncol* 2016; 18(2):195-205.
99. Han J, Hong Y, Lee YS. PD-L1 expression and combined status of PD-L1/PD-1-positive tumor infiltrating mononuclear cell density predict prognosis in glioblastoma patients. *J Pathol Transl Med* 2017; 51(1):40-48.

100. Hartley G, Faulhaber E, Caldwell A, et al. Immune regulation of canine tumour and macrophage PD-L1 expression. *Vet Comp Oncol* 2017; 15:534-549.
101. Maekawa N, Konnai S, Ikebuchi R, et al. Expression of PD-L1 on canine tumor cells and enhancement of IFN- γ production from tumor infiltrating cells by PD-L1 blockade. *PLoS One* 2014; 9:e98415.
102. Maekawa N, Konnai S, Okagawa T, et al. Immunohistochemical analysis of PD-L1 expression in canine malignant cancers and PD-1 expression on lymphocytes in canine oral melanoma. *PLoS One* 2016; 11:e0157176.
103. Kumar SR, Kim DY, Henry CJ, et al. Programmed death ligand 1 is expressed in canine B cell lymphoma and downregulated by MEK inhibitors. *Vet Comp Oncol* 2017; 15(4):1527-1536.
104. Coy J, Caldwell A, Chow L, et al. PD-1 expression by canine T cells and functional effects of PD-1 blockade. *Vet Comp Oncol* 2017; 15(4):1487-1502.
105. Bagley RS, Gavin PR, Moore MP, et al. Clinical signs associated with brain tumors in dogs: 97 cases (1992-1997). *J Am Vet Med Assoc* 1999; 215:818-819.
106. Bentley RT, Ahmed AU, Yanke AB, et al. Dogs are man's best friend: in sickness and in health. *Neuro Oncol* 2017; 19(3):312-322.
107. Truvé K, Dickinson P, Xiong A, et al. Utilizing the dog genome in the search for novel candidate genes involved in glioma development—genome wide association mapping followed by targeted massive parallel sequencing identifies a strongly associated locus. *PLoS Genet* 2016; 12(5):e1006000.
108. Fernández F, Deviers A, Dally C, et al. Presence of neural progenitors in spontaneous canine gliomas: a histopathological and immunohistochemical study of 20 cases. *Vet J* 2016; 209:125-132.

109. Recio A, de la Fuente C, Pumarola M, et al. Magnetic resonance imaging and computed tomographic characteristics of a glioma causing calvarial erosion in a dog. *Vet Radiol Ultrasound* 2019; 60:E1-E5.
110. Lobacz MA, Serra F, Hammond G, et al. Imaging diagnosis – Magnetic resonance imaging of diffuse leptomeningeal oligodendrogliomatosis in a dog with “dural tail sign”. *Vet Radiol Ultrasound* 2018; 59:E1-E6.
111. Zagzag D, Esencay M, Mendez O, et al. Hypoxia- and vascular endothelial growth factor-induced stromal cell-derived factor-1 α /CXCR4 expression in glioblastomas: one plausible explanation of Scherer’s structures. *Am J Pathol* 2008; 173:545-560.
112. Rossmeisl JH, Clapp K, Pancotto TE, et al. Canine butterfly glioblastomas: a neuroradiological review. *Front Vet Scie* 2016; 3:40.
113. Schweizer-Gorgas D, Henke D, Oevermann A, et al. Magnetic resonance imaging features of canine gliomatosis cerebri. *Vet Radiol Ultrasound* 2018; 59:180-187.
114. Vigerál M, Bentley RT, Rancilio NJ, et al. Imaging diagnosis – antemortem detection of oligodendroglioma “cerebrospinal fluid drop metastases” in a dog by serial magnetic resonance imaging. *Vet Radiol Ultrasound* 2018; 59:E32-E37.
115. Koch MW, Sánchez MD, Long S. Multifocal oligodendroglioma in three dogs. *J Am Anim Hosp Assoc* 2011; 47:e77-85.
116. Schkeeper AE, Moon R, Shrader S, et al. Imaging diagnosis – magnetic resonance imaging features of a multifocal oligodendroglioma in the spinal cord and brain of a dog. *Vet Radiol Ultrasound* 2017; 58:E49-E54.
117. Canal S, Bernardini M, Pavone S, et al. Primary diffuse leptomeningeal gliomatosis in 2 dogs. *Can Vet J* 2013; 54:1075-1079.

118. Sturges BK, Dickinson PJ, Bollen AW, et al. Magnetic resonance imaging and histological classification of intracranial meningiomas in 112 dogs. *J Vet Intern Med* 2008; 22:586-595.
119. Bittermann S, Lang J, Henke D, et al. Magnetic resonance imaging signs of presumed elevated intracranial pressure in dogs. *Vet J* 2014; 201:101-108.
120. Toyoda I, Vernau W, Sturges BK, et al. Clinicopathological characteristics of histiocytic sarcoma affecting the central nervous system in dogs. *J Vet Intern Med* 2020; 34:828-837.
121. Parker HG, Dreger DL, Rimbault M, et al. Genomic analyses reveal the influence of geographic origin, migration, and hybridization on modern dog breed development. *Cell Rep* 2017; 19:697–708.
122. Wood A, Garosi L, Platt S. Cerebrospinal fluid analysis. In: Platt S, Garosi L, eds. *Small animal neurological emergencies*. London: Manson Publishing, 2012; 121-136.
123. Rissi DR, Levine JM, Eden KB, et al. Cerebral oligodendroglioma mimicking intraventricular neoplasia in three dogs. *J Vet Diagn Invest* 2015; 27:396-400.
124. Schwartz M, Lamb CR, Brodbelt DC, et al. Canine intracranial neoplasia: clinical risk factors for development of epileptic seizures. *J Small Anim Pract* 2011; 52:632-637.
125. Vecht CJ, Kerkhof M, Duran-Pena A. Seizure prognosis in brain tumors: new insights and evidence-based management. *Oncologist* 2014; 19:751-759.
126. Wolff CA, Holmes SP, Young BD, et al. Magnetic resonance imaging for the differentiation of neoplastic, inflammatory, and cerebrovascular brain disease in dogs. *J Vet Intern Med* 2012; 26:589-597.
127. Khalid L, Carone M, Dumrongpisutikul N, et al. Imaging characteristics of oligodendrogliomas that predict grade. *AJNR Am J Neuroradiol* 2012; 33:852-857.
128. Walker C, Baborie A, Crooks D, et al. Biology, genetics and imaging of glial cell tumors. *Br J Radiol* 2011; 84:S90-S106.

129. Knopp EA, Cha S, Johnson G, et al. Glial neoplasms: dynamic contrast-enhanced T2*-weighted MR imaging. *Radiology* 1999; 211:791-798.
130. Reiche W, Grunwald I, Hermann K, et al. Oligodendrogliomas. *Acta Radiol* 2002; 43:474-482.
131. Jenkinson MD, du Plessis DG, Smith TS, et al. Histological growth patterns and genotype in oligodendroglial tumors: correlation with MRI features. *Brain* 2006; 129:1884-1891.
132. Van den Bent MJ, Reni M, Gatta G, et al. Oligodendroglioma. *Crit Rev Oncol Hematol* 2008; 66:262-272.
133. Ginsberg LE, Fuller GN, Hashmi M, et al. The significance of lack of MR contrast enhancement of supratentorial brain tumors in adults: histopathological evaluation of a series. *Surg Neurol* 1998; 49:436-440.
134. Matsukado Y, MacCarty CS, Kernohan JW. The growth of glioblastoma multiforme (astrocytomas, grades 3 and 4) in neurosurgical practice. *J Neurosurg* 1961; 18:636-644.
135. Rees JH, Smirniotopoulos JG, Jones RV, et al. Glioblastoma multiforme: radiologic-pathologic correlation. *Radiographics* 1996; 16:1413-1438.
136. Hardian RF, Goto T, Kuwabara H, et al. An autopsy case of widespread brain dissemination of glioblastoma unnoticed by magnetic resonance imaging after treatment with bevacizumab. *Surg Neurol Int* 2019; 10:137.
137. Walmsley GL, Chandler K, Davies ES, et al. Multi-focal cerebral oligoastrocytoma in a puppy. *J Small Anim Pract* 2009; 50:435-439.
138. Barnard RO, Geddes JF. The incidence of multifocal cerebral gliomas. A histologic study of large hemisphere sections. *Cancer* 1987; 60:1519-1531.
139. Ahn MS, Jackler RK. Exophytic brain tumors mimicking primary lesions of the cerebellopontine angle. *Laryngoscope* 1997; 107:466-471.

140. Wu B, Liu W, Zhu H, et al. Primary glioblastoma of the cerebellopontine angle in adults. *J Neurosurg* 2011; 114:1288-1293.
141. Kawakami S, Ochiai K, Azakami D, et al. R132 mutations in canine isocitrate dehydrogenase 1 (IDH1) lead to functional changes. *Vet Res Commun* 2018; 42:49-56.
142. Fraser AR, Bacci B, Chevoir MA, et al. Isocitrate dehydrogenase 1 expression in canine gliomas. *J Comp Pathol* 2018; 165:33-39.
143. Reitman ZJ, Olby NJ, Mariani CL, et al. IDH1 and IDH2 hotspot mutations are not found in canine glioma. *Int J Cancer* 2010; 127:245-246.
144. Amin SB, Anderson KJ, Boudreau CE, et al. Comparative molecular life history of spontaneous canine and human gliomas. *Cancer Cell* 2020; 37:243-257.e7.
145. Thomas R, Duke SE, Wang HJ, et al. ‘Putting our heads together’: insights into genomic conservation between human and canine intracranial tumors. *J Neurooncol* 2009; 94:333-349.
146. Rossmeisl JH Jr, Garcia PA, Pancotto TE, et al. Safety and feasibility of the NanoKnife system for irreversible electroporation ablative treatment of canine spontaneous intracranial gliomas. *J Neurosurg* 2015; 123:1008-1025.
147. Rossmeisl JH, Herpai D, Quigley M, et al. Phase I trial of convection-enhanced delivery of IL13RA2 and EPHA2 receptor targeted cytotoxins in dogs with spontaneous intracranial gliomas. *Neuro Oncol* 2020; 23(3):422-434.
148. Freeman AC, Platt SR, Holmes S, et al. Convection-enhanced delivery of cetuximab conjugated iron-oxide nanoparticles for treatment of spontaneous canine intracranial gliomas. *J Neurooncol* 2018; 137:653-663.
149. Bentley RT, Thomovsky SA, Miller MA, et al. Canine (pet dog) tumor microsurgery and intratumoral concentration and safety of metronomic chlorambucil for spontaneous glioma: a phase I clinical trial. *World Neurosurg* 2018; 116:e534-e542.

150. Suñol A, Mascort J, Font C, et al. Long-term follow-up of surgical resection alone for primary intracranial rostromedial tumors in dogs: 29 cases (2002–2013). *Open Vet J* 2017; 7:375–383.
151. Dolecek TA, Propp JM, Stroup NE, et al. CBTRUS statistical report: Primary brain and central nervous system tumors diagnosed in the united states in 2005–2009. *Neuro Oncol* 2012; 14:v1–49.
152. Herranz C, Fernández F, Martín-Ibáñez R, et al. Spontaneously arising canine glioma as a potential model for human glioma. *J Comp Pathol* 2016; 154:169–179.
153. Domingues P, González-Tablas M, Otero A, et al. Tumor infiltrating immune cells in gliomas and meningiomas. *Brain Behav Immun* 2016; 53: 1–15.
154. Filley A, Henriquez M, Bhowmik T, et al. Immunologic and gene expression profiles of spontaneous canine oligodendrogliomas. *J Neurooncol* 2018; 137(3):469–479.
155. Mostofa AGM, Punganuru SR, Madala HR, et al. The process and regulatory components of inflammation in brain oncogenesis. *Biomolecules* 2017; 7:1–33.
156. Huang Y, Wang F, Wang Y, et al. Intrahepatic interleukin-17⁺ T cells and FoxP3⁺ regulatory T cells cooperate to promote development and affect the prognosis of hepatocellular carcinoma. *J Gastroenterol Hepatol* 2014; 29:851–859.
157. Zhu S, Lin J, Qiao G, et al. Differential regulation and function of tumor-infiltrating T cells in different stages of breast cancer patients. *Tumor Biol* 2015; 36:7907–7913.
158. Wang L, Zhang B, Xu X, et al. Clinical significance of FOXP3 expression in human gliomas. *Clin Transl Oncol* 2014; 16:36–43.
159. Yue Q, Zhang X, Ye H, et al. The prognostic value of Foxp3⁺ tumor-infiltrating lymphocytes in patients with glioblastoma. *J Neurooncol* 2014; 116:251–259.

160. Biller BJ, Guth A, Burton JH, et al. Decreased ratio of CD8⁺ T cells to regulatory T cells associated with decreased survival in dogs with osteosarcoma. *J Vet Intern Med* 2010; 24:1118–1123.
161. Tominaga M, Horiuchi Y, Ichikawa M, et al. Flow cytometric analysis of peripheral blood and tumor-infiltrating regulatory T cells in dogs with oral malignant melanoma. *J Vet Diagn Invest* 2010; 22:438–441.
162. Porcellato I, Brachelente C, De Paolis L, et al. FoxP3 and IDO in canine melanocytic tumors. *Vet Pathol* 2019; 56:189–199.
163. Carvalho MI, Pires I, Prada J, et al. Intratumoral FoxP3 expression is associated with angiogenesis and prognosis in malignant canine mammary tumors. *Vet Immunol Immunopathol* 2016; 178:1–9.
164. Heimberger AB, Abou-Ghazal M, Reina-Ortiz C, et al. Incidence and prognostic impact of FoxP3⁺ regulatory T cells in human gliomas. *Clin Cancer Res* 2008; 14:5166–5172.
165. Han S, Zhang C, Li Q, et al. Tumour-infiltrating CD4⁺ and CD8⁺ lymphocytes as predictors of clinical outcome in glioma. *Br J Cancer* 2014; 110:2560–2568.
166. Sloma EA, Creneti CT, Erb HN, Miller AD. Characterization of inflammatory changes associated with canine oligodendroglioma. *J Comp Pathol* 2015; 153(2-3):92-100.
167. Kmiecik J, Poli A, Brons NHC, et al. Elevated CD3⁺ and CD8⁺ tumor-infiltrating immune cells correlate with prolonged survival in glioblastoma patients despite integrated immunosuppressive mechanisms in the tumor microenvironment and at the systemic level. *J Neuroimmunol* 2013; 264:71–83.
168. Hussain SF, Yang D, Suki D, et al. The role of human glioma-infiltrating microglia/macrophages in mediating antitumor immune responses. *Neuro Oncol* 2006; 8:261–279.

169. Orrego E, Castaneda CA, Castillo M, et al. Distribution of tumor-infiltrating immune cells in glioblastoma. *CNS Oncol* 2018; 7:CNS21.
170. Rissi DR, Porter BF, Boudreau CE, et al. Immunohistochemical characterization of immune cell infiltration in feline glioma. *J Comp Pathol* 2018; 160:15–22.
171. Yang I, Han SJ, Sughrue ME, Tihan T, Parsa AT. Immune cell infiltrate differences in pilocytic astrocytoma and glioblastoma: evidence of distinct immunological microenvironments that reflect tumor biology. *J Neurosurg* 2011; 115(3):505-511.
172. Jacobs JFM, Idema AJ, Bol KF, et al. Regulatory T cells and the PD-L1/ PD-1 pathway mediate immune suppression in malignant human brain tumors. *Neuro Oncol* 2009; 11:394–402.
173. Ebert LM, Tan BS, Browning J, et al. The regulatory T cell-associated transcription factor FoxP3 is expressed by tumor cells. *Cancer Res* 2008; 68:3001–3009.
174. Lohr J, Ratliff T, Huppertz A, et al. Effector T-cell infiltration positively impacts survival of glioblastoma patients and is impaired by tumor- derived TGF- β . *Clin Cancer Res* 2011; 17:4296–4308.
175. Kim YH, Jung TY, Jung S, et al. Tumor-infiltrating T-cell subpopulations in glioblastomas. *Br J Neurosurg* 2012; 26(1):21-27.
176. Boozer LB, Davis TW, Borst LB, et al. Characterization of immune cell infiltration into canine intracranial meningiomas. *Vet Pathol* 2012; 49: 784–795.
177. Pinheiro D, Chang Y-M, Bryant H, et al. Dissecting the regulatory microenvironment of a large animal model of Non-Hodgkin lymphoma: Evidence of a negative prognostic impact of FOXP3⁺ T cells in canine B cell lymphoma. *PLoS One* 2014; 9:e105027–15.
178. José-López R, Gutierrez-Quintana R, De la Fuente C, et al. Canine gliomas: clinical features, diagnosis and survival analysis. *J Vet Intern Med* 2021; 35(4):1902-1917.

179. Pi Castro D, José-López R, Fernández Flores F, et al. Expression of FOXP3 in canine gliomas: immunohistochemical study of tumor-infiltrating regulatory lymphocytes. *J Neuropathol Exp Neurol* 2020; 79(2):184-193.
180. Krane GA, O'Dea CA, Malarkey DE, et al. Immunohistochemical evaluation of immune cell infiltration in canine gliomas. *Vet Pathol*. 2021; doi:10.1177/03009858211023946.
181. DiDomenico J, Lamano JB, Oyon D, et al. The immune checkpoint protein PD-L1 induces and maintains regulatory T cells in glioblastoma. *Oncoimmunology* 2018; 7(7):e1448329.
182. Reardon DA, Brandes AA, Omuro A, et al. Effect of nivolumab vs bevacizumab in patients with recurrent glioblastoma: the CheckMate 143 phase 3 randomized clinical trial. *JAMA Oncol* 2020; 6(7):1003-1010.
183. Monroig-Bosque P, Driver B, Morales-Rosado JA, et al. Correlation between programmed death receptor-1 expression in tumor-infiltrating lymphocytes and programmed death ligand-1 expression in non-small cell lung carcinoma. *Arch Pathol Lab Med* 2018; 142(11):1388-1393.
184. Talay O, Shen CH, Chen L, Chen J. B7-H1 (PD-L1) on T cells is required for T-cell-mediated conditioning of dendritic cell maturation. *Proc Natl Acad Sci USA* 2009; 106(8):2741-2746.
185. Bloch O, Crane CA, Kaur R, et al. Gliomas promote immunosuppression through induction of B7-H1 expression in tumor-associated macrophages. *Clin Cancer Res* 2013; 19(12):3165-3175.
186. Pitter CL, Newcombe J, Antel JP, Arbour N. The majority of infiltrating CD8T lymphocytes in multiple sclerosis lesions is insensitive to enhanced PD-L1 levels on CNS cells. *Glia* 2011; 59(5):841-856.

187. Keffel S, Posch C, Barthel SR, et al. Melanoma cell-intrinsic PD-1 receptor functions promote tumor growth. *Cell* 2015; 162:1242-1256.